Current Awareness Bulletin

of

SCHOLARLY ARTICLES PUBLISHED BY

Faculty, Students and Alumni

~ September 2012 ~

DELHI TECHNOLOGICAL UNIVERSITY CENTRAL LIBRARY
(formerly Delhi College of Engineering, Bawana Road, DELHI)

PREFACE

This is the first Current Awareness Bulletin Service started by Delhi Technological University Library. The aim of the bulletin is to compile, preserve and disseminate information published by the Faculty, Students and Alumni for mutual benefits. The bulletin also aims to propagate the intellectual contribution of DTU as a whole to the academia. It contains information resources available in the internet in the form of articles, reports, presentation published in international journals, websites, etc. by the faculty and students of Delhi Technological University in the field of science and technology. The publication of Faculty and Students which are not covered in this bulletin may be because of the reason that either the full text was not accessible or could not be searched by the search engine used by the library for this purpose. To make the bulletin more comprehensive, the learned faculty and Students may provide their uncovered publication to the library either through email or in CD, etc.

This issue contains the information published during September 2012. The arrangement of the contents is alphabetical wise starting from A-Z. The Full text of the article which is either subscribed by the University or available in the web has been provided in this Bulletin.

CONTENTS

***** **Faculty**
@ **Students/Research Scholars**
**Alumni**

International Journal of Mathematics Research.
ISSN 0976-5840 Volume 3, Number 4 (2011), pp. 403-408

http://www.irphouse.com

Condition for Maxima and Minima between Two Points

[1]Chandan Kumar and [2]K. Jayakumar

[1]Department of Civil Engineering, Delhi Technological University
(Formerly: Delhi College of Engineering)
Delhi University, Bawana Road, Delhi-110042, India
E-mail: chandankumardce@gmail.com/yahoo.co.in
[2]Joint Secretary, Council of Scientific and Industrial Research,
Anusandhan Bhavan, 2, Rafi Marg, New Delhi-110001, India
E-mail: kjaykay@yahoo.com/jsa@csir.res.in

Abstract

In the present paper, we are going to find out and study the true relationship between the curve and the point of intersection of any two tangent drawn on the curve having product of their slope negative, also the condition for which maxima and minima exists between two points. since their is a general misconception that when the product of slope of two tangent is negative then their exist at least one point in between them whose slope is zero. In this paper we have find the condition when it will satisfy this result and when not, and also derived the other possible results, for any smooth curve which is continuous and differentiable in its domain.

AMS Subject Classification: 11*G*20, 14*H*50, 53*A*04.

Keywords: Continuity, Differentiability, Tangents, Slopes .motionatelligence, Stress Resiliency.

Introduction

Their is a general misconception that when the product of slope of two tangent is negative then their exist at least one point in between them whose slope is zero. In this

paper we have find the condition when it will satisfy this result, and also derived the other possible results. Let y = f(x) be any smooth curve which is continuous and differentiable in its domain. If the product of the slope of the tangents drawn on two points A[a,f(a)] and B[b,f(b)] lying on the curve is negative, then their exists at least one point C(cx,cy) lying on the curve between points A[a,f(a)] and B[b,f(b)] such that the angle of slope at point C(cx,cy) can be either zero or $\pi/2$.

Theorem

Let y = f(x) is a smooth curve such that:

1. It is continuous and differentiable in its domain.
2. Consider any two points A[a,f(a)] and B[b,f(b)] lying inside the domain.
3. The product of the slope of the tangents at points A[a,f(a)] and B[b,f(b)] be negative.
4. Let the point of intersection of two tangents drawn at points A[a,f(a)]and B[b,f(b)] be M(mx, my).
5. Then their exists a point C(cx,cy) lying on the curve between points A[a,f(a)] and B[b,f(b)] such that the angle of slope at point C(cx,cy) is either '0' or $\pi/2$.

Case (I): If $a < mx < b$, then their exists at least one point such that $f'(cx) = 0$.

Case (II): If $f(a) < my < f(b)$, then their exists at least one point such that

$$\frac{1}{f'(c_x)} = 0$$

Where

$$m_x = \frac{[bf'(b) - af'(a)] - [f(b) - f(a)]}{[f'(a) - f'(a)]}$$

and

$$m_y = \frac{[f'(a)f'(b)(b-a)] + [f(a)f'(b) - f(b)f'(a)]}{[f'(b) - f'(a)]}$$

Proof: Let y = f(x) is a curve

Since the product of the slope of two tangents is negative. Hence the slope of one tangent must be positive and the other negative. Since the product of slopes of two tangent is negative, they will definitely intersect at one point say M (mx,my).

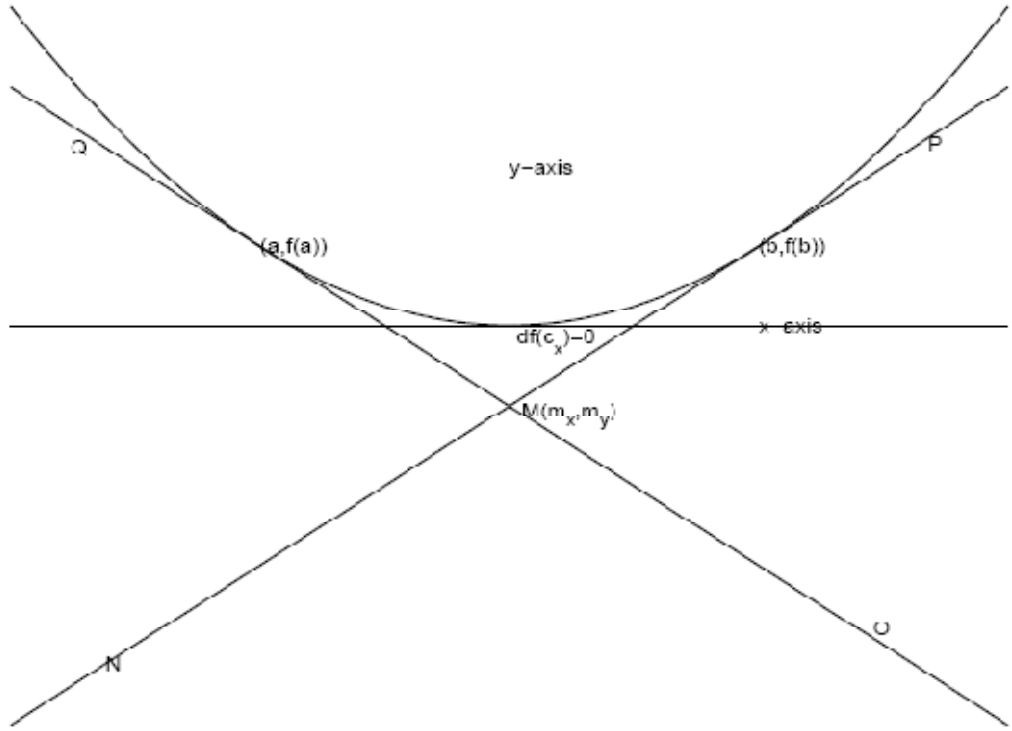

Graph of the curve when $a<m_x<b$.

Case (I): If $a < mx < b$, then their exists at least one point such that $f'(cx) = 0$.

Let NMP be any line whose slope is positive and

Let OMQ be other line whose slope is negative,

These two lines will behave like the tangent for the curve. Let point A[a,f(a)] lie anywhere between M and Q and point B[b,f(b)] lie anywhere between M and P. Since all the points on line MQ lie left side of point (mx) and all the points on line MP lie right side of point (mx).

Since $a < mx < b$ and the point C (cx,cy) lie on curve between points A[a,f(a)] and B[b,f(b)], hence the tangent MP or MQ must be rotated in such a way so that it can cover entire region between A[a,f(a)] and B[b,f(b)]. Hence rotating NMP clockwise or OMQ anticlockwise approaches and coincides with tangent OMQ and NMP respectively. Since slope of NMP is positive and OMQ is negative so, on rotating NMP to OMQ or OMQ to NMP there will exist at least one point such that $f'(cx) = 0$.

Case (II): If $f(a) < my < f(b)$, then their exists at least one point such that:

$$\frac{1}{f'(c_x)} = 0$$

Let NMP be any line whose slope is positive and

Let OMQ be other line whose slope is negative,

These two lines will behave like the tangent for the curve. Let point A [a,f(a)] lie anywhere between M and Q and point B[b,f(b)] will lie anywhere between M and N. since all the points on line MQ lie above the point (*my*) and all the points on line MN lie below the point (*my*).Since *f*(*a*) < *my* < *f*(*b*) and the point C (*cx,cy*) lie on curve between points A[a,f(a)] and B[b,f(b)] hence the tangent MQ or MN must be rotated in such a way so that it can cover entire region between A[a,f(a)] and B[b,f(b)]. Hence rotating OMQ clockwise or NMP anticlockwise to approach and coincides with tangent NMP and OMQ respectively. Since slope of NMP is positive and OMQ is negative so, on rotating NMP to OMQ or OMQ to NMP there will exist at least one points such that:

$$\frac{1}{f'(c_x)} = 0$$

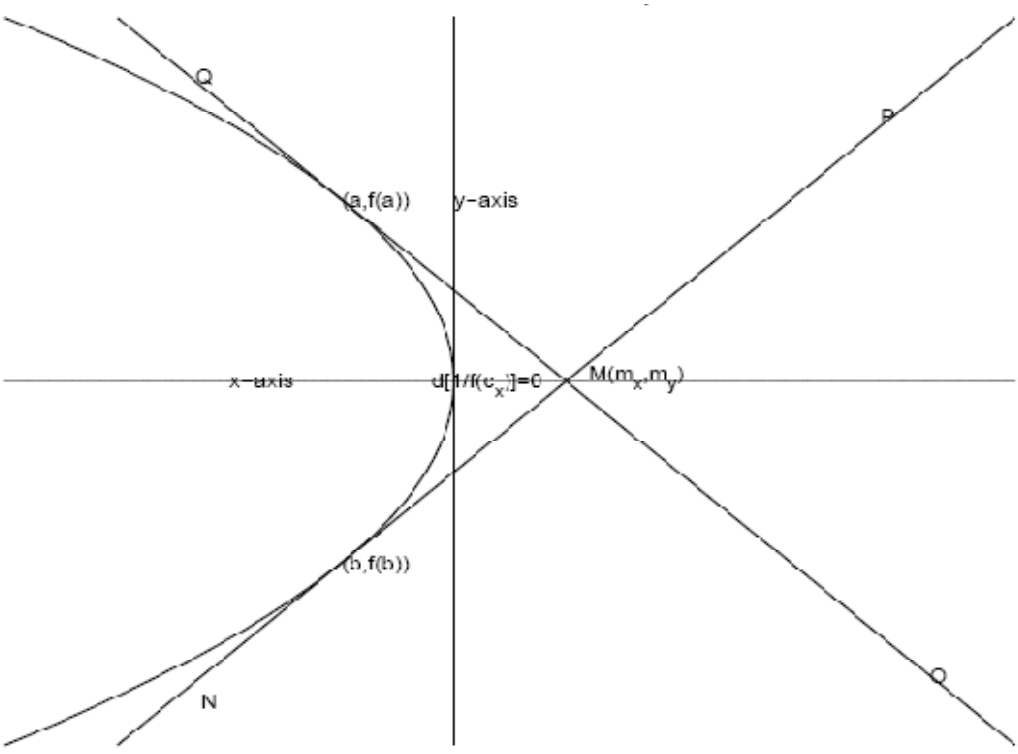

Graph of the curve when f(a)<m_y<f(b).

Calculation of the value of (m_x) and (m_y)

Since y=f(x)

Let $f'(a)$ is the slope at point A, and f'(b) is the slope at point B.

Equation of tangent at point A is:

$$(m_y) f'(b) - f(a) f'(b) + af'(a) f'(b) = (m_y) f'(c) = 0 - f(b) f'(a) + bf'(a) f'(b)$$

Equation of tangent at point A is:

$$f'(b) = \frac{Y - f(b)}{X - b}$$

Since the point of intersection of tangents is M (*mx,my*);

So, $Y = y = my$ and $X = x = mx$

On equating y value from both equations, we get:

$$f'(a)[m_x - a] + f(a) = f'(b)[m_x - b] + f(b)$$

$$[f'(b) - f'(a)](m_x) = [bf'(b) - af'(a)] - [f(b) - f(a)]$$

$$m_x = \frac{[bf'(b) - af'(a)] - [f(b) - f(a)]}{[f'(a) - f'(a)]}$$

On equating x value from both equations, we get:

$$\frac{m_y - f(a)}{f'(a)} + a = \frac{m_y - f(b)}{f'(b)} + b$$

$$\frac{m_y - f(a) + af'(a)}{f'(a)} = \frac{m_y - f(b) + bf'(b)}{f'(b)}$$

$$(m_y) f'(b) - f(a) f'(b) + af'(a) f'(b) = (m_y) f'(a) - f(b) f'(a) + bf'(a) f'(b)$$

$$m_y = \frac{[f'(a) f'(b)(b - a)] + [f(a) f'(b) - f(b) f'(a)]}{[f'(b) - f'(a)]}$$

Corollary

Condition for maxima and minima: (1) Let f(x) is continuous in [a,b] and differentiable in (a,b). (2) The product of $f'(a)$ and $f'(b)$ is negative. (3) The point of intersection of two tangents drawn at points A [a,f(a)] and B[b,f(b)] be M (*mx,my*). (4) If $a < mx < b$, (5) Then their will exists at least one point of maxima or minima between (a,b).

Where

$$m_x = \frac{[bf'(b) - af'(a)] - [f(b) - f(a)]}{[f'(a) - f'(a)]}$$

Proof

The proof of the corollary is same as stated above

The importance of this corollary is that for finding out maxima and minima between any two points the general rule is that "If the curve is continuous and differentiable between any two points and also if the slope of any point between this two points is zero i.e. $f'(c) = 0$, then their exists maxima or minima at this point" , but in this case we do not have to follow this given rule, since in this corollary the equation of curve is not given, only the value of slope at points A and B, the co-ordinate of point A and B, and the point of intersection of the tangents is given. So the above mentioned rule

Isn't be applying. Since this theorem and corollary is basics of the mathematics, so this corollary and above mention theorem can be very useful in the development of any branch mathematics, and may give new direction and approach to this theory.

Conclusion

The above theorem is a basic theorem whose results can be easily used in all branches of science. It is a more general theorem which uses co-ordinates of the point of intersection of the tangents to determine the nature of slope of the curves.

Acknowledgement

I would like to heartily dedicate this paper to my father Late Shri Mangal Das, mother Bibbo Devi, four brothers Manish Kumar, Parvat Raj, Vikas Kumar, Himanshu Kumar and Sisters Poonam Kumari, Sandhya Kumari, Rajani Kumari and Shivani Kumari who always supported me in the field of research. I would also like to thank our Vice Chancellor Prof. P.B. Sharma, Prof. S.K. Singh and Prof. R.K. Sinha for their guidance, teacher sister Rose Charles who really took pain to nurture me in beginning of my career and finally to my loving friends Mr. Thanvendra Singh and Mr. Prabhat Singh.

References

[1] Chandan Kumar (April 2011), "Integral of Bijective Function in a Bounded Region", International Journal of Emerging Technologies in Science and Engineering, Vol. 4, No.1: pp. 69-72.

[2] Chandan Kumar (2010), "Bounded Inverse Relational Function", International Journal of Mathematical Science Education, Vol. 3, No. 1, pp. 16-23.

[3] Chandan Kumar (November 2010), "Nine Multifunction Number", International Journal of Algorithms, Computing and Mathematics, Vol.3, No. 4, pp. 29-33.

[4] Lindgren. G., and H. Rootzen. 1987. Extreme values: Theory and technical applications. Scandinavian journal of statistics, Theory and Application 14:241-279.

Design of Model Predictive Control based Direct Neural Controller for Surge Tank Application

Rashmi Baweja
Reader, Department of Electronics Engg.
Modi Institute of Technology, Kota
Rajasthan, India

N. K. Bhagat,
Associate Prof., Department of Electrical Engg.,
Delhi Technological University,
Delhi, India

ABSTRACT
Model predictive control based direct neural controllers represent another class of computer application in the field of non-linear controls. These controllers can also be made adaptive such that the adaptation mechanism attempts to adjust a parameterized nonlinear controller to approximate an ideal controller. Various approximators such as linear mappings, polynomials, fuzzy systems, or neural networks can be used as parameterized nonlinear controller. In this paper, we proposed a model predictive control based neural network controller to control the liquid level in a surge tank, with respect to the reference input. The neural controller works on the normalized gradient-based approximator parameter update law used for a class of nonlinear discrete-time systems in direct cases. In our proposed design, the reduction in error is reached upon between the ideal and the actual controller and the direct adaptive control scheme is tested for performance via a simple surge tank example. The proposed controller algorithm performs well and can be physically implemented.

Keywords
Model predictive control, Direct neural control, Non linear systems.

1. INTRODUCTION
The present industrial scenario emphasizes on automated control to increase the productivity and improving the quality of products. In the case of process industries, more advanced and complex control systems needs to be implemented to fulfill the present needs. The non-linear process dynamics is a major area of research in the recent years. The neural approach to computation has emerged as the solution to tackle problems for which more conventional computational approaches have proven ineffective [1]-[4]. Model predictive control (MPC) techniques have been recognized as an efficient approach to improve operating efficiency and profitability. It has become an accepted standard for complex control problems in the process industries. It can be used for the control of non-linear systems if they are working around a reference set-point.

However, if the set point is moved away from the nominal work point, the controller is less effective, or even detrimental to the system operation. One solution to this kind of control problem is to develop a non-linear model predictive control strategy. The neural networks have been shown to have good approximation capability for non-linear systems [5].

The aim of controller design is to construct a controller that generates control signals which in turn generate the desired plant output subject to given constraints. Predictive control tries to predict, the plant output for a given control signal. This tells in advance, the effect of control, and by this knowledge the best possible control signal is chosen. Various model structures have been reported in the literature for identification of the non-linear systems. Neural network model has received much attention in the field of chemical process control as it possesses powerful function approximation properties that make them useful for representing nonlinear models or controllers [6, 7].

A large number of predictive control schemes have been developed based on various neural networks like Multi Layer Perceptron (MLP) or Radial Basis Functions (RBF). The major requirement for the successful application of non-linear MPC based on a neural network model is an accurate nonlinear model and an efficient optimization algorithm. A Multi Layer Perceptron commonly uses the back propagation learning algorithm, which is essentially a non-linear steepest descent algorithm [8]. An MLP approach for designing of NNMPC controller is presented in [9].The fuzzy systems can also be used as approximators to approximate the controller in the direct case. One good candidate of fuzzy systems is the Takagi–Sugeno fuzzy system (TSFS), which has shown to be successful in many applications [10].

In this paper, a control method based on prediction is developed for a nonlinear system of surge tank. Neural network model based on Radial basis function has been used to predict future plant behavior over a specified time horizon. The minimization routine of the control relevant cost function is based on the normalized gradient algorithm.

2. PREDICTIVE NEURAL CONTROL
Model Predictive Control (MPC), shown in Figure 1, optimizes the plant response over a specified time horizon [11]. This architecture requires a neural network plant model, a neural network controller, a performance function to evaluate system responses, and an optimization procedure to select the best control input. The optimization procedure can be computationally expensive. It requires a multi-step ahead calculation, in which the neural network model is used to predict the plant response. The neural network controller learns to produce the input selected by the optimization process. When training is complete, the optimization step can be completely replaced by the neural network controller. Here, the neural network controller is basically a Radial Basis Function neural network.

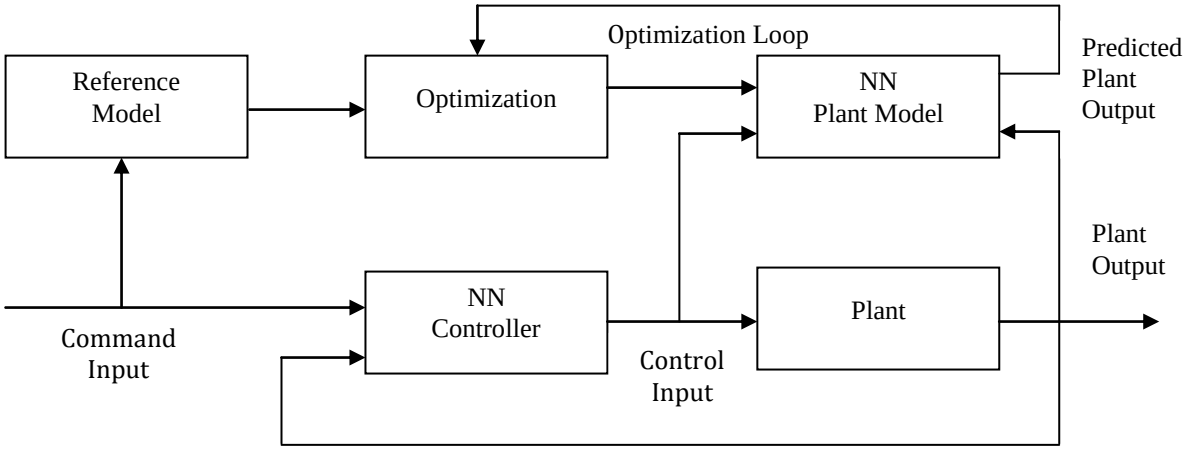

Fig 1: Generalized model predictive control structure

2.1 Radial Basis Function Networks

Radial Basis Function Networks (RBFN) consists of 3 layers, an input layer, a hidden layer and an output layer. The hidden units provide a set of functions that constitute an arbitrary basis for the input patterns. hidden units are known as radial centers. The transformation from input space to hidden unit space is nonlinear whereas transformation from hidden unit space to output space is linear. The radial basis functions in the hidden layer produce a significant non-zero response only when the input falls within a small localized region of the input space. Each hidden unit has its own receptive field in input space. An input vector which lies in the receptive field center, would activate the center and by proper choice of weights the target output is obtained. We are using the Gradient Descent Learning (On line) technique to update the weights and centers of the RBFN and the activation function is Gaussian in nature.

3. ADAPTIVE CONTROL

In this section, a description of the system considered for control is presented, along with its direct control law. Here, we consider the SISO discrete-time system described by [12]:

$$y(k+1) = f_0(x(k)) + g_0(x(k))u(k-d-1) \quad (1)$$

where $f_0(\cdot)$ and $g_0(\cdot)$ are unknown smooth functions, $x(k)$ is a vector of past inputs and outputs $[y(k-n+1),....., y(k), u(k-m-d+1),...., u(k-d)]^T$, where $m \le n$, y is the output, u is the input, and d is the time delay (relative degree) of the system. It is known that for the class of systems (2), there exists an ideal controller $(u^*(k))$ that drives the

output of the system to track a known reference trajectory after d steps. Such a controller is defined as

$$u^*(k) = \frac{-f_{d-1}(x(k)) + r(k)}{g_{d-1}(x(k))} \quad (2)$$

where it can be shown by recursive substitution as in [9] that $f_{d-1}(x(k)) = f_0(x(k+d-1))$ and $g_{d-1}(x(k)) = g_0(x(k+d-1))$. Here, we consider the same plant assumptions used in [9].

A direct adaptive controller that seeks to drive the system to track a known reference input $r(k)$ uses an approximator that attempts to approximate the ideal controller dynamics (u^*, that we assume to exist). Here, we assume that the ideal control can be approximated by

$$u(k) = A_u^T \zeta(x(k), r(k)) + u_k(k) \quad (3)$$

where $A_u(k)$ is an approximation of the ideal parameter vector A_u^*, $u_k(k)$ is the known part of the ideal control, and $\zeta(x,r)$ is the partial of the approximator output with respect to the parameter vector. The approximator parameter error is defined as $\phi(k) = A_u(k) - A_u^*$.

In the direct approach, let us consider the subclass of systems (2) which can be written as

$$y(k+d) = f_{d-1}(x(k)) + g_{d-1}(x(k))u(k)$$
$$= f_u(x(k)) + f_k(x(k)) + [g_u(x(k)) + g_k(x(k))]u(k) \quad (4)$$

where $f_k(\cdot)$ and $g_k(\cdot)$ are the known parts of the dynamics, and $f_u(\cdot)$ and $g_u(\cdot)$ are the unknown parts of the dynamics further, we can consider the case where $f_k \equiv g_k \equiv 0$.

Using the certainty equivalence approach, the control law is defined as

$$u(k) = \frac{-\hat{f}_{d-1}(x(k)) + r(k)}{\hat{g}_{d-1}(x(k))} \quad (5)$$

where $\hat{f}_{d-1}(x(k))$ and $\hat{g}_{d-1}(x(k))$ are estimates of $f_{d-1}(x(k))$ and $g_{d-1}(x(k))$, respectively. A projection algorithm may be used to ensure that $\hat{g}_{d-1}(x(k)) \ge \theta_0 > 0$ so that the control signal is well defined. The parameter errors for the direct adaptive neural controller is defined as $\phi_f(k) = A_f(k) - A_f^*$ and $\phi_g(k) = A_g(k) - A_g^*$.

The error equation for direct NNMPC case can be written as

$$e(k+1) = -\kappa\theta(x(k-d+1))\phi^T(k)\zeta(x()k-d+1) + \bar{\nu}(k) \quad (6)$$

where, $\theta(x(k)) = g_0(x(k+d-1))$ ($0 < \theta_0 \le \theta(x(k)) \le \theta_1$, and θ_0 and θ_1 are known constants related to the plant dynamics), in

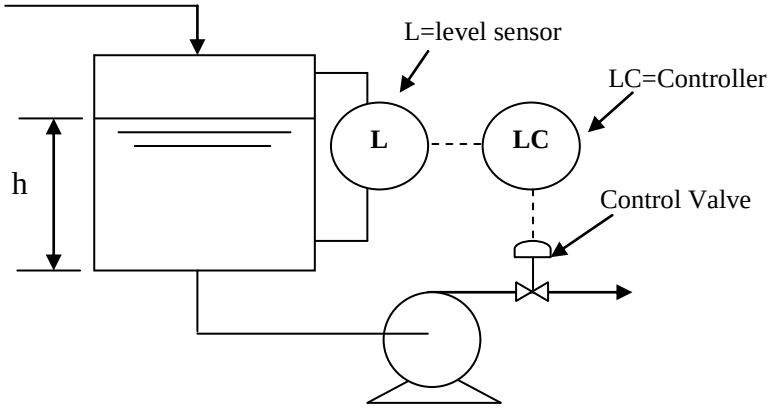

Fig 2: Diagram of surge tank system

the direct case $k=-1$. Also, $\bar{v}(k)$ is function of the approximation error. For simplicity, we will write (6) as

$$e(k+1) = -\kappa\theta(k-d+1)\phi^T(k)\zeta(k-d+1) + \bar{v}(k) \quad (7)$$

Here, the normalized gradient-based parameter update law that seeks to minimize the squared tracking error is used.

4. TANK DYNAMICS

Used to regulate fluid levels in systems, surge tanks act as standpipe or storage reservoirs that store and supply excess fluid. In a system that has experienced a surge of fluid, surge tanks can modify fluctuations in flow rate, composition, temperature, or pressure. Typically, these tanks (or "surge drums") are located downstream from closed aqueducts of feeders for water wheels. Depending upon its placement, a surge tank can reduce the pressure and volume of liquid, thereby reducing velocity. Therefore, a surge tank acts as a level and pressure control within the entire system.

To accurately model a surge tank, mass and energy balances need to be considered across the tank. From these balances, we will be able to develop relationships for various characteristics of the surge tank shown in Fig.2.

Consider the surge tank model that can be represented by the following differential equation [13]:

$$\frac{dh(t)}{dt} = \frac{-c\sqrt{2gh(t)}}{A_r(h(t))} + \frac{1}{A_r((h(t))}u(t) \quad (8)$$

Where $u(t)$ is the input flow (control input), which can be positive or negative. Also, $h(t)$ is the liquid level (output of the system); $A_r(h(t))$ is the cross-sectional area of the tank; $g = 9.8 m/\sec^2$ is the gravitational acceleration; and $c = 1$ is the known cross-sectional area of the output pipe. Let $A_r(h(t)) = \sqrt{ah(t)+b}$, where $a=1$ and $b=3$. Using Euler approximation to discretize the system, we have

$$h(k+1) = h(k) + T\left[\frac{-\sqrt{19.6h(k)}}{A_r(h(k))} + \frac{u(k)}{A_r(h(k))}\right] \quad (9)$$

Where $T=0.1$. Note that the system (9) belongs to the same class of systems (2), where $d=1$

$$f_0(x(k)) = h(k) - \frac{T\sqrt{19.6h(k)}}{A_r(h(k))} \quad (10)$$

and

$$g_0(x(k)) = \frac{T}{A_r(h(k))} \quad (11)$$

The system is tested for $h(k) > 0$ so that the response is realistic.

5. SIMULATION RESULTS

Testing of control quality of selected nonlinear system with RBFN based neural controller is realized in environment of MATLAB. For the purpose of testing, we used simulation models of nonlinear dynamic systems described by the differential equation. The nonlinear system has nonlinear transfer characteristic and dynamics of the system changes according to operating point. Initially, the surge tank shape parameters are characterized. The value of clogging factor representing dirty filter in pump is taken nominally as 1. Other parameters are, gravity=9.8, sampling rate=0.1, and lower and upper bounds on set point are taken as 0.25 and 0.5 respectively. The length of simulation is taken as 1000 samples. And a square wave is used as the reference input. Then the plant initial conditions are established, further the parameters of approximator are defined. The number of receptive field units taken in the RBF is 100. An optimization of no. of receptive units is reached upon by comparing the tracking error convergence rate and magnitude. It is been found that faster rate convergence with better steady state response is obtained in the designed neural controller, with 100 nos. of receptive field units.

Comparison of liquid level in the tank with the reference input w.r.t. time is plotted in Fig 3. In Fig 4 a comparison of tank input and ideal feedback linearizing input is shown for length of simulation taken as 100. Quality evaluation is done by plotting the norm of parameter error in Fig. 5 and by mapping of tracking error and dead-zone width in Fig.6. In Fig. 7 and 8 it has been revealed that the neural controller is causal and stable in nature and thus it is physically realizable.

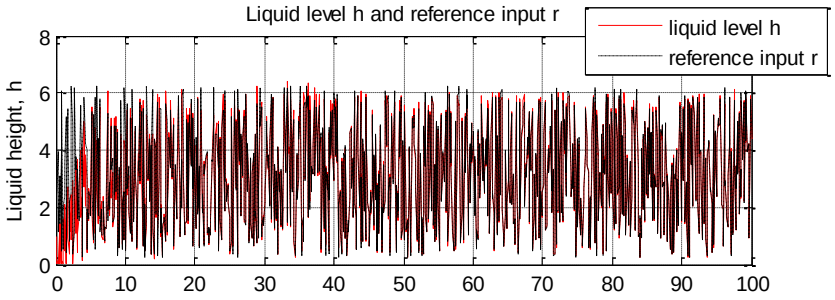

Fig 3: Comparison of liquid level in the tank and reference input w.r.t. time

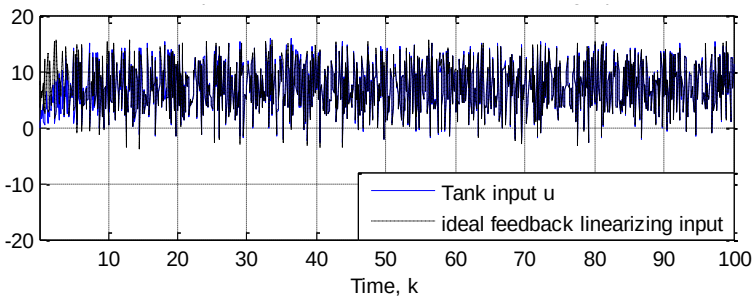

Fig 4: Comparison of tank input and ideal feedback linearizing input

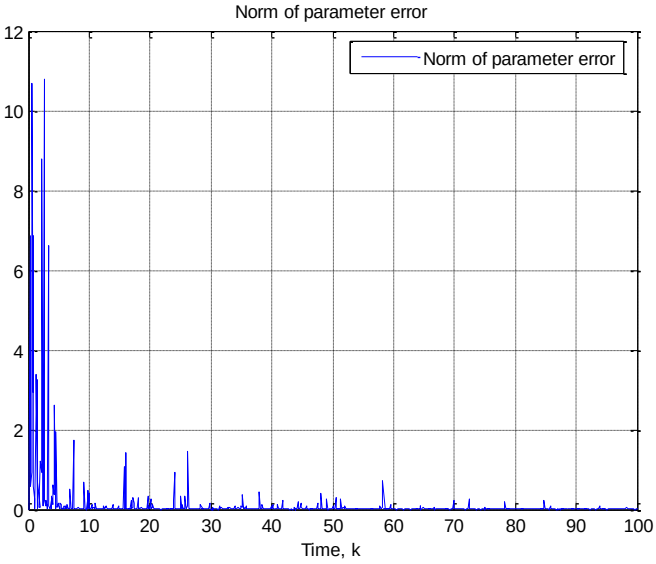

Fig 5: Norm of parameter error for proposed controller

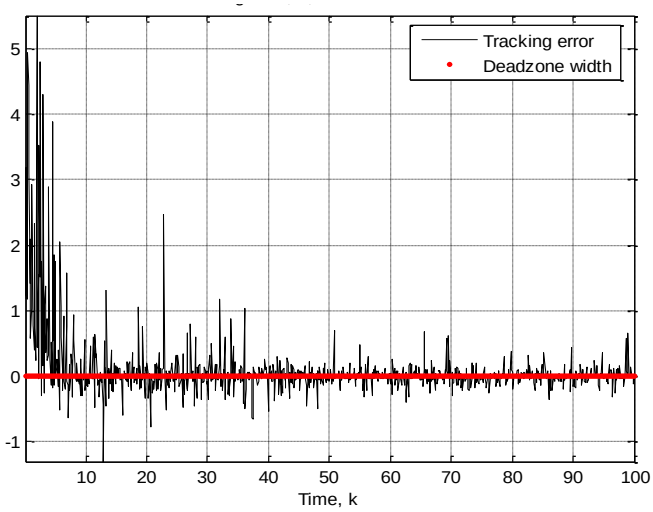

Fig 6: Mapping of tracking error and dead-zone width

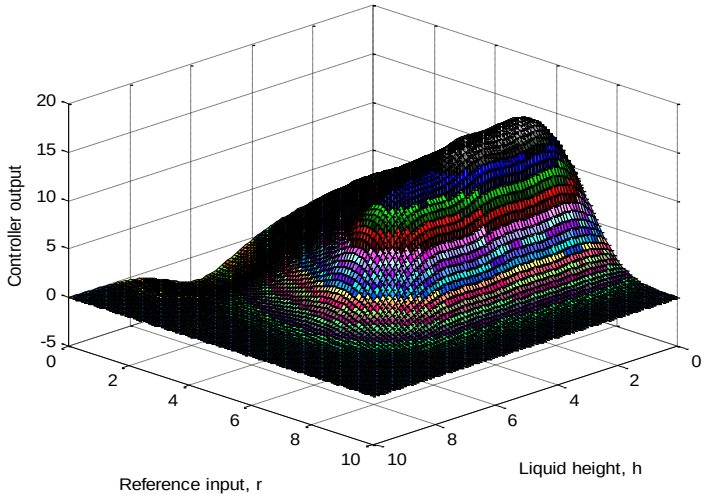

Fig 7: Direct neural controller mapping between inputs and output

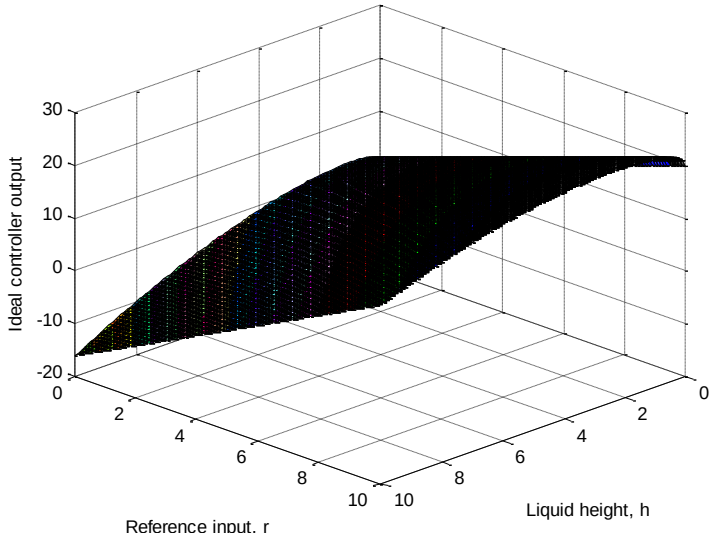

Fig 8: Ideal controller mapping between inputs and output

6. CONCLUSION

The main objective of this article is to control the non linear dynamics of surge tank via neural controller. In this paper the inclusion of dynamic neural models in predictive control for a benchmark nonlinear process, surge tank is presented. A Neural network approximator model was identified using Radial Basis Function(RBF), and validated on the data generated from simulation of surge tank dynamic equations. This model represents the dynamics of the nonlinear surge tank and is used as nonlinear predictor in the discussed predictive control technique, NNMPC. The control technique is tested on reference signals which exhibits, the possible nonlinear process dynamics occurring inside a real surge tank. On analysis of the response graphs it can be seen that the NNMPC strategy successfully tracks the random reference signal. The result obtained for the random reference signal illustrates and proves the tracking ability of controller. Also almost offset free and very close set point tracking is obtained using NNMPC strategy. This RBF based algorithm performs better than MLP as it has single hidden layer and is capable of fast learning.

7. REFERENCES

[1] Denker, J., 1986, AIP Con5 Proc. Neural Networks for Computing, American Institute of Physics, New York.

[2] J. Hopfield, "Neural Networks and Physical Systems with Emergent Collective Computational Abilities," Proc. Nut. Acad. Sci. U.S., 1982, 79, 2554-2558.

[3] Kohonen, T., 1984. Self Organization and Associative Memory. New York: Springer-Verlag.

[4] Rumelhart, D. and McClelland, J., 1986, Parallel Distributed Processing. Cambridge, MA: MIT Press.

[5] M. Morari, J.H. Lee, "Model Predictive Control: Past, Present and Future", Computers and Chemical Engineering, 1999, 23, 667-682.

[6] N. Bhat, T.J. McAvoy, "Use of Neural Network for Dynamic Modeling and Control of Chemical Process Systems", Computers and Chemical Engineering, 1990, 14, 573.

[7] A. Bjarne, T.A.J. Foss, V.S. Aage, "Nonlinear Predictive Control using Local Models-Applied to a Batch Fermentation Process", Control Engineering Practice, 1995, 3, 389.

[8] L.G. Lightbody, G.W. Irwin, "Neural Networks for Nonlinear Adaptive Control", in Proc. IFAC Symp. Algorithms Architectures Real-Time Control, Bangor, U.K. 1992, 1–13.

[9] P. Shrivastava, A.Trivedi "Control of Nonlinear Process using Neural Network Based Model Predictive Control" International Journal of Engineering Science and Technology (IJEST), 2011, 3, 2573-81.

[10] H.N. Nounou, K.M. Passino, "Stable Auto-Tuning of Adaptive Fuzzy/Neural Controllers for Nonlinear Discrete-Time Systems", IEEE Transactions on Fuzzy Systems, 2004, 12, 70-83.

[11] B. ZareNezhad, A. Aminian, "Application of the Neural Network-Based Model Predictive Controllers in Nonlinear Industrial Systems. Case Study", Journal of the University of Chemical Technology and Metallurgy, 2011, 46, 67-74.

[12] F.C. Chen, H. K. Khalil, "Adaptive Control of a Class of Nonlinear Discrete-Time Systems using Neural Networks", IEEE Trans. Automat. Contr., 1995, 40, 791–801.

[13] Passino, K.M., Yurkovich, S., 1998, Fuzzy Control. Menlo Park, CA: Addison-Wesley Longman.

Journal of Environmental Protection, **2012, 3, 533-537**
doi:10.4236/jep.2012.36064 Published Online June 2012 (http://www.SciRP.org/journal/jep)

Evaluation of Drinking Water Pollution and Health Effects in Baghdad, Iraq

Allaa M. Aenab, S. K. Singh

Civil & Environmental Engineering Department, Delhi Technological University (DTU), Delhi, India.
Email: allaaaenab@gmail.com

Received January 26th, 2012; revised February 21st, 2012; accepted March 20th, 2012

ABSTRACT

Contamination of water reserves by biological, chemical, and radiologic agents may affect the health of millions of residents in the Iraq as well as many others throughout the world. Fatal outbreaks of cholera struck several provinces of the country, including Baghdad. The United Nations Environment Programme (UNEP) also says air pollution, resulting from burning oil and aggravated by war, is cause for concern. The study area Baghdad has been divided into two parts: Central Baghdad and Outskirts of Baghdad (included in Baghdad but near the boundaries of Baghdad). The outskirts of Baghdad comprises of 4 cities: Al-Hussaniya located in northern part of Baghdad, Abu-Gurabe located in the western side of Baghdad, Jissr Diyala located in the eastern side of Baghdad and finally Al-Mahmodiya located in the southern side of Baghdad. These cities are in very poor situation in terms of water supply. The quality of water supplied is bad as no attention is given to WTP's in these places, which is also because of the fact that given the insecure war conditions, these areas are inaccessible. The sewage is thrown directly into the river because these areas do not have sewage treatment plants. In case of central Baghdad the water supply and sewerage network are broken in some places. Due to this there is mixing of water between the two networks. For this study we taking water supply samples and collect all the samples from WTPs and water supply network (houses, shops and different places). We made the analysis to parts first bacteriologies, second chlorine and after analysis these samples in lab we will give in our study numbers of fail samples, type of diseases and how many case during year 2007 in Baghdad City. Also in this study we will give Estimated Deaths from Water-Related Diseases 2010 to 2035.

Keywords: Drinking Water; Water Pollution; Water Supply; Drinking Water Network; Sewerage Network; WTP's; Wastewater; Iraq Environment and Water-Borne Diseases

1. Introduction

Country background. Iraq is rich in natural and human resources and was a middle-income country in the 1970s. But years of conflict, sanctions and wars have had a significantly negative effect on Iraq's economy with people suffering a severe decline in their standards of living. Although in the 1970s the health and educational institutions in Iraq were regarded as among the best in the Middle East, the current health and education indicators of Iraq are well below the regional average. An estimated 10 percent of the population has income of less than a dollar a day, and unemployment is estimated at 25 - 30 percent of the population. According to the United Nations, approximately 25 percent of the population is dependent on food rations. The agriculture sector has declined and is characterized by poor productivity and inefficient water use. Infrastructure in all sectors, including water and sanitation, is dilapidated and mostly dysfunctional. The current political and security environment remains unstable with negative impacts on basic services. Rebuilding the Iraqi economy and institutions remain a formidable challenge [1].

Environmental issues Iraq are also facing very serious environmental problems, including poor water quality, air pollution, waste management, contaminated sites and the deterioration of key ecosystems. With environmental problems neglected to a large extent prior to the war as well, the decades of war, conflicts and economic sanctions have further worsened the environmental conditions. The problems are aggravated by the country's weak environmental governance structure.

Before the Gulf War, Iraq's water supply system employed what was at the time up-to-date technology and functioned efficiently. However, with the imposition of economic sanctions, Iraq was unable to expand or update the system, resulting in extensive leaks throughout the network, and a steady decline in the volume and quality

of water supply. This, combined with the growth of urban populations, has affected everyday life, with some areas receiving almost no water. Waterborne infectious diseases, which had been eradicated prior to sanctions, also spread again due to the impossibility of importing chlorine disinfectants [2].

2. Objectives

- Current status of Iraq's environment and gather information on assistance initiatives in the environmental field being implemented.
- Evaluation of drinking water quality.
- Increased incidence of diseases will be attributable to degradation of normal preventive medicine, waste disposal and water purification/distribution.

3. Study Area

Iraq's quality of drinking water and water used for agriculture is poor, violating both Iraq National Standards and WHO guidelines. Leaking sewage pipes and septic tanks contaminate the drinking water network with wastewater [3].

- Only 17% of wastewater is treated before discharged into the environment [4].
- 80% of Iraqis do not treat their water before drinking [5].

Water-borne diseases are widespread due to polluted drinking water supplies. In the first six months of 2010, there were over 360,000 diarrhea cases as a result of polluted drinking water and a lack of hygiene awareness among local communities, particularly vulnerable groups such as women and children [6].

Iraqi Ministry of Environment in 2009 indicate that bacteriological contamination in the water supply varies between governorates, ranging from 2.5% up to 30%, with the current average of 16% greatly exceeding the Iraqi National Drinking Water Standards and WHO Guidelines for Drinking Water permissible limit of 5% [7].

- Every day at least 250,000 tonnes of raw sewage is pumped into the Tigris River threatening unprotected water sources and the entire water distribution system [8].
- Consumers directly and illegally puncture the main water supply lines with their individual and unhygienic leaky plastic hoses causing direct and continuous contamination [9].

During the hot summer months, the specter of widespread cholera outbreaks loomed over the country. Cholera is characterized by profuse diarrhea, which can lead to severe dehydration and death if left untreated. The World Health Organization (WHO) reported a total of 73 laboratory-confirmed cholera cases in Iraq from April 28 to June 4, 2010. 10 times more than WHO officials found during the same period last year [10].

4. Data Procurement

Samples were collected from central and outskirts of Baghdad for residual chlorine and bacteriology tests for the years 2007. The data of permissible quality of supplied water in ten cities, located in central Baghdad, also available. The health data containing the number of cases of various diseases for all the months of the year 2007 in Rusafa and Karakh districts this data showing us number and type of water born diseases in Baghdad.

5. Results

Table 1 present the design capacities, actual production and the capacity utilization in respect of different water treatment plants. It may be observed that other than 2 plants viz. Al Qarama and Sharaq Dijla, all other plants are operating at much lesser capacities, which need to be augmented for better performance.

Water samples were collected from central and outskirts of Baghdad and were made to undergo chlorine

Table 1. Capacity of WTP's in centre Baghdad.

NO.	Name of Project	Design Capacities	Actual Production	Capacity Utilization (%)	Year of establishment project	The network situated
1	Al-Qadisya	135,000 m^3/day	115,000 m^3/day	85%	1965 & 1970	Good
2	Sharaq Dijla	544,000 m^3/day	544,000 m^3/day	100%	1978	Good
3	Al-Karama	182,000 m^3/day	182,000 m^3/day	100%	1953, 1962 & 1984	Good
4	Al-Wathba	80,000 m^3/day	62,000 m^3/day	77%	1932 & 1976	Medium
5	Al-Wahda	70,000 m^3/day	50,000 m^3/day	71%	1942 & 1959	Good
6	Al-Dura	112,500 m^3/day	100,000 m^3/day	89%	1979	Good
7	Al-Za'afaranya	12,000 m^3/day	6000 m^3/day	50%	1980	Under the maintenance
8	Al-Rasheed	100,800 m^3/day	50,400 m^3/day	50%	1963	Bad
9	Al-Rashdya	68,000 m^3/day	60,000 m^3/day	88%	1993	Good
10	Al-Karkh	1365 million·l/day	1.1 M m^3/day	80%	1985	Very good

and bacteriology tests. The test results indicated that the water quality in the cities located in the outskirts of Baghdad is in a very erratic state. This is due to the insecure war conditions that make these areas inaccessible. Also the absence of wastewater treatment plants in these areas made the conditions worse as the waste is directly thrown in the river. The chlorine and bacteriology test results are shown in **Figures 1** and **2** respectively.

Table 2 and **Table 3** show that more number of water borne diseases cases was reported in Rusafa district as compared to the Karkh district. This is due to more pollution in water networks in the Rusafa area.

6. Estimate: Simple Proportional Projection

The simplest estimate of future deaths from water-related diseases comes from assuming that the proportion of deaths to total population experienced today will be maintained in the future. As total population grows, total water-related deaths will grow annually. This can be seen in Equation (1), which applies a simple proportional assessment of water-related deaths to official median estimates of future population growth to 2035.

Equation (1): Deaths from Water-Related Diseases 2010 to 2035:

Simple Proportional Assessment [11].

$$TD1 = \sum_{t=2010 \text{ to } 2035} (D/P)_{2010} (Pt)$$

where

TD1 = Total water-related deaths, 2010 to 2035.

$\sum_{t=2010 \text{ to } 2035}$ = Sum over the period 2010 to 2035.

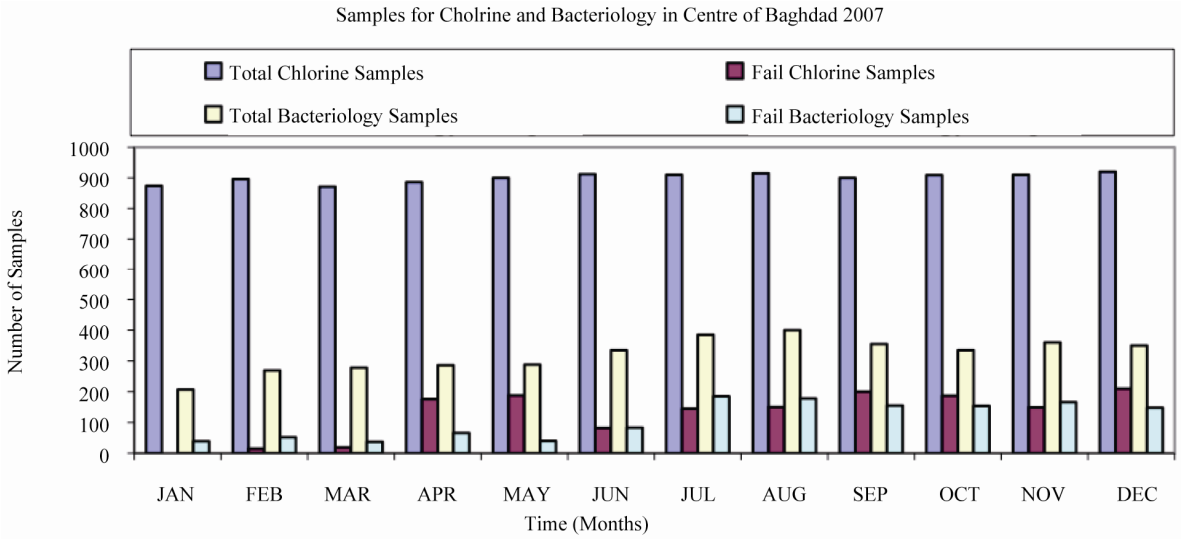

Figure 1. Samples for cholrine and bacteriology in centre of Baghdad 2007.

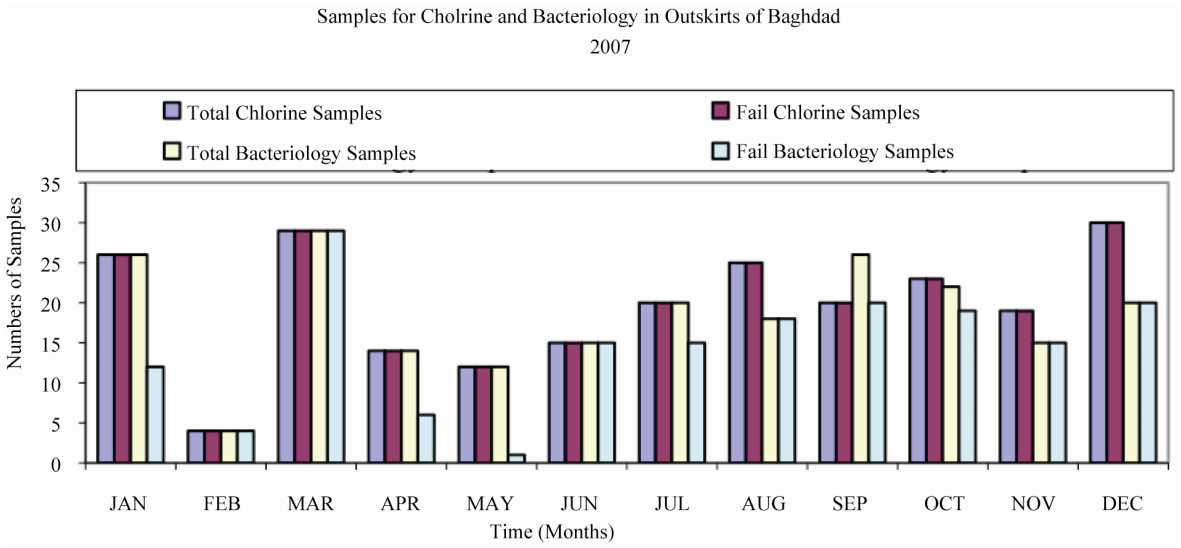

Figure 2. Samples for chlorine and bacteriology in outskirts of Baghdad 2007.

Table 2. Number of cases of mentioned diseases in Rusafa district in 2007

Month	AFP	Diphtheria	Pertussis	Measles	Rubella	Mumps	Chickenpox	Typhoid fever	Pneumonia	C. Leishmaiasis
JAN	1	0	4	3	0	12	94	29	318	3
FEB	5	0	17	1	0	5	85	65	339	4
MAR	7	0	31	5	0	11	157	126	465	4
APR	0	2	2	18	2	22	491	218	433	2
MAY	10	1	47	27	0	25	643	533	249	1
JUN	9	0	30	20	1	20	505	650	305	6
JUL	15	3	44	15	3	31	187	703	311	4
AUG	8	1	21	12	0	18	490	567	267	3
SEP	5	0	50	26	2	21	531	439	219	2
OCT	10	2	48	30	1	16	265	287	321	5
NOV	7	1	20	24	5	29	231	176	298	1
DEC	9	3	33	19	2	31	101	30	276	2

Table 3. Number of cases of mentioned diseases in Karkh district in 2007.

Month	AFP	Diphtheria	Pertussis	Measles	Rubella	Mumps	Chickenpox	Typhoid fever	Pneumonia	C. Leishmaiasis
JAN	0	9	4	0	0	5	35	20	220	6
FEB	2	0	5	1	0	1	41	85	243	4
MAR	1	0	7	0	0	5	44	45	236	2
APR	2	0	0	2	0	4	125	134	187	3
MAY	2	0	13	3	1	14	202	214	235	8
JUN	3	1	9	5	4	16	305	365	287	6
JUL	1	4	15	3	0	13	298	458	293	9
AUG	0	3	12	2	3	9	311	443	219	5
SEP	3	2	11	5	0	15	295	397	232	10
OCT	1	3	8	1	1	10	98	203	197	6
NOV	2	1	10	3	2	11	55	165	205	9
DEC	2	2	6	2	1	6	49	30	201	7

$(D/P)_{2010}$ = Water-related deaths in 2010/Population in 2010.

Pt = Population in a given year.

Given: D = 36000/year [12].

P_{2010} = 27,000,000 [13].

Growth Rate = 2.5% [13].

P_{2035} = 50,056,491.

7. Conclusions

The study area Baghdad has been divided into two parts: Central Baghdad and Outskirts of Baghdad (included in Baghdad but near the boundaries of Baghdad).

- The outskirts of Baghdad comprising of 4 cities: Al-Hussaniya, Abu-Gurabe, Jissr Diyala and Al-Mahmodiya were found in poor condition in terms of water supply and sewerage due to inaccessibility, lack of proper attention and insecure war conditions. In central Baghdad the water treatment plants are satisfying the standard conditions but the water supply network is in a poor condition.
- Efforts are needed from the concerned authorities for renovation of water treatment plants and network in inaccessible and war prone areas. The endeavors of the local people of Iraq are required in keeping their environment clean. Thus the people should be made aware about the dire consequences of negligence towards these issues.
- Around 100 infants die every day, many from water-borne diseases, with around 36,000 infants dying before they celebrate their first birthday.
- 1 child out of every 20 in Iraq dies before reaching their 5th birthday.
- At the present child mortality rate, around 1,300,000 Iraqi children will die, many from water-borne diseases, by 2035.
- Around 1,300,000 Iraqi children's lives will be saved

if Iraq succeeds in attaining the MDG target of reducing the current 41 deaths for every 1000 live births to 21 deaths for every 1000 live births by 2035. This will be much more likely to be achieved by improving the quality of drinking water as well as with the population adopting better hygiene practices.

REFERENCES

[1] World Bank, "Iraq Household Socio-Economic Survey," IHSES-2007 Tabulation Report.

[2] Wikipedia Foundation Inc., "Text is Available under the Creative Commons Attribution-Share Alike License," 2011.

[3] CCA, "Common Country Assessment IRAQ," 2009. http://www.iauiraq.org/reports/CCA_Final.pdf

[4] Geopolicity, "Iraq Water and Sanitation Scoping Study," 2010. http://www.geopolicity.com

[5] UNDAF, "An overview of the United Nations Development Assistance Framework Iraq," 2010. http://www.iauiraq.org/reports/UNDAF%20Booklet-English-WEB.pdf

[6] WHO, "World Health Organization Position Papers," 2010.

[7] UNAMI, "United Nations Assistance Mission for Iraq United Nations Country Team in Iraq Water Resource Management White Paper," 2010.

[8] UNICEF, "Iraq Wastes 50% of Water," 2011. http://www.google.com/hostednews/afp/article/ALeqM5ik87fAUtGSxTXLz5SszEVpX-CNIg?docId=CNG.261b2d3c66888006d3d84c66c4b96323.851

[9] UNICEF, "World Water Day 2011," 2011. http://iq.one.un.org/documents/155/UNICEF%20media%20advisory%20and%20facts.pdf

[10] Free Drinking Water News, 2010. http://www.freedrinkingwater.com/water_quality/quality1/1-dirty-water-or-bombs-dangerous.htm

[11] P. H. Gleick, "Dirty Water: Estimated Deaths from Water-Related Diseases 2000-2020," Pacific Institute for Studies in Development, Environment, and Security, 2002. http://www.pacinst.org

[12] UNICEF, "Iraq's Children 2007," 2007. http://www.unicef.org/infobycountry/files/Iraqs_Children_2007.pdf

[13] World Bank, "A Human Rights Report on Trafficking in Persons, Especially Women and Children," 2011.

Extensions and Analysis of Local Non-Linear Techniques

Rashmi Gupta
Ambedkar Institute of Advanced Communication Technologies and Research affiliated to Guru Gobind Singh Indraprastha University, Delhi, India

Rajiv Kapoor
Delhi Technological University, Bawana Road, (Formerly Delhi College of Engineering), Delhi, India

ABSTRACT
The techniques Conformal Eigenmap and Neighborhood Preserving Embedding (NPE) have been proposed as extensions of local non-linear techniques. Many of the commonly used non-linear dimensionality reduction, such as Local Linear Embedding (LLE) and Laplacian eigenmap are not explicitly designed to preserve local features such as distances or angles. In first proposed Conformal Eigenmap technique, a low dimensional embedding is constructed that maximally preserves angles between nearby data points. The embedding is derived from the bottom eigenvectors of LLE by solving an additional problem in Semidefinite Programming (SDP). In second proposed method, NPE minimizes the cost function of a local nonlinear technique for dimensionality reduction under the constraint that the mapping from the high-dimensional to the low-dimensional data representation is linear. The idea is to modify the LLE by introducing a linear transform matrix. The effectiveness of the proposed methods is demonstrated on synthetic datasets. Experimental results on several data sets demonstrate the merits of proposed techniques.

Keywords
Dimension reduction; Manifold Learning; Conformal Eigenmap; Neighborhood Preserving Embedding; Local Linear Embedding; Laplacian Eigenmap

1. INTRODUCTION
Dimensionality reduction is important in many domains, since it mitigates the curse of dimensionality and other undesired properties of high-dimensional spaces [1-2]. As a result, dimensionality reduction facilitates, among others, classification, visualization, and compression of high-dimensional data. Traditionally, dimensionality reduction was performed using linear techniques such as Principal Components Analysis (PCA), Linear Discriminant Analysis (LDA) and Multidimensional scaling (MDS). These techniques generate faithful low dimensional representations when the high dimensional input patterns are mainly confined to a low dimensional subspace. PCA, the most frequently used dimension reduction method seeks a projection that best represent the data in a least-squares sense [3]. MDS finds an embedding that preserves the interpoint distances, equivalent to PCA when those distances are Euclidean [4]. LDA, a supervised learning algorithm selects a transform matrix in such a way that the ratio of the between-class scatter and the within-class scatter is maximized [3]. If the input patterns are distributed more or less throughout this subspace, the Eigen value spectra from these methods also reveal the data set's intrinsic dimensionality. A more interesting case arises, however, when the input patterns lie on or near a low dimensional sub manifold of the input space. In this case, the structure of the data set may be highly non-linear, and linear methods are bound to fail.

In the last decade, a large number of non-linear techniques for dimensionality reduction have been proposed [5-10]. Recently, several manifold-embedding-based nonlinear approaches were developed such as locally linear embedding (LLE) [11], isometric feature mapping (Isomap) [12] and Laplacian Eigenmap (LEM) [13]. They all utilized local neighborhood relation to learn the global structure of nonlinear manifolds. But they have quite different motivations and objective functions. In contrast to the traditional linear techniques, the non-linear techniques have the ability to deal with complex non-linear data. On the other hand, such approaches also has several limitations: (i) the solutions do not yield an estimate of the underlying manifold's dimensionality; (ii) the geometric properties preserved by these embedding are difficult to characterize; (iii) the resulting embeddings sometimes exhibit an unpredictable dependence on data sampling rates and boundary conditions. Moreover, the original LLE, Isomap and Laplacian Eigenmap cannot deal with the out-of-sample problem [14] directly. Out-of-sample problem states that only the low dimensional embedding map of training samples can be computed but the samples out of the training set (i.e. testing samples) cannot be calculated at all.

An extension of Isomap was proposed to learn conformal transformations [15]; like Isomap, however, it relies on the estimation of geodesic distances, which can lead to spurious results when the underlying manifold is not isomorphic to a convex region of Euclidean space [16]. Hessian LLE is a variant of LLE that learns isometrics, or distance-preserving embeddings, with theoretical guarantees of asymptotic convergence [17].

In this paper, an extended analysis has been provided to remedy the key deficiencies of LLE and Laplacian Eigenmap. It is shown how to construct a more robust, angle-preserving embedding from the spectral decompositions of these algorithms as well as linear approximations to local non-linear techniques.

The rest of this paper is organized as follows: Section 2 described the proposed methods, Conformal Eigenmap and NPE. Experimental results are shown in Section 3. Finally, conclusions are drawn in Section 4.

2. EXTENSIONS OF LOCAL NON-LINEAR TECHNIQUES

The capability of local non-linear techniques to successfully identify complex data manifolds has led to the proposal of its several extensions. The original LLE, Isomap and Laplacian Eigenmap cannot deal with out of sample problem and cannot preserve local feature such as angle. To overcome the limitations of existing methods, extensions of local non-linear techniques have been discussed in this section. The difference between these methods lies in their different motivations and objective functions.

2.1 Conformal Eigenmap

A conformal mapping is a transformation that preserves the angles between neighboring datapoints when reducing the dimensionality of the data [18]. Conformal Eigenmap are based on the observation that local non-linear techniques for dimensionality reduction do not employ information on the geometry of the data manifold that is contained in discarded eigenvectors that correspond to relatively small Eigen values. Conformal Eigenmap initially perform LLE (or alternatively, another local nonlinear technique for dimensionality reduction) to reduce the high-dimensional data *D* to a dataset of dimensionality *m*. Conformal Eigenmap use the resulting intermediate solution in order to construct a *d*-dimensional embedding (where $d < m < D$) that is maximally angle-preserving.

A conformal map is a low-dimensional embedding where the angles formed by three neighboring points in the original high dimensional dataset are equal to the angles between those same three points in the embedding. Consider the point x_i and its neighbors x_j and x_k in *d*-dimensional space. Also, consider z_i, z_k and z_j to be the images of those points in the final embedding. If the transformation were a conformal map then the triangle formed by the x points would have to be similar to that formed by the *z* points. In the triangle formed by the *x* points the expression $|x_j - x_k|$ represents the length of one side of the triangle while the expression $|z_j - z_k|$ represents the corresponding side in the embedding. Since the triangles are similar there must exist $\sqrt{s_i}$ such that:

$$\sqrt{s_i} = \frac{|x_j - x_k|}{|z_j - z_k|} = \frac{|x_i - x_k|}{|z_i - z_k|} = \frac{|x_i - x_j|}{|z_i - zj|} \quad (1)$$

$$s_i = \frac{|x_j - x_k|^2}{|z_j - z_k|^2} = \frac{|x_i - x_k|^2}{|z_i - z_k|^2} = \frac{|x_i - x_j|^2}{|z_i - zj|^2} \quad (2)$$

It is usually not possible to find a perfect embedding where all of the triangles are exactly similar to each other. Therefore, the goal is to find a set of *z* coordinates such that the triangles are as similar as possible. This leads to the following minimization:

$$\min_{z,s_i} \sum_{j,k} \left(|z_j - z_k|^2 - s_i |x_j - x_k|^2 \right)^2 \quad (3)$$

Where the x_i represent the initial points and the z_i denote the points in the final embedding. Let y_i represent the points in the embedding produced by LLE (or LEM). The y_i points represent an intermediate step in the algorithm and so go part of the way to solving for z_i. Once LLE has produced, goal of the algorithm becomes a search for a transformation matrix L such that $z = Ly_i$ where the z_i value satisfy the minimization in Eq. (4)

$$\min_{L,s_i} \sum_{j,k} \left(|Ly_i - Ly_k|^2 - s_i |x_j - x_k|^2 \right)^2 \quad (4)$$

This should be done for all points x_i and with the condition that the points x_j and x_k are the neighbors of x_i.

$$\min_{L,s_i} \sum_{i} \sum_{j,k} \eta_{ij}\eta_{ik} \left(|Ly_i - Ly_k|^2 - s_i |x_j - x_k|^2 \right)^2 \quad (5)$$

Where η is an indicator variable and $\eta_{ij} = 1$ only if x_j is neighbor of x_i otherwise $\eta_{ij} = 0$ .The value for s_i can be calculated via least squares and the initial minimization (5) can be rewritten as:

$$\begin{aligned} &Minimize \quad t \\ &s.t. \quad P \succeq 0, \\ &\quad trace(P) = 1, \\ &\quad \begin{pmatrix} 1 & RVec(P) \\ RVec(P)^T & t \end{pmatrix} \succeq 0, \end{aligned} \quad (6)$$

Where $P = L^T L$, *t* is an unknown scalar, *I* and *R* are $m^2 \times m^2$ matrices: *I* denote the identity matrix, while *R* depends on $\{x_i, y_i\}_{i=1}^{n}$, but is independent of optimization variables *P* and *t*. The condition $trace(P) = 1$ is added to avoid the trivial solution where *P=0*. The optimization is an instance of SDP over elements of unknown matrix P [19]. After solving the SDP, the matrix can be decomposed back into $L^T L$ and the final embedding can be found by $z = Ly_i$ for all *i*. Conformal Eigenmap introduced the interesting idea of using spectral methods like LLE and LEM to find the low dimensional manifold and further modifying the output to produce a conformal map. The effectiveness of conformal map is limited by the computational complexity of SDP solvers.

Another extension of local non-linear dimension reduction technique is discussed in the section that follows.

2.2 Neighborhood Preserving Embedding

Neighborhood Preserving Embedding (NPE) is the linear approximation to local non-linear technique [20]. In contrast to traditional linear techniques such as PCA, local non-linear techniques for dimensionality reduction are capable of successful identification of complex data manifolds such as Swiss roll. This capability is due to the cost functions that are minimized by local non-linear dimensionality reduction techniques, which aim at preserving local properties of the data manifold. However, in many learning settings, the use of a linear technique for dimensionality reduction is desired, e.g., when an accurate and fast out-of-sample extension is necessary, when data has to be transformed back into its original space, or when one wants to visualize the transformation that was constructed by the dimensionality reduction technique. NPE is a technique that aims at combining the benefits of linear techniques and local non-

linear techniques for dimensionality reduction by finding a linear mapping that minimizes the cost function of LLE [11]. NPE minimizes the cost function of a local non-linear technique for dimensionality reduction under the constraint that the mapping from the high-dimensional to the low-dimensional data representation is linear.

Similar to LLE, NPE starts with the construction of a nearest neighbor graph in which every datapoint is connected to its nearest neighbors. The weights of the edges in the graph are computed and subsequently solves the generalized eigen problem.

Given a set of points $X = \{X_1, X_2, ...X_N\}$, in R^D, NPE attempts to seek an optimal transformation matrix *P* to map high-dimensional data *X* onto a low-dimensional data $Y = \{Y_1, Y_2, ...Y_N\}$, in R^d *(d << D)* in which the local neighborhood structure of *X* can be preserved, namely, $Y = P^T X$.

NPE algorithm can be stated in three steps.

Step 1: Compute the neighbors of each data point $\mathbf{X_i}$. There are two ways to compute neighbors:

- K nearest neighbors (KNN): Put a directed edge from node i to j if $\mathbf{X_j}$ is among the K nearest neighbors of $\mathbf{X_i}$.
- ε neighborhood: Put an edge between nodes *i* and *j* if $\left\| \boldsymbol{x_i} - \boldsymbol{x_j} \right\| \leq \varepsilon$

The graph constructed by the first method is a directed graph, while the one constructed by the second method is an undirected graph. In many real world applications, it is difficult to choose a good ε . In this work, the KNN method is adopted to construct the adjacency graph. When computational complexity is a major concern, one may switch to ε neighborhood.

Step 2: Compute the weights W_{ij} that best reconstruct each data point from its neighbors. In this step, the weights on the edges are computed. Let W denote the weight matrix with W_{ij} having the weight of the edge from node *i* to node *j*, and 0 if there is no such edge. The weights on the edges can be computed by minimizing the following objective function,

$$\min \sum_i \left\| \mathbf{X_i} - \sum_j W_{ij} \mathbf{X_{ij}} \right\|^2 \qquad (7)$$

Where $\sum_j W_{ij} = 1, \quad j = 1, 2, ..., m$, is enforced to make sure that the reconstruction weight matrix W is invariant to translation of the data point.

Step 3: Computing the projections Y_i of each data points X_i in space $\mathbf{R}^D$ can be reconstructed by W, then the corresponding point by Y_i in space $\mathbf{R}^d$ can be reconstructed by *W* also. Therefore, the mapping transformation matrix *P* can be obtained by solving the following minimization problem:

$$\boldsymbol{P}_{opt} = \arg\min_P \left[\sum_i \left\| \mathbf{Y_i} - \sum_{j=1}^{k} W_{ij} \mathbf{Y_j} \right\|^2 \right] \qquad (8)$$

$$\arg\min_A tr\left(\boldsymbol{P}^T \boldsymbol{XMX}^T \boldsymbol{P} \right)$$

$$\textbf{\textit{s.t.}}\ \boldsymbol{P}^T \boldsymbol{XMX}^T \boldsymbol{P} = 1, M = (I - W)^T (I - W)$$

Where *I* represent the *n x n* identity matrix. Using Lagrange multiplier, the minimization problem of equation (8) becomes a generalized eigenvalue problem:

$$\boldsymbol{XMX}^T \boldsymbol{P} = \lambda \boldsymbol{XX}^T \boldsymbol{P} \qquad (9)$$

Then, the column vectors of the transformation matrix $\boldsymbol{P}$ are given by the bottom d eigenvectors of (9), which are ordered according to their eigenvalues $\lambda_0 \leq \lambda_1 \leq ... \leq \lambda_{d-1}$. Therefore, and the projection can be obtained through the formula $Y = P^T X$.

3. RESULTS

In this section, some results of proposed algorithms are presented for a number of synthetic datasets. The datasets are specifically selected to investigate how the dimensionality reduction techniques deal with data that lies on a low-dimensional manifold.

The synthetic datasets on which the algorithms are implemented are the swissroll dataset, the helix dataset and twinpeaks dataset. Figure 1 shows plots of the three artificial datasets. All artificial datasets consist of 5,000 samples. The experiments are run for parameter k (nearest neighbors of data point) ranges from 5 to 15.

Figures 2-4 show the results of Conformal Map and NPE dimension reduction techniques on Swiss roll, helix and twinpeaks dataset respectively. From the results, it is clear that the angle preserving embedding more faithfully preserves the shape of the underlying manifold's boundary. The maximally angle preserving embedding exploits structure in the few bottom eigenvectors of LLE, not just in the bottom two eigenvectors. The semidefinite programming (SDP) in Eq. (6) mixes all of the bottom eigenvectors from LLE or Laplacian Eigenmap to obtain the maximally angle-preserving embedding.

Conformal transformations cast a new light on older algorithms, such as LLE and Laplacian Eigenmap. Viewing these bottom eigenvectors as a partial basis for functions on the data set, it is shown how to compute a maximally angle-preserving embedding by solving an additional problem in SDP. At little extra computational cost, Conformal Eigenmap significantly extends the utility of LLE and Laplacian Eigenmap, yielding more faithful embeddings as well as a global estimate of the data's intrinsic dimensionality.

The proposed NPE is able to search a direction projected onto which neighborhood relations are preserved along the curve of the manifold. From Fig. 2(c), Fig. 3(c) and Fig.4(c), it is

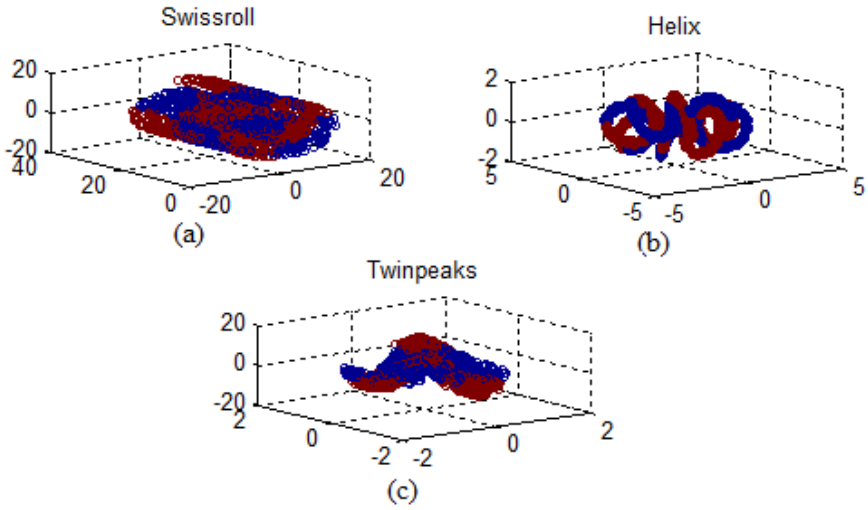

Fig 1: Four artificial datasets (a) Swissroll (b) Helix (c) Twinpeaks

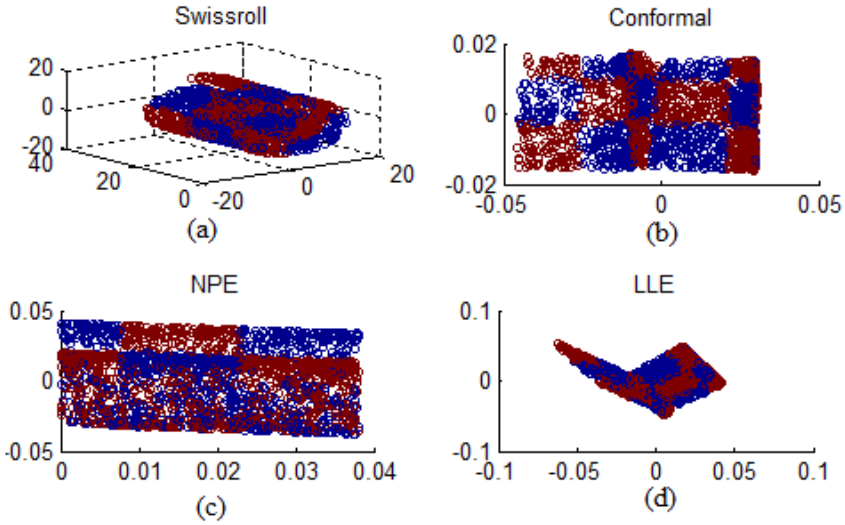

Fig 2: Results of dimensionality reduction on Swiss roll dataset (a) Swiss roll (b) Conformal (c) NPE (d) LLE

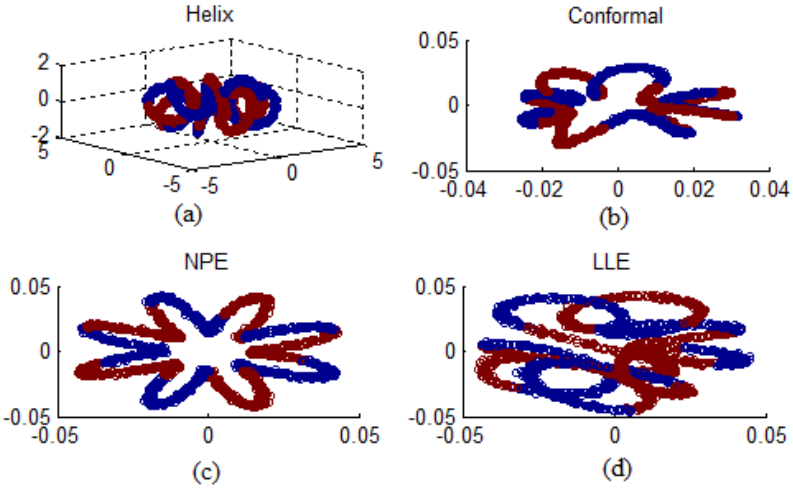

Fig. 3: Results of dimensionality reduction on Helix dataset (a) Helix (b) Conformal (c) NPE (d) LLE

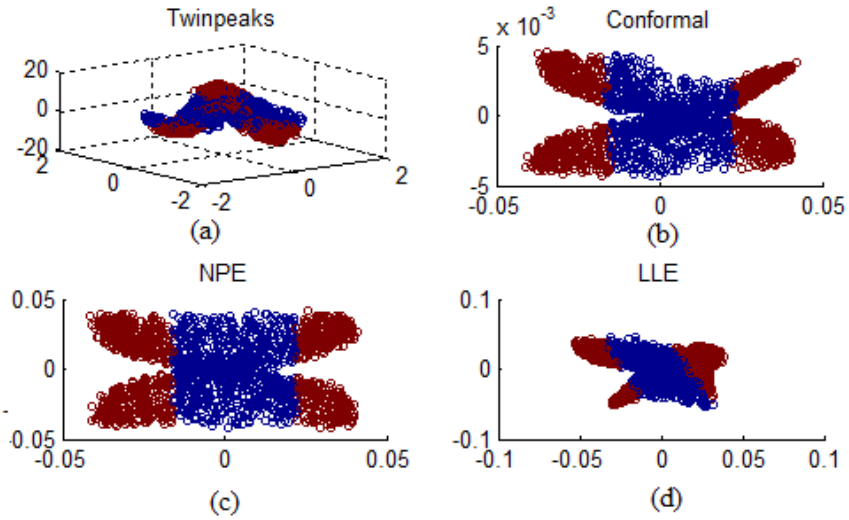

Fig. 4: Results of dimensionality reduction on Twinpeaks dataset (a) Twinpeaks (b) Conformal (c) NPE (d) LLE

	LLE	Conformal	NPE
Speed	Fast	Slow	Very Fast
Handle Curvature	Maybe	Yes	No
Handles noise	No	Yes	No
Preserves angles	No	Yes	No

observed that NPE cannot always unfold the manifold as LLE can. Furthermore, many neighbors are collapsed into a single point in the low dimensional space. The reason is that NPE is a linear transform instead of non-linear one like LLE. Nevertheless, the NPE has favorable properties against other linear transform methods such as PCA. The techniques are compared based on various parameters such as speed, noise, non-convexity, curvature, non-uniform sampling. First, it is observed for manifold geometry swissrollLLE is pretty slow, LLE and Laplacian can't handle this data. Twin Peaks: fold up the corners of a plane. LLE will have trouble because it introduces curvature to plane. LLE distort the mapping the most. Add noise to the Helix sampling. LLE cannot recover the circle. When the sampling rate is changed along the torus, Laplacian starts to mess up and Hessian is completely thrown off. Hessian LLE code crashed frequently on this example.

4. CONCLUSIONS

Conformal Map and NPE build on LLE and Laplacian Eigenmap, thus inheriting their strengths as well as their weaknesses. Results show that the Conformal Map algorithm has the potential to preserve the angles from their high dimensional data. NPE, due to linear in nature, might not outperform as good as non-linear LLE, Isomap and Laplacian Eigenmap. However, it is a novel and useful linear dimension reduction method. However the effectiveness of conformal mapping is limited by the computational complexity of SDP solver. In future work, the algorithm can be developed that does not require SDP solution so that it can be applied to wide variety of datasets.

5. REFERENCES

[1] Jain, A.K., Duin, R.P.W., and Mao, J. 2000. Statistical Pattern Recognition: A Review, IEEE Transactions on Pattern Analysis and Machine Intelligence, vol. 22, no. 1, 4-37.

[2] Jimenez, L.O. and Landgrebe, D.A. 1997. Supervised classification in high-dimensional space: geometrical, statistical, and asymptotical properties of multivariate data, IEEE Transactions on Systems, Man and Cybernetics, vol. 28, no.1, 39–54.

[3] Belhumeur, P.N., Hepanha, J.P., and Kriegman, D.J. 1997. Eigenfaces vs. fisherfaces: recognition using class specific linear projection, IEEE. Trans. Pattern Analysis and Machine Intelligence, vol. 19, no. 7, 711-720.

[4] Torgerson, W.S. 1952. Multidimensional scaling I: Theory and method, Psychometrika, vol. 17, 401–419.

[5] Burges, C.J.C. 2005. Data Mining and Knowledge Discovery Handbook: A Complete Guide for Practitioners and Researchers, chapter Geometric Methods for Feature Selection and Dimensional Reduction: A Guided Tour. Kluwer: Academic Publishers.

[6] Saul, L.K., Weinberger, K.Q., Ham, J.H., F. Sha, and Lee, D.D 2006. Spectral methods for dimensionality reduction, In Semisupervised Learning, Cambridge, MA: The MIT Press.

[7] Maaten, L.J.P., Postma, E.O., and Herik, H.J. 2008. Dimensionality reduction: A comparative review.

[8] Scholkopf, B., Smola, A., and Muller, K.R., 1998. Nonlinear Component Analysis as a Kernel Eigenvalue Problem" Neural Computation, vol. 10, no. 5, 1299-1319.

[9] Baudat, G. and Anouar, F. 2000. Generalized discriminant analysis using a kernel approach, Neural Computation, vol. 12, 2385-2404.

[10] He, X. and Niyogi, P. 2003. Locality Preserving Projections, Advances in Neural Information Processing Systems16, Vancouver, British Columbia, Canada.

[11] Roweis S.T. and Saul, L.K. 2000. Nonlinear dimensionality reduction by Locally Linear Embedding, Science, vol. 290, no. 5500, 2323–2326.

[12] Tenenbaum, J.B., Silva, V. de and J.C. Langford, 2000. A global geometric framework for nonlinear dimensionality reduction, Science, vol. 290, no. 5500, 2319–2323.

[13] Belkin, M. and Niyogi, P. 2000. Laplacian Eigenmaps and spectral techniques for embedding and clustering, In Advances in Neural Information Processing Systems, vol. 14, 585–591, Cambridge, MA: The MIT Press.

[14] Bengio, Y., Paiement, J., Vincent, P., Dellallaeu, O., Roux, N.L, Quimet, M. 2003. Out-of sample Extensions for LLE, Isomap, MDS, Eigenmaps, and Spectral Clustering, Neural Information Processing Systems.

[15] Silva, V. de and Tenenbaum, J. B. 2003. Global versus local methods in nonlinear dimensionality reduction," Advances in Neural Information Processing Systems 15, 721–728, Cambridge, MA: MIT Press.

[16] Donoho, D. L. and Grimes, C. E. 2002. When does Isomap recover the natural parameterization of families of articulated images? (Technical Report 2002-27). Department of Statistics: Stanford University.

[17] Donoho, D. L. and Grimes, C. E. 2003. Hessian eigenmaps: locally linear embedding techniques for high dimensional data, Proceedings of the National Academy of Arts and Sciences, 100, 5591–5596.

[18] Sha, F. and Saul, L.K. 2005. Analysis and Extensions of Spectral Methods for Nonlinear Dimensionality Reduction, Proceedings of twenty second International Conference on Machine Learning, Germany.

[19] Vandenberghe, L. and Boyd, S. 1996. Semidefinite programming. SIAM Review, vol. 38, no. 1, 49–95.

[20] . He, X., Cai, D., Yan, S., and Zhang, H. 2005. J Neighborhood preserving embedding, Proceedings of Tenth International Conference on Computer Vision, Piscataway: IEEE Press, 1208-1213.

2012 Second International Conference on Advanced Computing & Communication Technologies

Fuzzy Based Real Time Traffic Signal Controller to Optimize Congestion Delays

Parveen Jain
Dept. of Computer Engg.
Delhi Technological University
Delhi, India
e-mail: parveenain1@gmail.com

Manoj Sethi
Dept. of Computer Engg.
Delhi Technological University
Delhi, India
e-mail: manojsethi@dce.ac.in

***Abstract*—With the increasing number of vehicle on roads, current traffic load cannot be maintained by preset Traffic signal controller. There is need to regularly monitor the traffic at roads and controller should work accordingly. Better Traffic prediction will result in better controller output. So, only solution to the problem of dynamic nature of traffic load is Dynamic or Intelligent Traffic Signal Controller. The main goal of controller is to avoid jams without any conflict in the signals. Real Time Controller is based on Sensor Mechanism and Controller unit, both will decide whether to extend or terminate the current phase. There are various ways to implement intelligent traffic signal controller, but a small amount of delay or conflict can affect the performance of whole system.**

Here, Work shows an optimization method for Real Time Traffic Controller using fuzzy logic that reduces waiting time significantly and its comparison with other controllers [1]. The fuzzy controller is dependent on the two factors considered here are: distance covered by vehicles over roads and total free space among vehicles on the road. The time of signal required changes dynamically depending on above defined two factors.

Keywords- Real Time; Controller; Fuzzy; Signal; Delay; Time.

I. INTRODUCTION

A majority of people uses roads for traveling in their daily life. There are various works where a small amount of delay may result into unfruitful things. So, Main aim of controller is smooth flow of traffic without any jams, delays. Everybody accept that proper traffic signals ensure safety and mobility and cost saving.

Intelligent Transportation system includes route-planning, optimization of transport, Infrastructures. Main goals of a Traffic Controller are: improving safety, minimizing travels time, which will indirectly beneficial to health, economy and environment [2]. There are two different types of traffic signal control:

1) Preset Time Control: As name indicates, time is predefined and is based on the past data; a local field signal controller uses the preset timing plan to control intersection signals. Since the traffic demand is changing all time in the real world, the preset time signal control is obviously not satisfactory.
2) Adaptive Signal Control: This type of controller depends on the output of sensors. The operations of signal control depends on actual traffic conditions.[3]

As adaptive signal controller is complex and very expensive as compared to preset time control. In preset time control, time was already preset for a particular lane irrespective of traffic load on roads. Controller has to just change the signal for a preset amount of time, but an adaptive controller can do two things.

1) On roads, at different timing different traffic load would be there, so to set the controller according to different timings. For example: on a road in morning timing, load will be more as compared to noon timing.
2) A dynamic model, in which traffic conditions are measured every time, when a signal changes.

There are various ways to implement intelligent traffic signal controller, but a small amount of delay or conflict can affect the performance of whole system. So an adaptive fuzzy controller will consider second case i.e. measure traffic condition when signal changes, whereas in first case, effort is required if there is need to add one more traffic condition.

II. CONTROLLER USING FUZZY LOGIC

Fuzzy controller will collect the real time traffic conditions where as in the Preset traffic signal controller (fixed time controller), where time for each signal was fixed, whether there is any number of traffic. Before switching to next state, fuzzy controller will examine the conditions.

Fuzzy logic technology allows the implementation of real-life rules similar to the way humans would react. For example, humans would react in the following way to control traffic situation at a certain junction: “if the road is loaded on the first and second lanes and the road is less loaded on the third and fourth lanes is less, then the traffic lights should stay green longer for the first and second lanes”. Fuzzy logic can easily implement these rules. But enough knowledge is required to prepare knowledge database or rules for a controller. The fuzzy controller has to collect data for the updating of the traffic situation model,

978-0-7695-4640-7/12 $26.00 © 2012 IEEE
DOI 10.1109/ACCT.2012.55

which is the base of determination of signal sequence and timings.

III. Structure of Fuzzy Controller

Fuzzy logic controller is responsible for controlling the length of green or red lights. Fuzzy based traffic controller consists of two parts.

1) Dynamic part: It collects traffic information on roads.
2) The Information is given to the fuzzy controller (fuzzy model) to calculate the length of signal.

Diagram below shows gathering and flow of information in the fuzzy traffic controller. Here first detector detects the traffic conditions and data is collected dynamically. Detectors will detect the condition of road. These conditions are fed to the fuzzy controller to process and then fuzzification is applied to convert the real terms into fuzzy terms.

In Fuzzy Inference system rules are there. Then rules are applied on fuzzy terms; then we get the output in fuzzy terms. Then again fuzzy terms are converted into real terms or mathematical terms with appropriate units. After proper mapping, the output of controller is used as the length of green or red signals. Actually diagram is divided into three parts, First part is from Traffic conditions to Fuzzification, second part is Fuzzy Inference System and third part is Defuzzification to signal status.

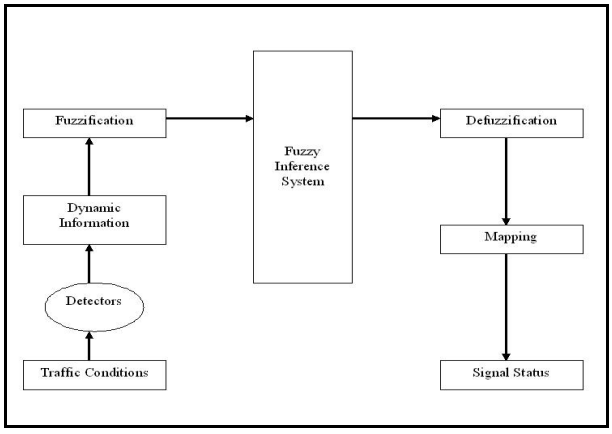

Figure 1. Structure of Fuzzy Traffic Controller

For making rules for fuzzy inference system, a lot of experience or knowledge is required. Larger the number of rules better will be fuzzy controller, because the fuzzy data has to pass these numbers of rules. One of the fuzzy rules is selected based on the input conditions. Number of fuzzy rules will vary with number of input variables and number of value each input variable is having. Fuzzy rules define the each possible combination of input variables and corresponding output variable.

IV. Designing of Fuzzy Controller

Here we are considering two variables to design a fuzzy controller. Two variables considered are:

1) Distance covered by Vehicles
2) Total Free Space Between Vehicles on the road

These two variables can tell the condition of traffic over the roads. The output of the controller will be the length of green signals so as to optimize the traffic flow. Here it is considered that the vehicle can go either straight or right side. The Diagram for the controller is as below in Fig. 2,which represent how two variables, after scaling are fed to controller and output is taken as required Signal length and fuzzy controller defined is shown in Fig. 1.

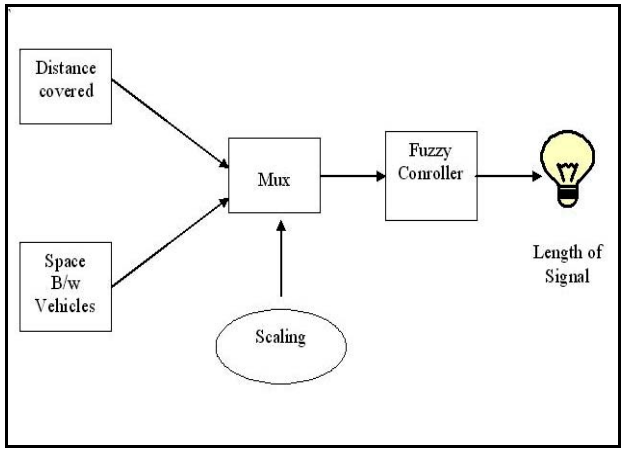

Figure 2. Fuzzy Controller

Each Input and output variable can have four values as below:

Distance	Space	Time of Signal
Very small	Very Less	Very less
Small	Less	Less
Far	Medium	Medium
Very far	Large	large

So these three variables will help to define and design a fuzzy controller. We can increase and decrease the number of parameter value based on the design and requirement of the controller.

V. Membership Diagrams of Input and Output Variables

Membership functions of the input and output variables are simulated using Fuzzy toolbox in Matlab. Fig. 3 and Fig. 4 represent the membership functions for input variables. The shape of membership diagram tells how the value of a variable will change. Number of membership values can be increased or decreased based on the parameter value.

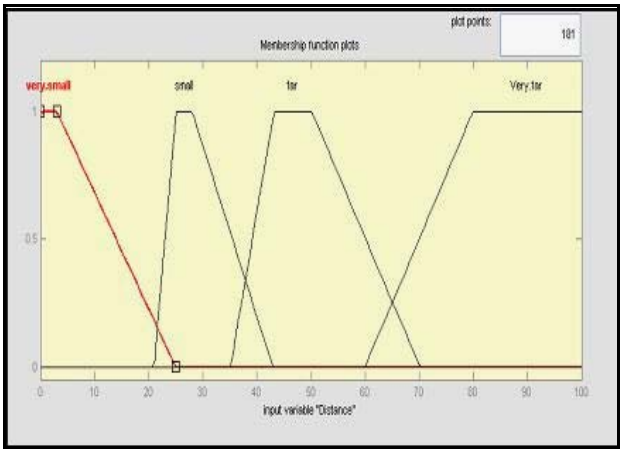

Figure 3. Membership Diagram of Distance

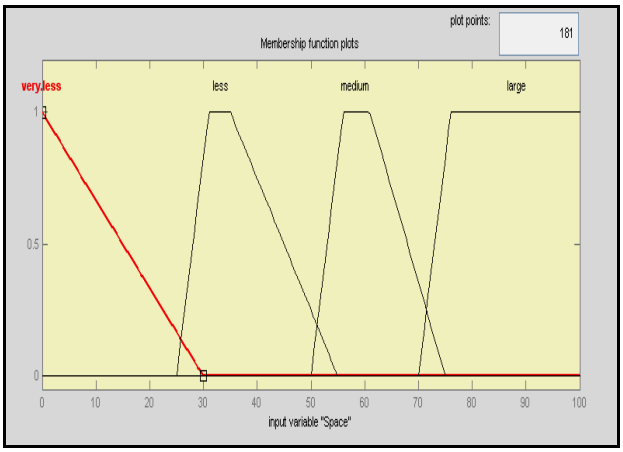

Figure 4. Membership Diagram of Space b/w Vehicle

(Distance covered on the roads and Total free space b/w vehicles) and Output variable (Time of Signal Required) by combination of input variables can be represented by membership diagram. As each variable is having four values so each variable is having four membership functions and having either trapezoidal shape or triangular depend upon how their value changes.

VI. Fuzzy Inference System

Total sixteen fuzzy rules can be created using input variables; four rules are defined below:

1) If (Distance is very small) and (Space b/w Vehicle is very less) then (Time is less).
2) If (Distance is small) and (Space b/w Vehicle is very large) then (Time is medium)
3) If (Distance is far) and (Space b/w Vehicle is very large) then (Time is medium)
4) If (Distance is very far) and (Space b/w Vehicle is very large) then (Time is large)

These sixteen rules define the working of Fuzzy Controller. We can increase the number of rules by defining more values for input variable. Basically Rules define the mapping between input and output variables.

VII. Comparison Using Surface Diagram

Surface Diagram shown below is the three dimensional representation of the input and output variables. In First diagram below; along x-axis we have Distance covered, along y-axis we have Total Free Space b/w Vehicles and along z-axis we have output variable Time of Signal required to control the traffic at junction without any conflict.

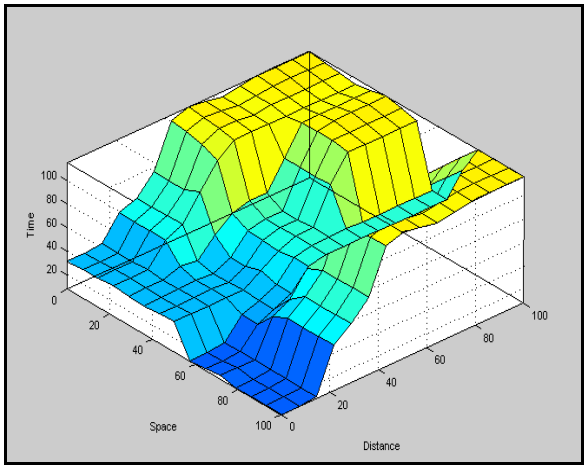

Figure 5. Surface Diagram for proposed Controller

The approach defined in [1] considers Distance covered by vehicle over road and Total Number of vehicles over road. In Figure 6, along x-axis we have Distance covered, along y-axis we have Total No. of Vehicles and along z-axis we have output variable Time of Signal Required.

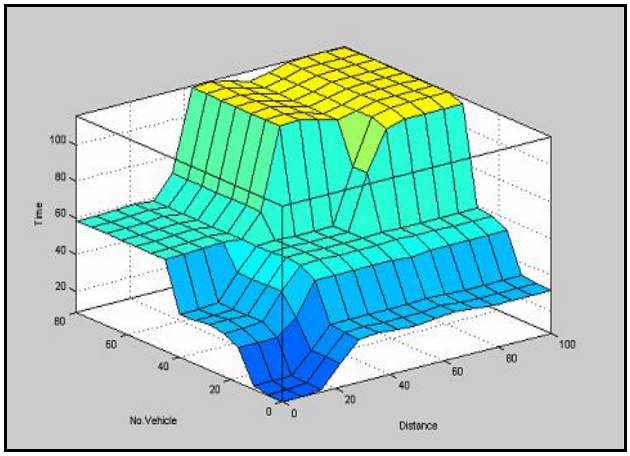

Figure 6. Surface Diagram for Earlier Controller

In Fig 5. Time of signal is increasing smoothly with the changing input parameters as compared to fig.6. Proposed controller is responding more effectively to every changing traffic condition.

VIII. Result Analysis

The figures shown below represent the difference between two fuzzy controllers under different traffic conditions over road. One Fuzzy controller considers Number of vehicles on roads and other fuzzy controller considers the Total Free Space in between vehicles. Here, we have taken three cases of traffic conditions. The figures shown below represent the difference between two fuzzy controllers.

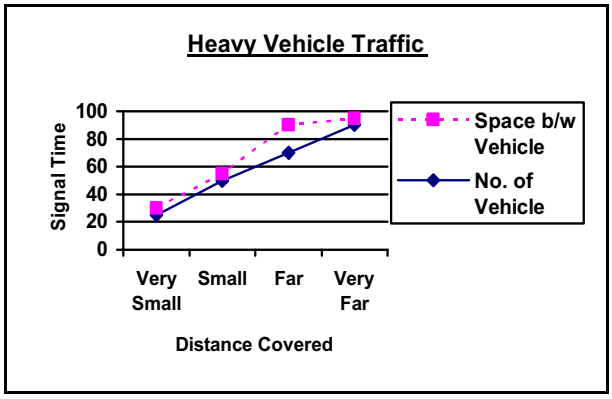

Figure 7: Heavy Traffic vehicle comparison

As we can see in Fig. 7, In case of road covered by Heavy Traffic Vehicles, both controllers are giving approximately same results for each of four traffic conditions.

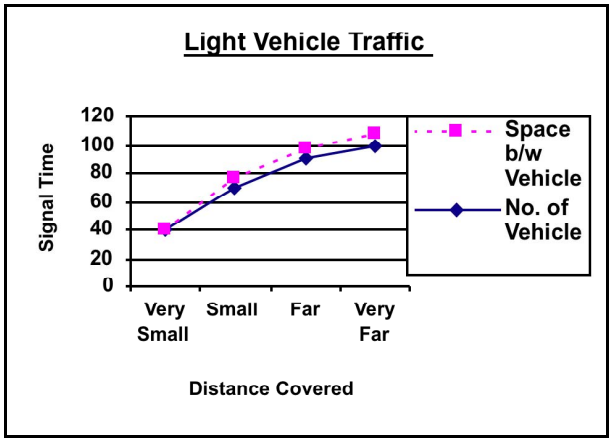

Figure 8: Light Traffic vehicle Comparison

In case of Light Traffic vehicles shown in Fig 8, Result is same for both the controllers. Both the controllers are calculating same time for each condition.

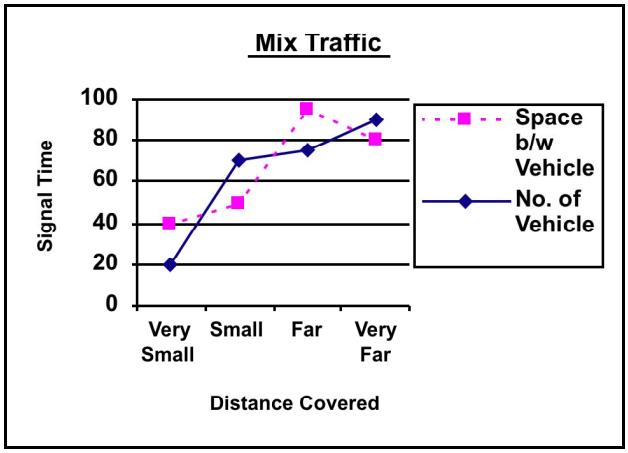

Figure 9: Mix Traffic Comparison

When the mix traffic will be there on roads, as shown in Fig. 9 then proposed fuzzy controller considering Space b/w vehicle is useful and gives better result. Overall, Proposed controller is giving better result as compared to earlier controller.

Conclusion and Future Work

Fuzzy controller will definitely reduce the waiting time for a vehicle as compared to predefined signal controller. Fuzzy Controller using space gives much better result than as compared to previous fuzzy controller, which was considering the number of vehicles on the road. Fuzzy logic technology deals with real time scenarios just like human do. Future work considers the defining the Service oriented architecture (SOA) to control the traffic of overall city and to provide better transportation system.

References

[1] Jain P, "Automatic Traffic Signal Controller for Roads by Exploiting Fuzzy Logic" Springer-Verlag Berlin Heidelberg 2011,CCIS 142, pp. 273-277, 2008.

[2] Wiering Macro, Veenen Jelle Van, Vreeken Jilles, Koopmam Arne, "Intelligent Traffic Light Control" www.cs.uu.nl, Techincal Report UU-CS-2004-029, pp.1–26, 2004.

[3] Lin Qinghui, Kwan B.W., Tung L.J., "Traffic Signal Control using Fuzzy Logic" IEEE 0-7803-4053-1/97, pp. 1644-1649, 1997.

[4] Xiao-Feng Chen, Zhong-ke Shi, Kai Zhao, "Research on an Intelligent Traffic Signal Controller", IEEE Transaction on Intelligent Transportation System, Vol. 1, pp. 884-887, 2003.

[5] Hoyer Robert and Jumar Ulrich, "Fuzzy Control of Traffic Lights", IEEE International Conference on Fuzzy Systems, vol. 3, pp. 1526-1531, 2007.

[6] Jan Jantzen, "Design of Fuzzy Controller", Technical University of Denmark, http://fuzzy. iau.dtu.dk/download/design.pdf .

[7] Jarkko Niittymaki, "Using Fuzzy Logic to Control Traffic Signals at Multi-phase Intersections", http://www.springerlink.com/content/ 981 502 q147x5t82g,2007.97.

2012 IEEE Control and System Graduate Research Colloquium (ICSGRC 2012)

Implementation of Interval Type-2 Fuzzy Systems with Analog Modules

Mamta Khosla, R K Sarin
Department of Electronics and Communication Engineering
Dr B R Ambedkar National Institute of Technology
Jalandhar- 144011, India
khoslam@nitj.ac.in

Moin Uddin
Delhi Technological University
Delhi

Prof_moin@yahoo.com

Abstract – **The objective of this paper is to present the implementation of Type-2 Fuzzy Logic System (T2 FLS) with analog modules. Specifically, this implementation focuses on Interval T2 FLSs (IT2 FLS) since they are computationally much simpler than general T2 FLSs and hence the most widely used in almost all the applications. The realization of IT2 FLS has been done by using two Type-1 Fuzzy Logic Systems (T1 FLS) which in turn have been implemented through analog modules built around operational-amplifiers (op-amps) and discrete components. The suggested implementation approach is based on rule-by-rule architecture and hence truly captures the inherent parallel nature of fuzzy systems.**

Keywords- Type-2 fuzzy logic systems, Interval type-2 fuzzy logic systems, analog modules, footprint of uncertainty.

I. INTRODUCTION

Type-2 fuzzy sets (T2 FSs) introduced by Zadeh [1] as an extension to the concept of fuzzy sets, now known as Type-1 Fuzzy Sets (T1 FSs) [2], are now well established and are gaining more and more popularity. T2 FSs allow us to handle linguistic uncertainties, as typified by the adage, "*words can mean different things to different people* [3]". Therefore, fuzzy logic systems based on T2 FSs are expected to perform better as they are capable of handling higher order of uncertainties, but at the same time are computationally intensive due to the involvement of a third dimension [4][5]. The third dimension in T2 FSs and footprint of uncertainty (FOU) provide an additional degree of freedom for T2 FLS to directly model and handle uncertainties.

Implementation of fuzzy systems depends on the application towards which it is addressed. Non-real time fuzzy systems are implemented through software with a high level programming language and this approach provides a high flexibility. On the other hand, software implementation is not adequate for applications demanding small size, low power consumption and high inference speed. A wide range of domains such as control, robotics, automotive etc. requires real-time operation and thus calls for hardware realization, The approaches for implementing T1 FLSs cover technologies like microcontrollers, Field Programmable Gate Arrays (FPGAs) among others [6]. The three basic processing stages of a T1 FLS are viz. fuzzification, inference and defuzzification. Since the general-purpose processors are exclusively sequential, so that these operations have to be performed serially that results in a low inference speed. The requirement of low inference speed or high response time can only be met by using dedicated hardware. The hardware realization of T1 FLSs is a well known and established area. On the contrary, the hardware realization of T2 FLSs in a relatively nascent research area. Their design and realization is more challenging due to high computational complexity, difficulty in visualization and non-availability of development tools. A few digital implementations reported in literature have been around microcontrollers, FPGAs etc. [7][8].

To the best of our knowledge, there is no report of a parallel hardware implementation of an IT2 FLS. This paper presents a simple arrangement for implementing IT2 FLS based on the averaging of two T1 FLSs, which have been realized with some standard analog modules built around op-amps and discrete components [9].

The paper is organized as follows. Section II briefly presents T2 FLS. The implementation of IT2 FLS presented in this paper is based on the use of two T1 FLSs and is explained in Section III. Simulation results are also presented in this section that validate the proposal. Section IV presents the various analog modules and their organization for IT2 FLS implementation. Finally, Section V draws conclusions.

II. INTRODUCTION TO T2 FUZZY SYSTEMS

Type-2 fuzzy system is a rule based fuzzy system that uses T2 FSs to describe its linguistic variables. A T2 FS can be informally defined as a fuzzy set that is characterized by a fuzzy or non-crisp membership function. This means there is uncertainty in the primary membership grades of a T2 membership function (MF) which introduces a third dimension to the MF, defined by the secondary membership grades [4].

A T2 FS denoted by $\tilde{A}$ is characterized by a T2 MF $\mu_{\tilde{A}}(x,u)$, where $x \in X$ and $u \in J_x \subseteq [0,1]$. $\tilde{A}$ can be expressed mathematically in the following form

$$\tilde{A} = \{(x,u), \mu_{\tilde{A}}(x,u) \mid \forall x \in X, J_x \subseteq [0\,1]\} \quad (1)$$

Uncertainty in the primary memberships of a T2 FS set consists of a bounded region that we call the *footprint of uncertainty* (FOU). It is the union of all primary memberships [4] as in (2)

$$FOU(\tilde{A}) = \bigcup_{x \in X} J_x \quad (2)$$

All the embedded FSs of FOU are T1 FSs and their union covers the entire FOU. FOU provides a very convenient verbal description of the entire domain of support for all the secondary grades of a T2 MF. It also lets us depict a T2 FS in two-dimensions instead of three dimensions which is easier to draw and makes it easy to understand the uncertainties inherent in that specific MF. The 2-D shape of the FOU depends on the type of uncertainty in the primary MF. However, because of the computational complexity of using a general T2 FLS, most designers only use IT2 FSs in a T2 FLS, the result being an IT2 FLS.

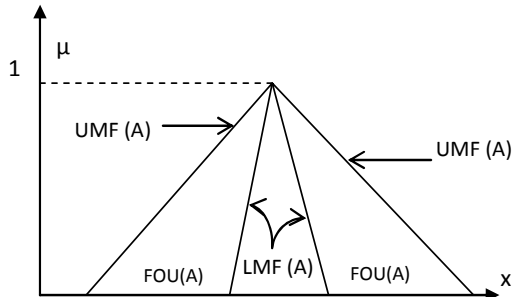

Figure 1. FOU of an IT2 FS

IT2 is a special case of a T2 FS where all the secondary membership grades equal one. IT2 FS is completely characterized by its 2-D FOU that is bound by a Lower MF (LMF) and an Upper MF (UMF) as shown in Fig. 1. IT2 FSs are the most widely used T2 FSs to date used in almost all applications because all calculations are easy to perform. LMF and UMF together are popularly used in most of research papers to represent IT2 FLSs [10].

III. Implementation Methodology for IT2 FLSs

The implementation of IT2 FLS presented in this paper is based on the use of two T1 FLSs to emulate a T2 FLS. The first T1 FLS is constructed using LMFs and the second one with the UMFs so as to emulate the FOU in a T2 FLS. The fuzzification, fuzzy inference and defuzzification are done as traditionally for two T1 FLSs and the outputs are averaged as shown in the Fig. 2.

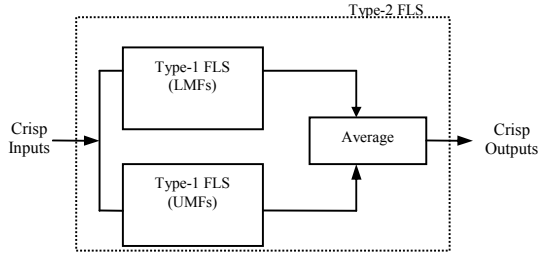

Figure 2. Implementation methodology for IT2 FLS

This methodology has been validated though two case studies by the authors [11]. The advantage of using this approach is that all the existing realization methods for T1 FLSs can be adopted for T2 FLSs. This realization methodology has been utilized by Sepúlveda *et al.* [12, 13] in their works and they implemented the IT2 FLS on FPGA. The authors have also designed an IT2 fuzzy controller chip in 0.18μm CMOS technology based on this methodology [16]. This realization methodology reduces the computational burden while preserving the advantages of IT2 FLSs as it eliminates the requirement of type-reduction.

IV. Organization of Analog Modules for IT2 FLS Implementation

From architectural point of view, fuzzy systems are parallel systems and parallelism can be built into the system by adopting rule-by-rule architecture, which provides a data path for each rule [6]. The design of T1 FLS based on rule-by-rule architecture is shown in Fig. 3.

Each T1 FLS realizes a type of fuzzy inference where the rule consequents are constant values called singletons and each rule has the following format.

$$\textit{IF } (x \textit{ is } A) \textit{ AND } (y \textit{ is } B) \textit{ THEN } z = c \quad (3)$$

In the above, x and y are input variable, A and B are fuzzy labels of x and y. Furthermore, z is an output variable and c is some constant. As compared to general case where the consequents are fuzzy sets, this type of fuzzy inference requires much less complex hardware [14].

Although each block in the figure can be implemented in analog or digital domain, but in this paper the focus is only on analog implementation. Each module in Fig. 3 can be realized using op-amps and other discrete components. Analog modules based design has been reported in literature [9] for T1 FLS realization that has been used for different applications [15]. We have arranged these analog modules to build two T1 FLSs and designed an additional *Averager* analog module that averages the defuzzified outputs of two T1 FLSs so as to give the overall output of IT2 FLS. The membership function generators (MFGs) are used for fuzzification i.e. to find the membership grades corresponding to the input variables.

For the purpose of simplicity, a fuzzy system with only two inputs and single output is considered. Further each input variable is represented by three IT2 FSs. Analog modules for implementing membership functions of different shapes viz. Z, triangular/trapezoidal and S are shown in Figs. 4, 5 and 6 respectively. The input variables are scale-mapped that transfer the range of input variables in the corresponding universe of discourse [0 +Vcc] and output voltage will be zero for all negative voltages, since Vee=0.

The fuzzy operator AND can be implemented using MIN module, which computes the rule firing strength. Scalar circuit calculates the weighted rule strength and MAX module is used for defuzzification. Analog modules for MIN operation (2 inputs), scaling operation for a single input, and for performing the MAX operation (9 inputs) are shown in Figs. 7, 8 and 9 respectively. The *Averager* circuit that averages the defuzzified outputs of the two T1 FLSs is shown in Fig 10. The parameters of the MFGs viz. slope and position are adjustable through the feedback resistor values RF and the

reference voltages Vref. Also the scaling factor of the *Scalar* and the averaging ratio of the *Averager* can be adjusted through the resistor values RF and R1. The simulations of these analog modules are shown in Figs. 11 to13.

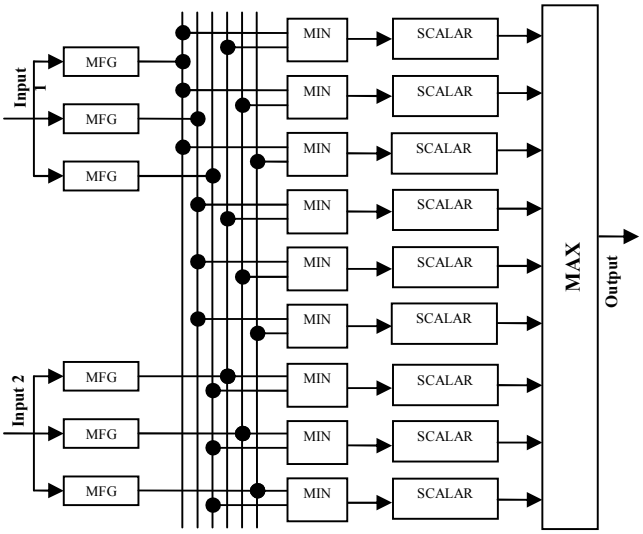

MFG – Membership Function Generator

MIN – Minimum
MAX – Maximum

Figure 3. T1 FLS based on Rule-by-Rule Architecture

The values of the control feedback resistors and Vref are so chosen as to obtain the desired shapes of the fuzzy sets. The variation of slope of MF with different values of FB resistors is shown in Fig. 14. And the variation of the position of the MF with Vref values is shown on Fig. 15.

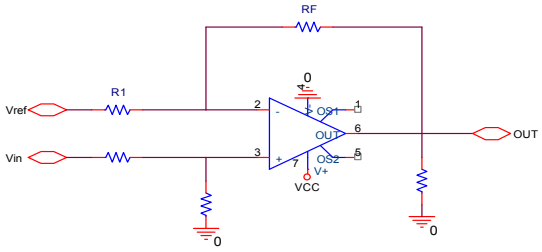

Figure 4. Analog Module for Z MFG

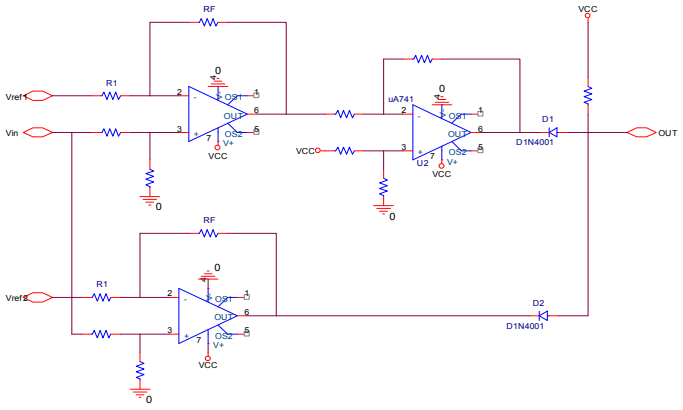

Figure 5. Analog Module for Triangular/Trapezoidal MFG

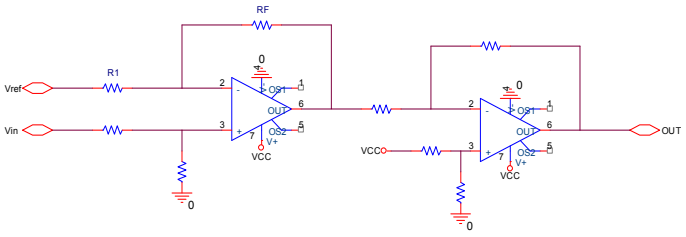

Figure 6. Analog Module for S MFG

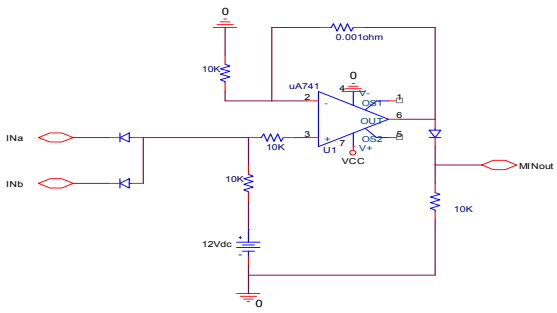

Figure 7. Analog Module for MIN Operation (2 inpits)

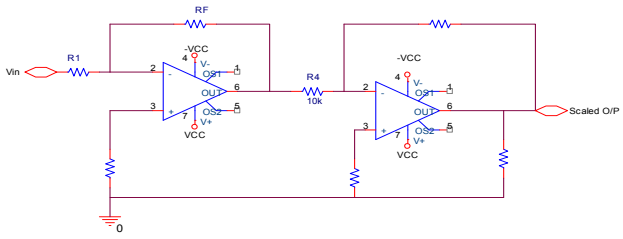

Figure 8. Analog Module for *Scalar*

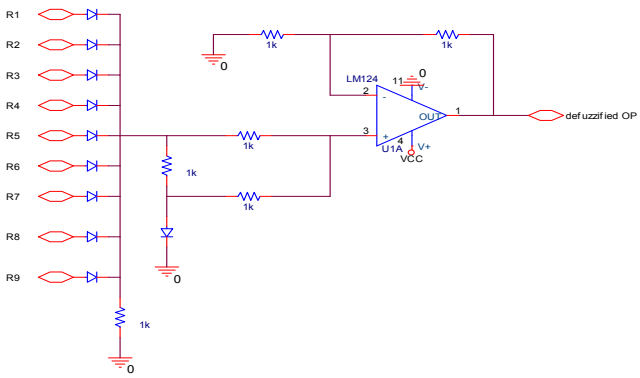

Figure 9. Analog Module for MAX Operation (9 inputs)

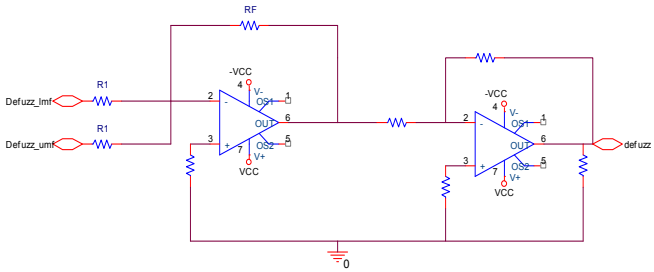

Figure 10. Analog Module for *Averager* (2 inputs)

An IT2 FLS based on the implementation methodology described in Section III and using various analog modules described in this section was created in OrCAD Spice simulator and the arrangement is shown in Fig. 16. The response of fuzzifier corresponding to the sweep of one of the two input variables that generate LMFs and UMFs is shown in Fig. 17. The load resistors shown in MIN, MAX and *Scalar* modules are connected only for measuring the individual responses. However, these load resistors are not required in the complete IT2 FLS realization as per the arrangement shown in Fig. 16. The number of discrete components required for implementation of each analog module is given in Table I. And the hardware budget for the realization of IT2 fuzzy processor is given in Table II.

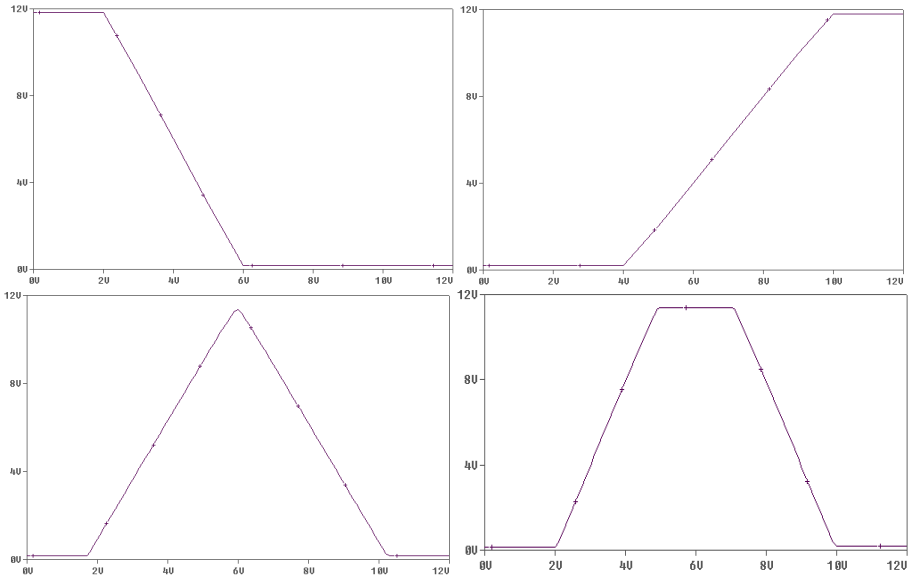

Figure 11. Simulation Results for (a) Z MF (b) S MF (c) Triangular MF (d) Trapezoidal MF

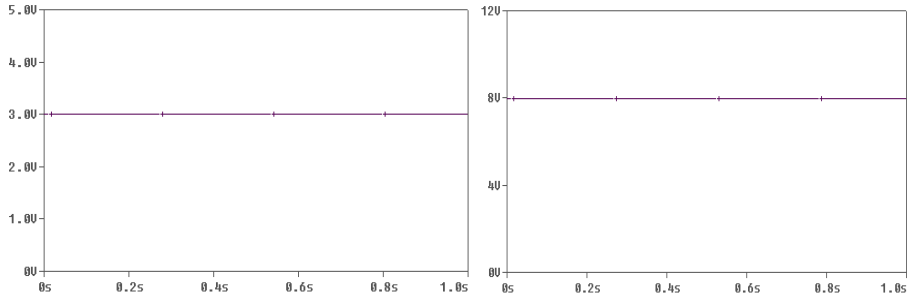

Figure 12. Simulation Results for (a) MIN (INa=8V, INb=3V) (b) MAX (2V, 3V, 4V, 5V, 6V, 7V, 8V, 1V, 4.5V)

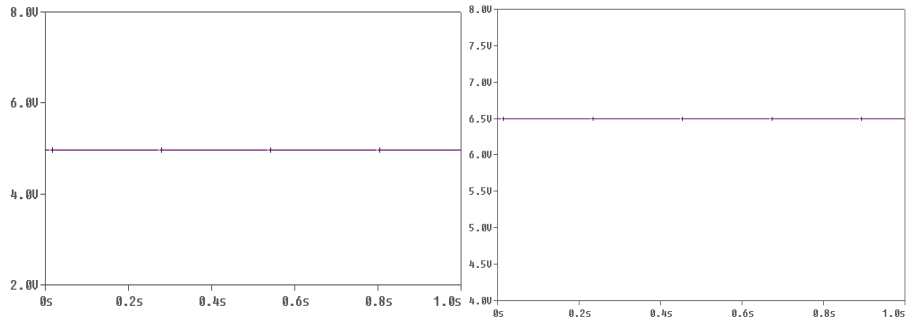

Figure 13. Simulation Results for (a) *Scalar* (input voltage=0.5V, scaling factor=10) (b) *Averager* (average of 8V and 5V)

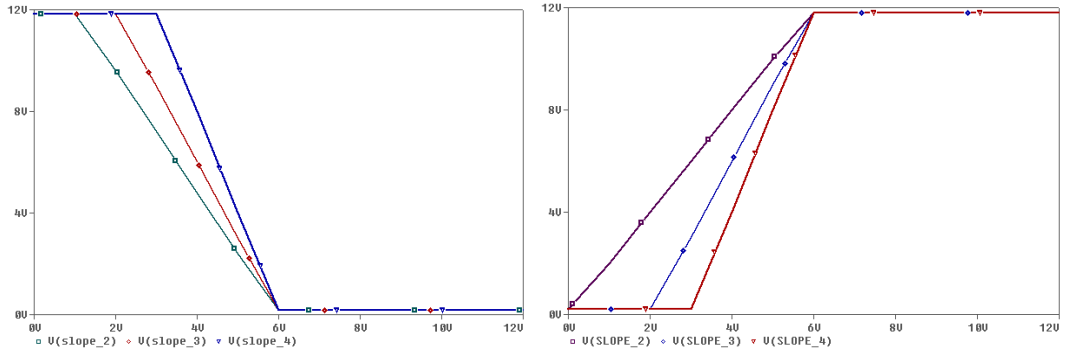

Figure 14. Slope variation (a) Z MF with slope (RF/R1)=2, 3, 4, (Vref=6V) (b) S MF with slope (RF/R1)=2, 3, 4, (Vref=6V)

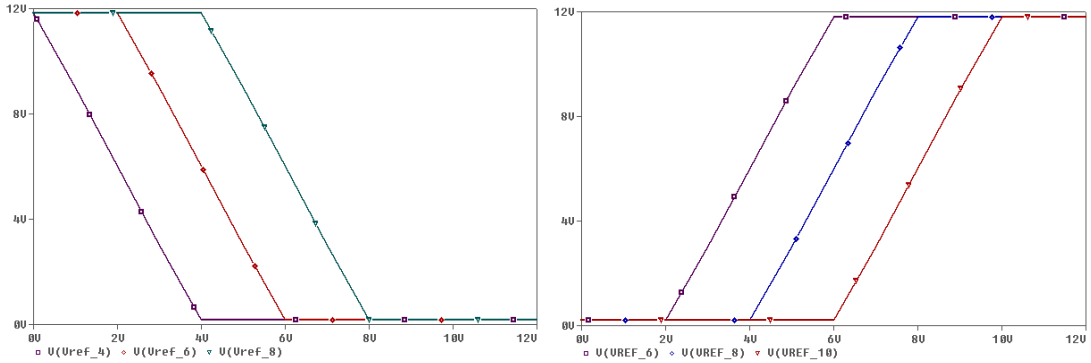

Figure 15. Position Variation (a) Z MF with Vref=4, 6, 8V {slope (RF/R1)=3}, (b) Z MF with Vref=6, 8, 10V {slope (RF/R1)=3}

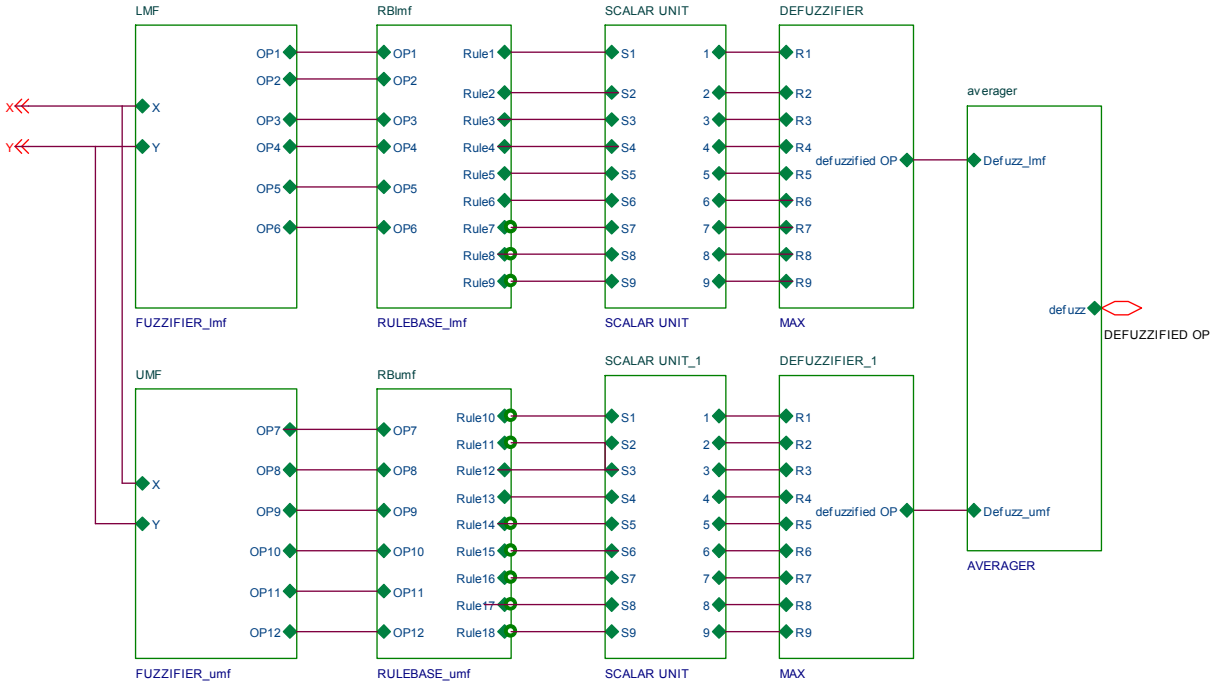

Figure 16. IT2 FLS Implementation created in OrCAD

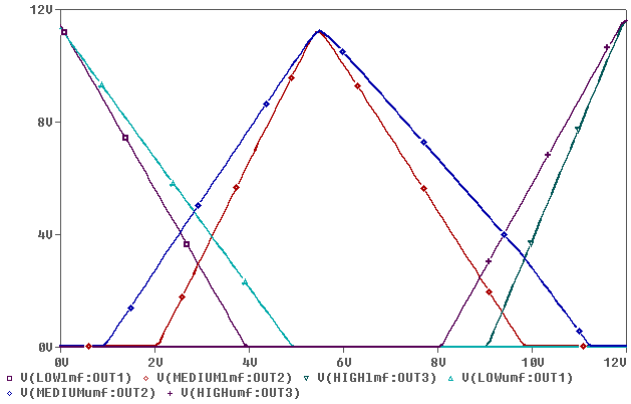

Figure 17. Simulation Results of Fuzzifier corresponding to one input variable

TABLE I. HARDWARE BUDGET FOR EACH ANALOG MODULE

Analog Module	OP-Amp	Diode	Resistor
Z MFG	1	0	4
Triangular MFG	3	2	13
S MFG	2	0	8
MIN	1	3	4
MAX	1	10	6
Scalar	2	0	6
Averager	2	0	8

TABLE II. HARDWARE BUDGET FOR IT2 FLS

Analog Module	No.	OP-Amp	Diode	Resistor
Z MFG	2	2	0	8
Triangular MFG	2	6	4	26
S MFG	2	4	0	16
MIN	18	18	54	72
MAX	2	2	20	12
Scalar	18	36	0	108
Averager	1	2	0	8
Total no. of Components		**70**	**78**	**250**

V. CONCLUSIONS

This paper presents a simple, easy and effective implementation of IT2 FLS with analog modules built around op-amps and discrete components. The realization is based on use of two T1 FLSs. The implementation follows rule-by-rule architecture and would provide a very high inference speed and hence good performance. Even people with non-electrical background and having little understanding of basic electronic components can realize IT2 FLS for their applications. However, the limitation of this arrangement is lack of flexibility and excessive wiring.

REFERENCES

[1] L. A Zadeh, "The Concept of a Linguistic Variable and Its Application to Approximate Reasoning – 1", Information Sciences 8, pp. 199–249 1975.

[2] L. A Zadeh, "Fuzzy Sets", Information and Control, vol. 8, pp. 338–353, 1965.

[3] J. M. Mendel, "Computing with Words, When Words can Mean Different Things to Different People", Proceedings of 3rd International ICSC Symposium on Fuzzy Logic and Applications, Rochester University, Rochester, NY. 1999.

[4] J. M. Mendel and R.I. John, "Type-2 Fuzzy Sets Made Simple", IEEE Transaction on Fuzzy Systems, vol. 10, no. 2, pp. 117–127, 2002.

[5] N. N. Karnik and J.M. Mendel, "Applications of Type-2 Fuzzy Logic Systems to Forecasting of Time-Series", Information Sciences 120, pp. 89–111, 1999.

[6] Baturone, Barriga, Carlos Jimenez-Fernandez and Diego, R. Lopez, Microelectronic Design of Fuzzy-Logic Based Systems, CRC Press, 2000.

[7] J. Bulla, G. Sierra and M. Melgarejo, "Implementing a Simple Microcontroller-Based Interval Type-2 Fuzzy Processor", Proceedings of 51st Midwest Symposium on Circuits and Systems (MWSCAS), pp. 69-72, 2008.

[8] M. A. Melgarejo and C.A. Pena-Reyes, "Hardware architecture and FPGA implementation of a type-2 fuzzy system", Proc. ACM GLSVLSI, Boston, MA, p. 458–461, 2004.

[9] A. Sanz, "Analog Implementation of Fuzzy Controller," Proceedings of 3rd IEEE Conference on Fuzzy Systems, pp. 279-283, 1994.

[10] Q. Liang, J.M. Mendel, "Interval type-2 fuzzy logic systems: Theory and design", IEEE Trans. Fuzzy Syst., vol. 8, no. 5, pp. 535–549, 2000.

[11] Mamta Khosla, Rakesh Kumar Sarin, Moin Uddin, Satvir Singh, Arun Khosla, *Realizing Interval Type-2 Fuzzy Systems with Type-1 Fuzzy Systems,* Book Chapter for the Book Cross-Disciplinary Applications of Artificial Intelligence and Pattern Recognition: Advancing Technologies, Eds.: Vijay Mago and Nitin Bhatia, IGI Global, USA, 2012, pp. 412-427.

[12] Roberto Sepúlveda, Oscar Castillo, Patricia Melin, Oscar Montiel: An Efficient Computational Method to Implement Type-2 Fuzzy Logic in Control Applications. Analysis and Design of Intelligent Systems using Soft Computing Techniques 2007, pp. 45-52.

[13] Roberto Sepúlveda, Oscar Montiel, Gabriel Lizárraga, Oscar Castillo: Modeling and Simulation of the Defuzzification Stage of a Type-2 Fuzzy Controller Using the Xilinx System Generator and Simulink. Evolutionary Design of Intelligent Systems in Modeling, Simulation and Control 2009, pp. 309-325.

[14] T. Yamakawa, "A Fuzzy Inference Engine in Nonlinear Analog Mode and its Application to a Fuzzy Logic Control", IEEE Transanction on Neural Network, Vol. 4, pp 496-522, May 1993.

[15] Satvir Singh and J.S. Saini, "Captive Power Management using Op-amp based FLS", Proceedings of Asian Conference on Intelligent Systems and Networks, Jagadhari, February 24-25, 2006,India, pp. 160-166.

[16] Mamta Khosla, Rakesh Kumar Sarin and Moin Uddin, "Design of an Analog CMOS based Interval Type-2 Fuzzy Logic Controller Chip", International Journal of Artificial Intelligence and Expert Systems, vo. 2, no.4, pp. 167-183, 2011.

Investigations of Dielectric and Ferroelectric Properties of Yttrium Substituted $SrBi_2Ta_2O_9$ Ferroelectric Ceramics

Investigations of yttrium substituted SBT Ferroelectric ceramics

Sugandha[1] and A. K. Jha[1, 2]

[1]Thin Film and Material Science Laboratory, Department of Applied Physics, Delhi Technological University (Formerly Delhi College of Engineering), Delhi-110042, India.

[2]Department of Applied Sciences, A.I.A.C.T.R. Geeta Colony, Delhi-110031, India.

Email: miglani.sugandha@gmail.com, prof.akjha@gmail.com

***Abstract*—In the present work yttrium substituted samples of compositions $Sr_{1-x}Y_xBi_2Ta_2O_9$ (x=0.0-0.1) were synthesized by solid state reaction method. The synthesized specimens were characterized for their structural and electrical properties. X-ray diffractograms of the samples reveal the single phase layered perovskite structure formation for yttrium content x ≤ 0.05. The temperature variation of dielectric constant shows that the Curie temperature (T_c) decreases on increasing the yttrium concentration. The dielectric loss reduces significantly with yttrium substitution. The ferroelectric properties improve with Y substitution and the maximum value of remnant polarization is observed for the composition with x =0.05. The observations have been discussed in terms of contribution from the cation vacancies introduced into the lattice structure due to donor substitution.**

Keywords-c Electroceramics, Y substituted SBT, Dielectric property, Ferroelectric property.

I. INTRODUCTION

A large number of ferroelectric materials have been intensely investigated for applications in non-volatile ferroelectric random access memories (FeRAMs), piezoelectric transducers, actuators, pyroelectric sensors, high dielectric constant capacitors, etc. [1-5]. Among various ferroelectric materials, Lead Zirconate Titanate (PZT) has been regarded as the best potential material for memory device applications because of its superior ferroelectric properties [6, 7]. However, PZT has a few limitations such as environmentally hazardous lead content, high leakage current and poor fatigue endurance [8]. Bismuth layered ferroelectric materials such as Strontium Bismuth Tantalate (SBT) has attracted a lot of attention of the researchers as an alternative ferroelectric material to PZT. Being lead free, it has various advantages such as low leakage current and high fatigue endurance up to 10^{12} switching cycles [9-12].

SBT is a member of bismuth layer structured ferroelectric material with a general formula of $(Bi_2O_2)^{2+}(A_{n-1}B_nO_{3n+1})^{2-}$, where A = Ca^{2+}, Ba^{2+}, Sr^{2+}, Bi^{3+}, La^{3+}, Sm^{3+}, etc. and B = Fe^{3+}, Ti^{4+}, Nb^{5+}, Ta^{5+},W^{6+},Mo^{6+}, etc; and n indicates the number of corner sharing octahedra forming the perovskite like slabs [13, 14]. The crystal structure of $SrBi_2Ta_2O_9$ comprises of pseudo-perovskite blocks $(SrTa_2O_7)^{2-}$ that are sandwiched between $(Bi_2O_2)^{2+}$ layers. Here, Sr occupies the A-site of the perovskite blocks and Ta occupies the B-site. However, SBT suffers from two major limitations: high dielectric loss and low remnant polarization values [15, 16]. Significant efforts have been made to improve the dielectric and ferroelectric properties of the compound. It has been reported that substitution at A or B- site can effectively taylor the physical and chemical properties of SBT for various device applications [17-19]. A-site (Sr^{2+}) substitution by various trivalent cations such as Bi^{3+}, La^{3+}, Pr^{3+}, Ce^{3+}, Nd^{3+}, etc. have been widely investigated and has showed a significant enhancement in the polarization values and fatigue endurance [20, 21].

Detailed literature survey showed that even though a lot of work has been done on pristine SBT compound, however, hardly any systematic work dealing with the characterization of yttrium (Y^{3+}) substituted SBT as a function of composition has been reported. This prompted the authors to conduct a detailed study of $Sr_{1-x}Y_xBi_2Ta_2O_9$ (SYBT) compounds and characterize their structural and electrical properties.

II. EXPERIMENTAL TECHNIQUE

Samples of compositions $Sr_{1-x}Y_xBi_2Ta_2O_9$ with x = 0.0, 0.01, 0.025, 0.05, 0.075 and 0.1 were synthesized by solid-state reaction method taking $SrCO_3$, Bi_2O_3, Ta_2O_5 and Y_2O_3 (all from Aldrich) in their stoichiometric proportions. The powder mixtures were thoroughly ground and passed through a sieve of appropriate size and then calcined at 900°C in air for 2 h. The calcined mixtures were ground and admixed with 1–1.5 wt% polyvinyl alcohol (Aldrich) as a binder and then pressed at 300 MPa into disk shaped pellets. The pellets were sintered at 1200°C for 2 h in air.

X-ray diffractograms of the sintered pellets were recorded using Bruker Diffractometer (model D8 Advance) in the range $20^\circ \leqslant 2\theta \leqslant 70^\circ$ with Cu Kα radiation(λ= 1.5405 Å) at a scanning rate of 1°/min. The sintered pellets were polished and

978-1-4673-2669-8/12/$31.00 ©2012 IEEE

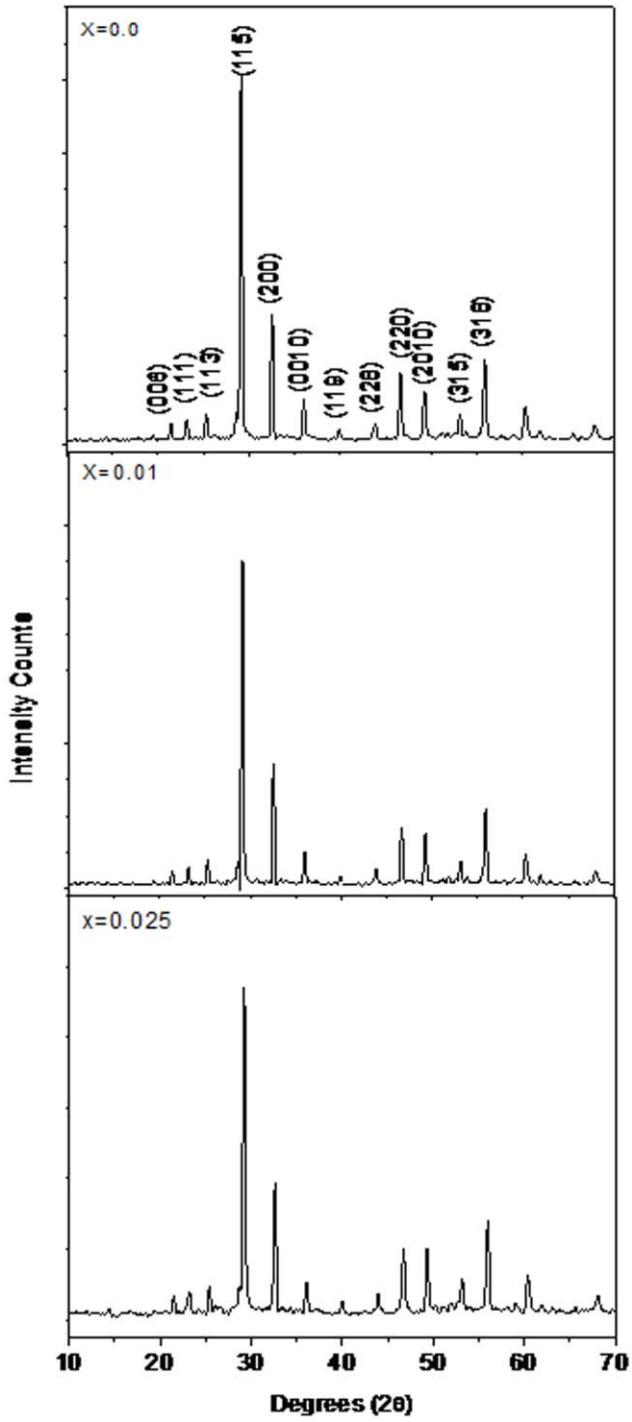

silver pasted on both sides and cured at 500°C for 1 h. The dielectric measurements were carried out using a precision LCR meter (Agilent 4284A) operating at oscillation amplitude of 1V. The polarization–electric field (P–E) hysteresis loops were recorded using a P–E loop tracer based on Sawyer–Tower circuit. The dc electrical resistivities of the samples were measured using a programmable electrometer (Kiethley, 6517A).

III. Results and Discussions

A. Microstructural Studies

Fig. 1 shows the XRD patterns of various SYBT sintered samples. The XRD peaks are similar to those of the standard diffraction pattern of $SrBi_2Ta_2O_9$ on the JCPDS card (JCPDS file no- 072-7073). It is observed in the diffractograms that the

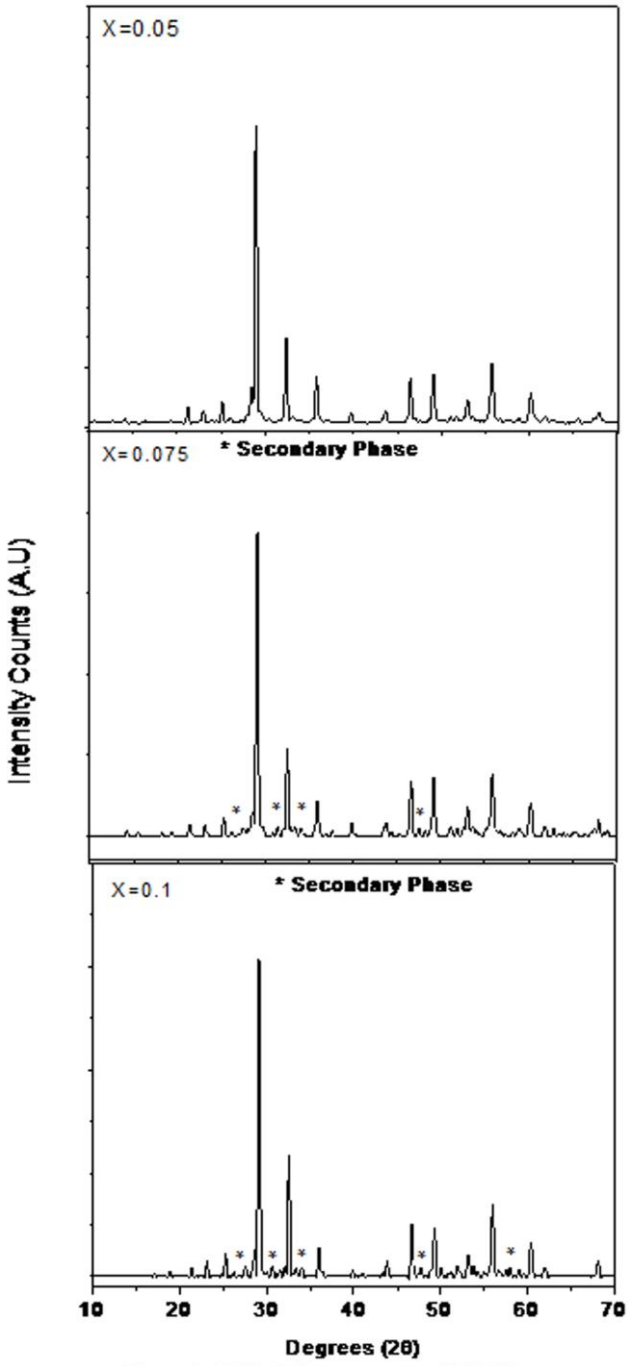

Figure 1: XRD Diffractograms of SYBT samples for x=0.0-0.1

specimen remain single phase up to x≤ 0.05 confirming the incorporation of Y^{3+} at Sr^{2+} site in the SBT lattice. For the samples with composition x>0.05, additional peaks are also

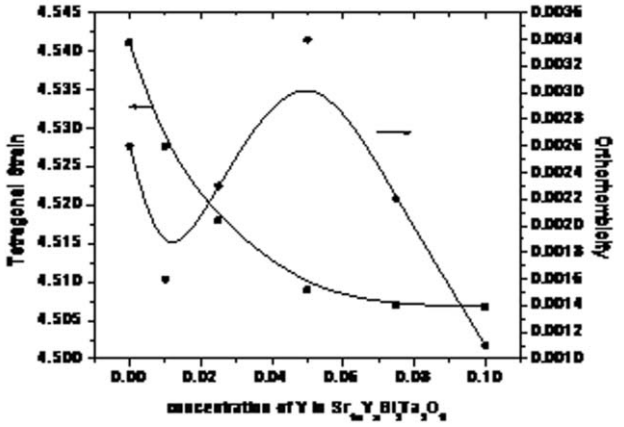

Figure 2: Compositional variation of tetragonal strain and orthorhombicity

observed indicating the formation of secondary phase. A comparison of the additional peaks with standard XRD patterns of (JCPDS file no- 074-6546) indicates the formation of $YTaO_4$ as the secondary phase. Lattice parameters were calculated from the XRD patterns and refined using least square refinement method by a computer programmed package powder-X [22] and are listed in Table 1. A decrease in lattice constants is observed which can be understood on the basis of ionic radii. The ionic radius of Y^{3+} (1.02 Å) is smaller than that of Sr^{2+} (1.44 Å) [23]. It is worth mentioning here that Y^{3+} is substituted at Sr^{2+} site (A- site), however, substitution of some Y^{3+} at the vacant bismuth –site, due to bismuth volatilization, cannot be ruled out. The ionic radius of Y^{3+} is close to the radius of Bi^{3+} (0.96 Å) and both have similar valency, therefore some of the Y^{3+} ions occupying the Bi site in the Bi_2O_2 layer is also possible. The crystal structure distortion parameters, namely, tetragonal strain (c/a) and orthorhombicity [2(a-b)/ (a+b)] have been calculated and plotted as function of yttrium concentration (Fig. 2). It is observed that tetragonal strain decreases as the yttrium concentration is increased. However, the orthorhombic distortion is observed to increase upto x≤ 0.05 and decreases thereafter.

B. Dielectric Property

Fig. 3 illustrates the temperature variation of the dielectric constant (Fig. 3(a)) and dielectric loss (Fig. 3(b)) of the studied samples at a frequency of 100 kHz. As seen in Fig. 3(a), dielectric constant increases gradually with increasing temperature up to the transition temperature T_c and then decreases with a broadened peak near the transition. Further, the Curie temperature (T_c) decreases with increase in yttrium concentration. It is also observed that dielectric constant decreases as the concentration of yttrium increases (Table 1). This is possibly due to the decrease in the net polarization of the compound with increase in yttrium concentration as the ionic polarizability (α_I) of Y^{3+} is lower (3.81Å^3) compared to

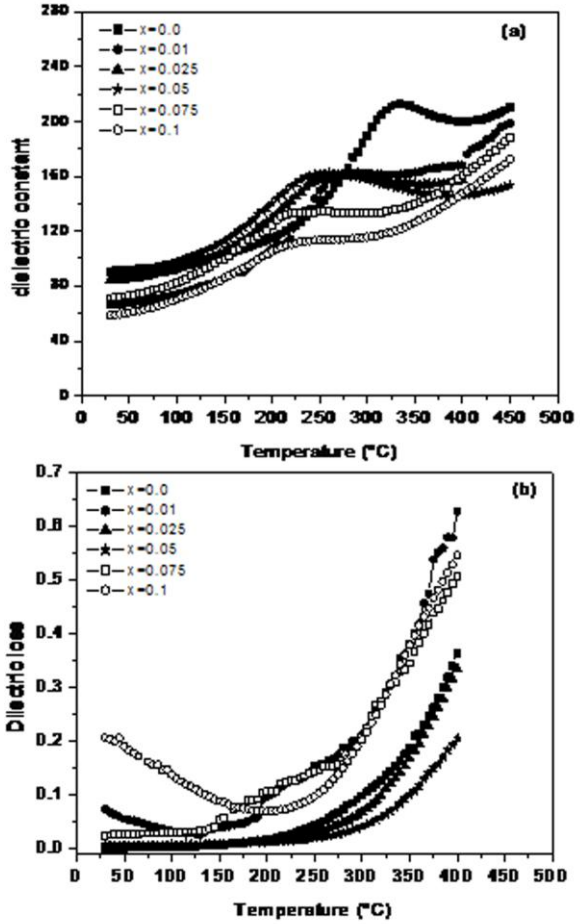

Figure 3: (a) Variation of dielectric constant and (b) dielectric loss with temperature of $Sr_{1-x}Y_xBi_2Ta_2O_9$ (x=0.0-0.1) compounds

that of Sr^{2+} (4.24 Å^3) [24, 25]. The broadened peaks, as observed in Fig. 3(a), indicate that the transition in all the samples is of the diffuse type, an important characteristic of a disordered perovskite structure [26]. The broadening or diffuseness of a peak occurs mainly due to the compositional fluctuation and/or substitution disordering in the arrangement of cations at one or more crystallographic sites in the lattice structure [27]. Also, there is a possibility of cation-disordering, i.e., some Y atom intended for A-site substitution also occupy the Bismuth sites, in the bismuth layered structures. Comprehensive structural analysis of SBT with the aid of neutron diffraction and Raman scattering have shown disorder in the distribution of the A-site ions and Bi ions [28, 29]. Also, it is known that the pristine $SrBi_2Ta_2O_9$ is not perfectly stoichiometric, but contains a certain amount of inherent defects (e.g. oxygen vacancies) resulting from the volatilization of Bi_2O_3 at high temperatures [30, 31]. When Bi_2O_3 is lost, bismuth and oxygen vacancy complexes are formed in the $(Bi_2O_2)^{2+}$ layers [32, 33]. Also, due to the

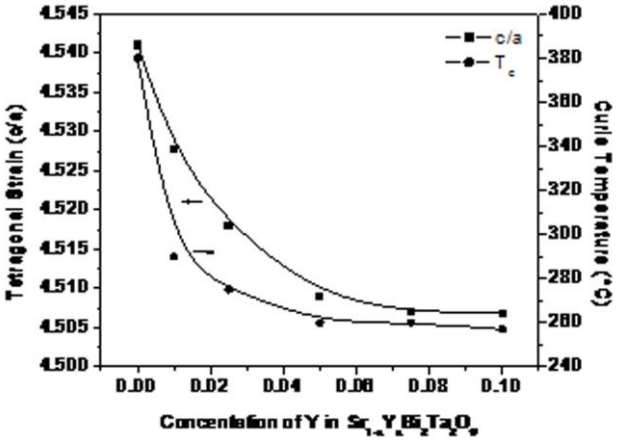

Figure 4:Compositional variation of tetragonal strain and Curie Temperature.

similar ionic radius it is possible that some Y^{3+} ions might occupy the vacant bismuth sites in the Bi_2O_2 layer. This results in disorder in the arrangements of cations at A-sites and Bismuth-sites in Bi_2O_2 layers leading to a microscopic heterogeneity [34, 35] in the structure which results in the creation of different local Curie points [26, 34] and hence, broadening of the peak is observed near the transition temperature [35]. The broadening or diffuseness of the peak is measured in terms of diffusivity constant calculated using the empirical relation [36]:

$$\ln(1/\varepsilon - 1/\varepsilon_{max}) = \gamma \ln (T-T_c) + \text{constant} \qquad (1)$$

where ε_{max} is the maximum ε value at $T = T_c$. The value of γ at 100 kHz for all the samples was calculated from the slope of $\ln((1/\varepsilon) - (1/\varepsilon_{max}))$ versus $\ln(T - T_c)$ curve. In the studied compositions, γ is found to be between 1 (obeying Curie–Weiss law) and 2 (for completely disordered sys tem) confirming the diffuse phase transition in all the samples. The value of γ for the samples with composition $0.01 \leq x \leq 0.05$ is observed to decrease from 1.47 to 1.38. However, an increase in diffusivity from 1.64 to 1.68 is observed for the samples with composition x=0.075 and x=0.1 respectively. This suggests disorderness increases in the system at higher yttrium concentration (x> 0.05).

The fall in Curie temperature for yttrium substituted SBT (Fig. 4) can be understood on the basis of the observed tetragonal strain variation. It is observed that c/a decreases as strontium is substituted by yttrium. Tetragonal strain is the internal strain in the lattice which affects the phase transition temperature [37, 38]. Smaller value of the strain indicates that a lesser amount of thermal energy is required for the phase transition and therefore a decrease in T_c is expected with a decrease in the strain. Another possible reason for the decrease in transition temperature is attributed to the increase in value

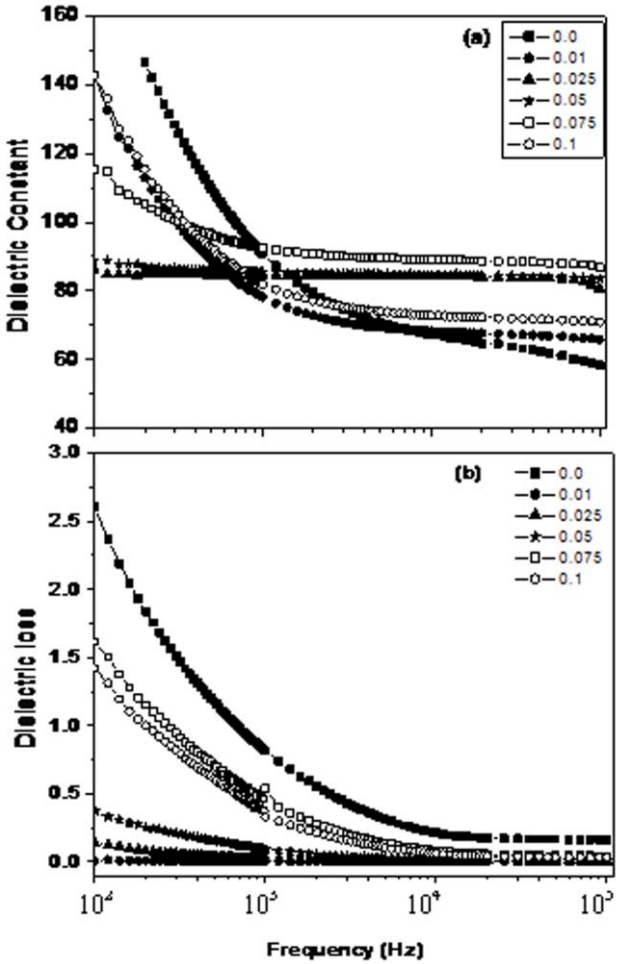

Figure 5: (a) Variation of dielectric constant and (b) dielectric loss with frequency

of tolerance factor due to the partial substitution of the smaller size cation Y at Sr- site [39].The tolerance factor 't' for the perovskite structure is given by [40]:

$$t = (R_o + R_A)/ 1.414 (R_B + R_o) \qquad (2)$$

where R_A, R_B and R_o are the respective ionic radii of A-site, B-site and Oxygen ions. It is observed that the substitution of Y^{3+} at the A-site results in slight increase of 't' value from 0.912 (x=0.01) to 0.919 (x=0.1). The observed behaviour is in good agreement with the reports by Suraez et. al. [41] for Aurivillius compounds, where a linear decrease of T_c was observed with an increase of 't'.

Fig. 3(b) shows the dielectric loss (at 100 kHz) as a function of temperature for the studied samples. It is observed that the dielectric loss reduces on yttrium substitution. The source of dielectric loss in these ceramics is space charge polarization/domain wall relaxation [42]. The presence of defects like oxygen vacancies, V•• act as space charge and contribute to the dielectric loss in these materials [43]. The

pure SBT has inherent oxygen vacancies resulting from the volatilization of Bi_2O_3 [30]. The additional charge, in the case of donor substituted compounds, is compensated through the formation of cation vacancies to maintain the overall charge neutrality of the unit structure. In the compositions studied in the present work, Y^{3+} acts as a donor and the constraint of maintaining the overall charge neutrality of the structure results in the formation of cation vacancies, possibly at the A-site [44]. For substitution of two Y^{3+} ions, one A-site (Sr-site) should remain vacant. The corresponding formation of vacancy can be represented as:

$$\text{Null} = Y^{\bullet}_{Sr} + \tfrac{1}{2} V''_{Sr} \qquad (3)$$

where $Y^{\bullet}_{Sr}$ denotes the yttrium at Sr site and V''_{Sr} denotes the strontium vacant site. Similar observations have been made in various rare-earth (La^{3+}, Nd^{3+}, etc.) substituted SBT [45, 46]. Noguchi et al. [47] concluded from the neutron diffraction and XPS analyses on praseodymium (Pr) added SBT that Pr occupies the A-site and that the formation of V''_{Sr} compensates the charge difference between Pr^{3+} and Sr^{2+}. Similarly, it can be inferred that for Y added SBT, Y occupies the A-site and the charge difference between Sr^{2+} and Y^{3+} is compensated by the formation of cation vacancies. These cation vacancies effectively reduce the number of oxygen vacancies that are present in the prepared samples. It is this reduction in the number of oxygen vacancies that effectively reduces the dielectric loss.

Fig. 5(a) shows the variation of dielectric constant with frequency from 100 Hz to 100 kHz at room temperature for all the studied specimens. It is observed that the dielectric constant decreases up to about 1 kHz and remains nearly constant beyond this frequency. The dielectric constant of a material has four polarization contributions: electronic, ionic, dipolar and space charge [48]. Response frequencies for ionic and electronic polarizations are $\sim 10^{13}$ and 10^{16} Hz, respectively; and at frequencies beyond 1 kHz, contribution from space charge polarization is not expected [48]. As discussed above, pristine $SrBi_2Ta_2O_9$ is not perfectly stoichiometric, but contains a certain amount of inherent defects (e.g. oxygen vacancies), acting as space charges [30, 43]. The high value of dielectric constant for low frequencies in case of undoped SBT can therefore be attributed to the presence of such space charges. However, samples with composition $0.01 \leq x \leq 0.05$ exhibit negligible change of dielectric constant as frequency increases from 1 KHz to 100 KHz. This implies that there is no appreciable contribution of space charges, confirming the suppression of the defects by cation vacancies when A-site is substituted by higher valent cation [33].

Fig. 5(b) shows the variation of dielectric loss with frequency at room temperature for all the specimens. It also decreases up to 1 KHz and remains nearly independent beyond this frequency. It is known that at lower frequencies, the dipoles can follow the alternating field resulting in higher values of dielectric loss while at higher frequencies the dipoles are unable to follow the rapidly changing field leading to the reduction in the values of dielectric loss.

C. *Ferroelectric Property*

To confirm the ferroelectric nature of the studied compounds, hysteresis loops were recorded at room temperature at a frequency of 100 Hz. Fig. 6 shows the variation of polarization as a function of electric field for all the samples. The observed values of remnant polarization ($2P_r$) for all the samples are given in Table 1. It is observed that the remnant polarization (P_r) value increases with increase in the concentration of yttrium in SBT up to $x \leq 0.05$ and decreases thereafter considerably. The maximum $2P_r$ value of $\sim 15 \mu C/cm^2$ is observed for the composition with x = 0.05.

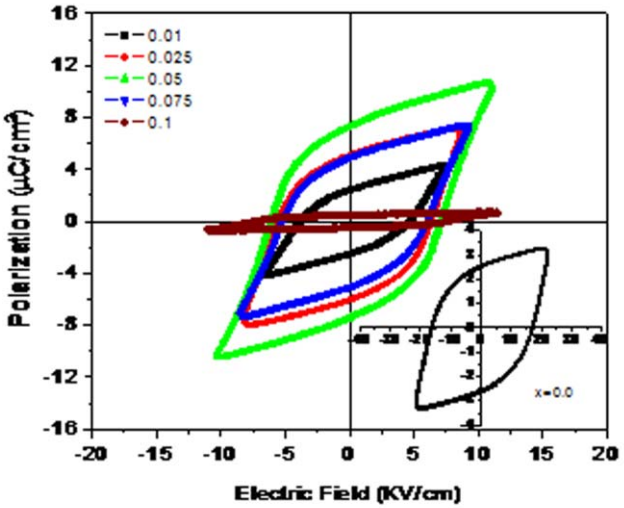

Figure 6: P–E hysteresis loops of $Sr_{1-x}Y_xBi_2Ta_2O_9$ (x=0.0-0.1) compounds at room temperature.

As observed in Fig. 5, yttrium substitution significantly enhances the ferroelectric properties of the studied compositions. The observed behavior can be explained as follows. It is well known that the polarization switching behavior of ferroelectric material is strongly influenced by defects like oxygen vacancies [49]. The oxygen vacancies assemble near domain walls and the polarization reversal of these domains is suppressed due to "pinning" by these defects near the domain boundaries resulting in smaller remnant polarization values [45]. There is sufficient experimental evidence to indicate that the defects accumulated at electrode-ferroelectric interfaces (and/or grain and domain boundaries) are mainly oxygen vacancies which have a direct effect on the ferroelectric properties [50, 51]. In the present case, the observed ferroelectric behavior can be understood in terms of the reduction in the amount of oxygen vacancies due to the formation of cation vacancies, as discussed earlier. These cation vacancies suppresses the concentration of oxygen vacancies, which are the major cause for degradation in the ferroelectric properties and fatigue behavior of Bi-based layered perovskite structures [47, 52]. A reduction in the concentration of oxygen vacancies reduces the pinning effect on the domain walls, leading to the enhanced remnant

polarization values. Also, due to these A- site vacancies, the rotation of TaO_6 octahedra in the a-b plane may double whereas the tilting from the c-axis changes very slightly. Thus the A-site vacancies greatly enhance the rotation of the TaO_6 octahedra in the a-b plane accompanied by an entire shift of TaO_6 octaherdra to the a-axis, resulting in an increase in polarization [48, 53]. This explains the observed increase in ferroelectric properties of yttrium substituted SBT samples. However, $2P_r$ values decreases for composition with x> 0.05. This is possibly due to the presence of secondary phases [46, 54], as discussed earlier.

D. Conductivity Studies

The total conductivity σ_{tot} of the material comprises of the dc conductivity, σ_{dc}, and the ac conductivity, σ_{ac},

$$\sigma_{tot} = \sigma_{dc} + \sigma_{ac}(\omega) \qquad (4)$$

The σ_{dc} accounts for the free charges available and is independent of the frequency. The σ_{ac} accounts for the bound and free charges and can be expressed in terms of the dielectric constant ε_r and the dissipation factor tan δ as [48]:

$$\sigma_{ac} = \omega\varepsilon_o\varepsilon_r \tan\delta \qquad (5)$$

where ω is the angular frequency and ε_o the free-space permittivity.

Fig 7(a) shows the variation of dc conductivity ($\sigma dc = 1/\rho$) with inverse of temperature (103/T) for all the compositions. It can be seen in the figure that at low temperatures the conductivity is constant. However, at higher temperatures, it increases with temperature indicating negative temperature coefficient of resistance (NTCR) behaviour in all the studied SYBT samples. It is observed that donor doping in SBT results in reduced dc conductivities. As seen in the figure, there are two predominant types of conduction regions, one is the lower temperature region in which dc conductivity remains invariant with temperature and the other is higher temperature region in which dc conductivity increases sharply with temperature. In lower temperature region, from room temperature to approximately ~300°C, the electrical conduction is dominated by extrinsic defects. Whereas, in higher temperature region ~300°C to ~700°C the conduction is dominated by intrinsic defects such as oxygen vacancies [55, 56]. Table 1 summarizes the dc conductivity (at higher temperature, 400°C) and activation energy values calculated using the Arrhenius equation [57]:

$$\sigma = \sigma_o \exp(E_a/K_BT) \qquad (6)$$

where σ indicates the conductivity, E_a the activation energy and K_B the Boltzman constant. It is observed in Table 1 that the E_a values increases and dc conductivity decreases with yttrium content. The observed behaviour can be understood as follows. The oxygen vacancy $V_o^{\cdot\cdot}$ is doubly positively charged with respect to the neutral lattice and is considered to be the most mobile intrinsic ionic defect in the perovskite oxides [58]. Their motion in perovskites is manifested through

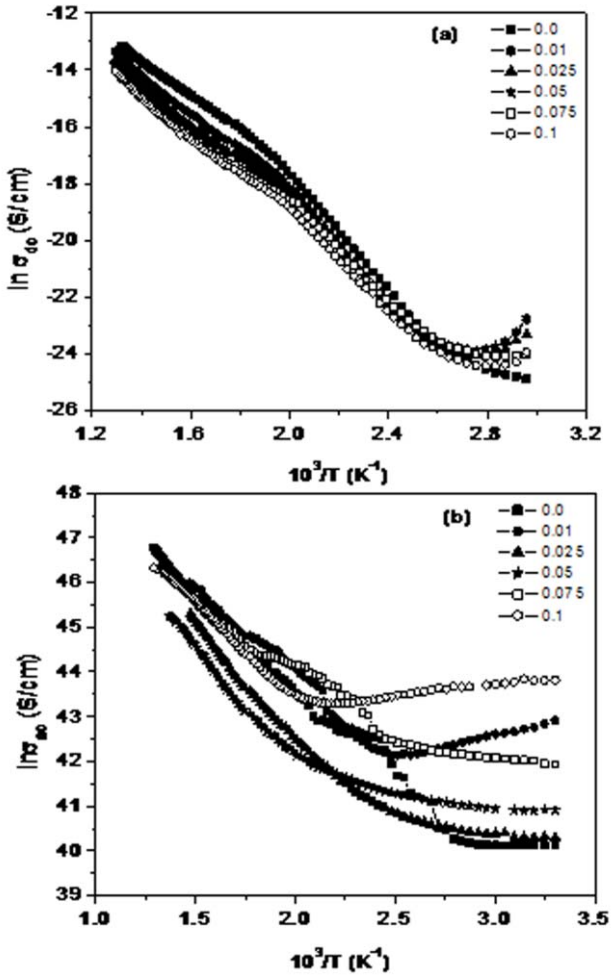

Figure 7: Variation of (a) dc conductivity and (b) ac conductivity with inverse of temperature

enhanced conductivity and activation energy value of ~ 1 eV [59]. From the obtained values of E_a in Table 1, for composition x=0.0, it seems that the conductivity is basically due to oxygen vacancies. As discussed earlier, in SYBT samples, the substitution of Y in SBT results in the formation of cation vacancies and subsequent elimination of oxygen vacancies. Therefore, the energy needed for the charge carriers to migrate (by hopping) also increases, leading to higher activation energy. As a result, the conductivity decreases because there are fewer oxygen vacancies available with sufficient energy to move around and the energy barrier between the scarcer vacancies increases [60]. Also, the obtained higher activation energy values for SYBT samples can be understood in terms of the stability of perovskite structure. The substitution of Y^{3+} onto Sr^{2+} sites enhances the stability of perovskite structure due to larger chemical bond strength of Y–O bond (719.7 KJ/mole) as compared to Sr–O bond (425.5KJ/mole) [61]. The substitution of stronger bond would suppress the formation of intrinsic defect resulted in an increased activation energy values [62].

The variation of ac conductivity as a function of inverse of temperature (10^3/T) for all the compositions at 100 kHz is shown in Fig. 7(b). The conductivity of the compounds at higher temperature is higher, which is a common behaviour in most of the dielectric ceramics [63, 64]. The nature of variation of σ_{ac} over a wide temperature range supports the thermally activated conduction process in these materials. This is due to the presence of defects like oxygen vacancies whose mobility increases at higher temperatures [59].

IV. CONCLUSION

A single phase layered perovskite structure is maintained in $Sr_{1-x}Y_xBi_2Ta_2O_9$ (SYBT) samples up to x=0.05 and secondary phases appear for higher Y content. The Curie temperature decreases with increase in yttrium content and the dielectric loss reduces significantly. The ferroelectric properties get enhanced on yttrium substitution. The maximum $2P_r$ value of ~15 μC/cm^2 is obtained for x = 0.05. The substitution of yttrium into SBT is found to be effective in eliminating oxygen vacancies improving the ferroelectric properties.

REFERENCES

[1] S.B. Desu, D.P.Vijay, Mater. Sc. & Eng. B, 32 (1995) 75.

[2] J. F. Scott, C.A.P.de Araujo, Science, 246 (1989) 1400.

[3] K. Takemura, T. Noguchi and M. Miyasaka, Appl. Phys. Lett. 73 [12] (1998) 1649-51.

[4] R.R. Neurgaonkar, W. F. Hall, J. R. Oliver, W. W. Ho, W. K. Cory, Ferroelectrics, 87 (1998) 167.

[5] Sugandha and A. K. Jha Mater. Charact. 65 (2012) 126-132.

[6] B. H. park, B. S. Kang, S. D. Bu, T. W. Noh, W. Jo, Nature 40 (1992) 682.

[7] D. Wu, A. Li, T. Zhu, Z. Liu, N. Ming, J. Appl. Phys. 88 (2000) 5941.

[8] S. Ezhilvalan, J. M. Xue, J. Wang, Mater. Che. & Physis, 75 (2002) 50-55.

[9] C. A. P. de Araujo, J. D. Cuchlaro, L. D. Mcmillan, M. C. Scott, J. F. Scott, Nature, 374 (1995) 627.

[10] M. Nagata, D. P. Vijay, X. Zhang, S. B. Desu, Phys. Status Solidi A 159 (1996) 75.

[11] L. S. Zheludev, Physics of Crystalline Dielectrics, Electrical properties, vol 2, Plennum, New york, (1971) 474.

[12] V. Shrivatava, A. K. Jha and R. G. Mehdiratta, Solid St. Commu. 133 (2004) 125.

[13] B. Aurivillius, Ark. Kemi. 1 (1949) 463.

[14] E. C. Subbaro, J. Phys. Chem.. solids, 23, (1962) 665.

[15] J. F. Scott, Annu. Rev. Mater. Sci. 28 (1998) 79.

[16] F. Kulcsar, J. Am. Carem. Soc. 42 (1959) 343.

[17] R. B. Atkin, R. L. Holman and R. M. Fulrath, J. Amer. Ceram. Soc. 54 (1971) 113.

[18] P. Duran Martin, A. Catro, P. Millan R. Jimnez, J. Mater. Res. 13 (1998) 2565.

[19] R. R. Das, P. Bhattacharya, W. Perez, R. S. Katiyar, S. B. Desu, Appl. Phys. Lett. 80 (2002) 637.

[20] T. J. Boyle, P. G. Clem, B. A. Juttle, T. D. Dunbarb, W. F. Hammetter, J. Mater. Res. 17 (2002) 4.

[21] S. Sahoo, R. N. P. Choudhary, B. K. mathur, Physica B, doi: 10.1016/ J. Phys b.2010.12.072.

[22] C. Dong, J. Appl. Cryst. 32 (1999) 838.

[23] R.D. Shannon, C.T. Prewitt, Acta Crystallogr. B25 (1965) 925.

[24] R. D. Shannon, J. Appl. Phys. 73 (1993) 348–366.

[25] P. Ganguly and A. K. Jha J. Alloys & Cmpds. 495 (2010) 7-12.

[26] R. Rai, S. Sharma, R.N.P. Choudhary, Solid State Commun. 133 (2005) 635.

[27] R. Rai, S. Sharma, R.N.P. Choudhary, Mater. Lett. 59 (2005) 3921.

[28] S.M. Blake, M.J. Falconer, M. McCreedy, P. Lightfoot, J. Mater. Chem. 7 (1997) 1609.

[29] S. Kojima, J. Phys.: Condens. Matter 10 (1998) L327.

[30] B.H. Park, S.J. Hyun, S.D. Bu, T.W. Noh, J. Lee, H.D. Kim, T.H. Kim, W. Jo, Appl. Phys. Lett. 74 (1999) 1907.

[31] M.M. Kumar, Z.G. Ye, J. Appl. Phys. 90 (2001) 934.

[32] I. Coondoo, A.K. Jha, S.K. Agarwal, J. Eur. Ceram. Soc. 27 (2007) 253.

[33] I. Coondoo, A.K. Jha, S.K. Agarwal, Ceram. Int. 33 (2007) 41.

[34] M.E. Lines, A.M. Glass, Principles and Application of Ferroelectric and Related Materials, Oxford University Press, Oxford, 1977.

[35] S. Singh, O.P. Thakur, C. Prakash, K.K. Raina, Physica B369 (2005) 64.

[36] S.M. Pilgrim, A.E. Sutherland, S.R. Winzer, J. Am. Ceram. Soc. 73 (1990) 3122–3125:

[37] Y.H. Xu, Ferroelectric Materials and their Applications (Elsevier Science Publishers, Amsterdam, 1991) pp. 131.

[38] Priyanka Arora Jha and A. K. jha, J. Alloys & Cmpds. 513 (2012) 580-585.

[39] E. V. Ramana, V. V. Kiran, T. B. Sankaran, J. Alloys & Cmpds. 456 (2008) 271-76.

[40] S.K. Rout, E. Sinha, S. Panigrahi, Mater. Chem. Phys. 101 (2007) 428.

[41] D. Y. Suarez, I. M. Reany, W. E. Lee, J. Mater. Res. 16 [11] (2001) 3139.

[42] I.S. Zheludev, Physics of Crystalline Dielectrics, Electrical Properties, vol. 2, Plenum, New York, 1971, p. 474.

[43] Y. Noguchi, M. Miyayama, Appl. Phys. Lett. 78 (2001) 1903.

[44] A. K. Jha and Sugandha Ferroelectrics, 421 (2011) 1-8.

[45] Y. Noguchi, M. Miyayama, K. Oikawa, T. Kamiyama, M. Osada, M. Kakihana, Jpn. J. Appl. Phys., Part 1 41 (2002) 7062.

[46] Y. Noguchi, M. Miyayama, T. Kudo, Phys. Rev. B 63 (2001) 214102.

[47] Y. Noguchi, A. Kitamura, L. Woo, M. Miyayama, K. Oikawa, T. Kamiyama, J. Appl. Phys. 94 (2003) 6749.

[48] R.C. Buchanan, Ceramic Materials for Electronics: Processing, Properties and Applications, Marcel Dekker, Inc., New York, 1991.

[49] W.L. Warren, D. Dimos, B.A. Tuttle, J. Am. Ceram. Soc. 77 (1994) 2753.

[50] Q.Y. Jiang, L.E. Cross, J. Mater. Sci. 28 (1993) 4536.

[51] J.F. Scott, C.A. Araujo, B.M. Melnik, L.D. McMillan, R. Zuleeg, J. Appl. Phys. 70 (1991) 382.

[52] Y. Noguchi, I. Miwa, Y. Goshima, M. Miyayama, Jpn. J. Appl. Phys. 39 (2000) L1259.

[53] G. Z. Liu, C. Wang, H. S. Gu, H. B. Lu, J. Phys. D: Appl. Phys. 40 (2007) 7817-7820

[54] T. Sakai, T. Watanabe, M. Osada, M. Kakihana, Y. Noguchi, M. Miyayama, and H. Funakubo, Jpn. J. Appl. Phys. 42, 2850 (2003).

[55] Shulman HS, Testorf M, Damjanovic D, Setter N. J Am Ceram Soc 1996; 79: 3124.

[56] Smyth, D. M Ferroelectrics, 1991, 117, 117–124.

[57] W.D. Kingery, Introduction to Ceramics, Wiley, New York, 1960.

[58] Warren, W. L., Vanheusden, K., Dimos, D., Pike, G. E. and Tuttle, B. A., J. Am. Ceram. Soc., 78 (1995)536–538

[59] Robertson, J., Chen, C. W., Warren, W. L. and Guttleben, C. D., Electronic Appl. Phys. Lett., 69 (1996) 1704–1706.

[60] J. J. Dih and R. M. Fulrath, J. Am. Ceram. Soc., 61, 448 (1978).

[61] D. R. Liden, CRC Handbook of Cemistry and Physics, CRC press, 81st edition, 2000-2001.

[62] D. Dhak, P. Dhak, P. Pramanik, Appl. Surf. Sc. 254 (2008) 3078-92.

[63] K.S. Singh, R. Sati, R.N.P. Choudhary, Pramana 38 (1992) 161–166.

[64] K.S. Rao, T.N.V.K.V. Prasad, A.S.V. Subrahmanyam, J.H. Lee, J.J. Kim, S.H. Cho, Mater. Sci. Eng. B 98 (2003) 279–285.

x	a (Å)	b (Å)	c(Å)	ε_{max} (100 KHz)	$2P_r$ ($\mu C/cm^2$)	$\sigma_{dc\ X\ 10^{-7}}$ (400°C)	E_a (eV)
0.0	5.4983	5.5131	24.9688	212.374	5.106	7.0876	0.82
0.01	5.5077	5.5069	24.8759	162.260	4.938	3.6143	0.96
0.025	5.4875	5.5006	24.6932	161.118	11.090	2.5924	1.12
0.05	5.4775	5.4964	24.7536	162.779	14.696	1.9869	1.26
0.075	5.4761	5.4882	24.6812	134.759	9.972	1.8001	1.29
0.1	5.4757	5.4818	24.6781	113.795	0.970	1.7014	1.31

Table 1: Variation of different parameters of $Sr_{1-x}Y_xBi_2Ta_2O_9$ (x=0.0-0.1) compound.

I.J. Intelligent Systems and Applications, **2012, 10, 1-14**
Published Online September 2012 in MECS (http://www.mecs-press.org/)
DOI: 10.5815/ijisa.2012.10.01

Sentiment Analysis: A Perspective on its Past, Present and Future

Akshi Kumar
Department of Computer Engineering, Delhi Technological University, Delhi, India
Email:akshi.kumar@gmail.com

Teeja Mary Sebastian
Department of Computer Engineering, Delhi Technological University, Delhi, India
Email: teeja.sebastian@gmail.com

***Abstract*—**The proliferation of Web-enabled devices, including desktops, laptops, tablets, and mobile phones, enables people to communicate, participate and collaborate with each other in various Web communities, viz., forums, social networks, blogs. Simultaneously, the enormous amount of heterogeneous data that is generated by the users of these communities, offers an unprecedented opportunity to create and employ theories & technologies that search and retrieve relevant data from the huge quantity of information available and mine for opinions thereafter. Consequently, Sentiment Analysis which automatically extracts and analyses the subjectivities and sentiments (or polarities) in written text has emerged as an active area of research. This paper previews and reviews the substantial research on the subject of sentiment analysis, expounding its basic terminology, tasks and granularity levels. It further gives an overview of the state- of – art depicting some previous attempts to study sentiment analysis. Its practical and potential applications are also discussed, followed by the issues and challenges that will keep the field dynamic and lively for years to come.

Index Terms— Sentiment Analysis, Opinion, Web 2.0, Tasks, Levels, Applications, Issues

I. Introduction

A vital part of the information era has been to find out the opinions of other people. In the pre-web era, it was customary for an individual to ask his or her friends and relatives for opinions before making a decision. Organizations conducted opinion polls, surveys to understand the sentiment and opinion of the general public towards its products or services. In the past few years, web documents are receiving great attention as a new medium that describes individual experiences and opinions. With proliferation of Web 2.0 [1] applications such as micro-blogging, forums and social networks came. Reviews, comments, recommendations, ratings, feedbacks were generated by users. Hence, with the advent of World Wide Web[1] and specifically with the growth and popularity of Web 2.0 where focus shifted to user generated content, the way people express opinion or their view has changed dramatically. People can now make their opinion, views, sentiment known on their personal websites, blogs, social networking sites, forums and review sites. They are comfortable with going online to get advice. Organizations have evolved and now look at review sites to know how the public has received their product instead of conducting surveys. This information available on the Web is a valuable resource for marketing intelligence, social psychologists and others interested in extracting and mining views, moods and attitude [2].

There is a vast amount of information available on the Web which can assist individuals and organization in decision making processes but at the same time present many challenges as organizations and individuals attempt to analyze and comprehend the collective opinion of others. Unfortunately finding opinion sources, monitoring them and then analyzing them are herculean tasks. It is not possible to manually find opinion sources online, extract sentiments from them and then to express them in a standard format. Thus the need to automate this process arises and sentiment analysis [3] is the answer to this need.

Sentiment analysis or Opinion mining, as it is sometimes called, is one of many areas of computational studies that deal with opinion oriented natural language processing. Such opinion oriented studies include among others, genre distinctions, emotion and mood recognition, ranking, relevance computations, perspectives in text, text source identification and opinion oriented summarization [4]. Sentiment analysis has turned out as an exciting new trend in social media with a gamut of practical applications that range from applications in business(marketing intelligence; product and service bench marking and improvement), applications as sub component technology(recommender systems;

[1]World Wide Web Consortium(W3C) www.w3.org/WWW/

summarization; question answering) to applications in politics. It has great potential to be used in business strategies and has helped organizations get a real-time feedback loop about their marketing strategy or advertisements from the reaction of the public through tweets, posts and blogs. For a new product launch it can give them instant feedback about the reception of the new product. It can gauge what their brand image is, whether they are liked or not.

As the field of sentiment analysis is relatively new, the terminology used to describe this field of research is many. The terms opinion mining, subjectivity analysis, review mining and appraisal extraction are used interchangeably with sentiment analysis. Subjectivity analysis or subjectivity classification is focused on the task of whether the sentence or document is expressing opinions or sentiments of the author or just merely stating facts. Majority of the papers which use the phrase "sentiment analysis" focus on the specific application of classifying reviews as to their polarity (either positive or negative) [4]. The term opinion mining was first noticed in a paper by Dave et al. [5]. The paper defined that an opinion mining tool would "process a set of search results for a given item, generating a list of product attributes (quality, features, etc.) and aggregating opinions about each of them (poor, mixed, good)". This definition has been broadened to include various other works in this area. The evolution of the phrase sentiment analysis is similar to that of Opinion Mining. We have used these terms interchangeably in this paper.

Recently a lot of interest has been generated in the field of sentiment analysis, with researchers recognizing the scientific trials and potential applications supported by the processing of subjective language. Some factors substantiated by research till date, that push the development of the research area, include, augmenting of machine learning methods in natural language processing and information retrieval, increase in World Wide Web to provide training datasets for machine learning algorithms and the realization of commercial and intelligent applications that the area provides. As an example of one of the latest applications of sentiment analysis, Twitter[1], Inc. incorporated an advanced tweet-searching function based on sentiment direction, where users can search for positive or negative tweets on a particular topic.

This paper gives an overview of sentiment analysis, its basic terminology, tasks and levels and discusses practical and potential applications of sentiment analysis further expounding its significant open research directions. The paper is organized as follows: the first section introduces sentiment analysis and discusses its history. It is followed by a section which explains the basic terminology. Section 3 expounds how different Web 2.0 applications add dimensions to the sentiment analysis tasks, which are illustrated in section 4 followed by section 5 which explains the granularity at which these tasks can be performed. Section 6 explicates the current state- of- art and describes how machine learning has proved its worth as a technique used for solving the sentiment analysis tasks. Section 7 presents the various applications of sentiment analysis. Lastly, section 8 discusses the various issues that turn out as open problems to be addressed which urge researchers to make significant improvements to understand and work in the sentiment analysis domain.

II. Basic Terminology of Sentiment Analysis

Formally stating Sentiment Analysis is the computational study of opinions, sentiments and emotions expressed in text [3]. The goal of sentiment analysis is to detect subjective information contained in various sources and determine the mind-set of an author towards an issue or the overall disposition of a document.

Wiebe et al. [6] described subjectivity as the linguistic expression of somebody's opinions, sentiments, emotions, evaluations, beliefs and speculations. The words opinion, sentiment, view and belief are used interchangeably but there are subtle differences between them [4].

- *Opinion:* A conclusion thought out yet open to dispute ("each expert seemed to have a different opinion").
- *View:* subjective opinion ("very assertive in stating his views").
- *Belief:* deliberate acceptance and intellectual assent ("a firm belief in her party's platform").
- *Sentiment:* a settled opinion reflective of one's feelings ("her feminist sentiments are well-known").

Sentiment analysis is done on user generated content on the Web which contains opinions, sentiments or views. An opinionated document can be a product review, a forum post, a blog or a tweet, that evaluates an object. The opinions indicated can be about anything or anybody, for e.g. products, issues, people, organizations or a service.

Lui [3] mathematically represented an opinion as a quintuple (o, f, so, h, t), where o is an object; f is a feature of the object o; so is the orientation or polarity of the opinion on feature f of object o; h is an opinion holder; t is the time when the opinion is expressed.

- *Object:* An entity which can be a product, person, event, organization, or topic. The object can have attributes, features or components associated with it. Further on the components can have subcomponents and attributes

[1] http://twitter.com/

- *Feature:* An attribute (or a part) of the object with respect to which evaluation is made.
- *Opinion orientation or polarity:* The orientation of an opinion on a feature f indicates whether the opinion is positive, negative or neutral. Most work has been done on binary classification i.e. into positive or negative. But opinions can vary in intensity from very strong to weak [7]. For example a positive sentiment can range from content to happy to ecstatic. Thus, strength of opinion can be scaled and depending on the application the number of levels can be decided.
- *Opinion holder:* The holder of an opinion is the person or organization that expresses the opinion.

The following example in Fig. 1 illustrates the basic terminology of sentiment analysis:

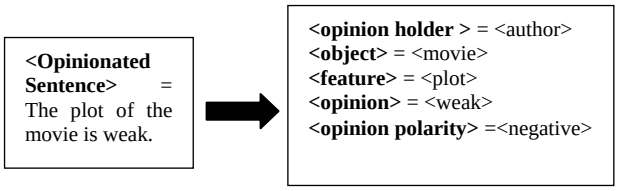

Fig.1 Example corresponding to Terminology of Sentiment Analysis

III. Web 2.0 and Sentiment Analysis

The term Web 2.0 was made popular by Tim O'Rielly in the O'Reilly Media Web 2.0 conference in late 2004. Web 2.0 is an evolution from passive viewing of information to interactive creation of user generated data by the collaboration of users on the Web. Every facet of Web 2.0 is driven by contribution and collaboration. The evolution of Web from Web 1.0 to Web 2.0 was enabled by the rise of read/write platforms such as blogging, social networks, and free image and video sharing sites. These platforms have jointly allowed exceptionally effortless content creation and sharing by anyone.

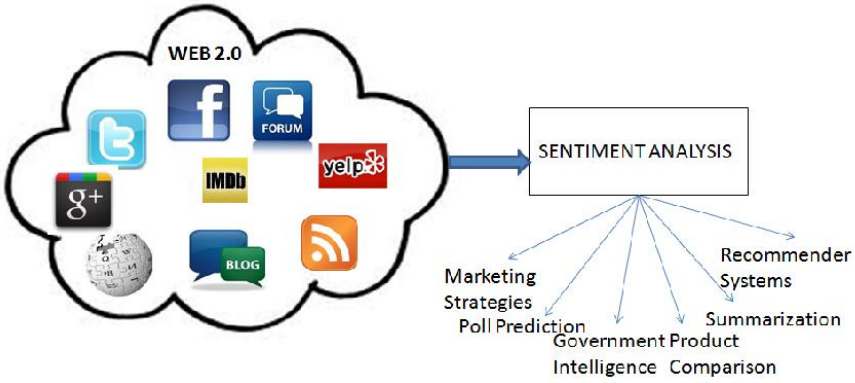

Fig.2 Conceptual model of Sentiment Analysis

The research field of sentiment analysis has been rapidly progressing because of the rich and diverse data provided by Web 2.0 applications. Blogs, review sites, forums, microblogging sites, wikis and social networks have all provided different dimensions to the data used for sentiment analysis.

A. *Review Sites*

A review site is a website which allows users to post reviews which give a critical opinion about people, businesses, products, or services. Most sentiment analysis work has been done on movie and product review sites [5, 7, 9]. The purpose of a review is to appraise a specific object, thus it is a single domain problem. Sentiment analysis on review sites is useful to both manufacturers and potential consumers of the product. The manufacturers can gauge the reception of a product based on the reviews. They can derive the features liked and disliked by the reviewers.

B. *Blogs*

The term web-log or blog, refers to a simple webpage consisting of brief paragraphs of opinion, information, personal diary entries, or links, called posts, arranged chronologically with the most recent first, in the style of an online journal [10]. The bloggers post at hourly, daily or weekly basis which makes the interactions faster and more real-time. Different blogs have different styles of presentation, content material and writing techniques. Sentiment analysis on blogs [11, 12, 13] has been used to predict movie sales, political mood and sales analysis.

C. *Forums*

Forums or message boards allow its members to hold conversations by posting on the site. Forums are generally dedicated to a topic and thus using forums as a database allows us to do sentiment analysis in a single domain.

D. *Social Networks*

Social networking is online services or sites which try to emulate social relationships amongst people who know each other or share a common interest. Social networking sites allow users to share ideas, activities, events, and interests within their individual networks.

Social network posts can be about anything from the latest phone bought, movie watched, political issues or the individual's state of mind. Thus posts give us a richer and more varied resource of opinions and sentiments.

1) *Twitter*

Twitter is an online social networking and micro blogging service that enables its users to send and read text-based posts of up to 140 characters, known as "tweets". Sentiment analysis on twitter [14, 15, 16] is an upcoming trend with it being used to predict poll results [17] among various other applications.

2) *Facebook*

Facebook[1] is a social networking service and website launched in February 2004. The site allows users to create profiles for themselves, upload photographs and videos. Users can view the profiles of other users who are added as their friends and exchange text messages.

Social media is the new source of information on the Web. It connects the entire world and thus people can much more easily influence each other. The remarkable increase in the magnitude of information available calls for an automated approach to respond to shifts in sentiment and rising trends

IV. Sentiment Analysis Tasks

Sentiment analysis is a challenging interdisciplinary task which includes natural language processing, web mining and machine learning. It is a complex task and encompasses several separate tasks, viz:

- Subjectivity Classification
- Sentiment Classification
- Complimentary Tasks
  - Object Holder Extraction
  - Object/ Feature Extraction

Fig. 3 illustrates the major tasks in a sentiment analysis:

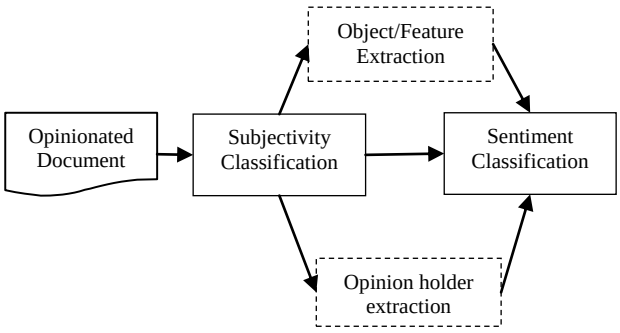

Fig.3 Tasks of Sentiment Analysis

[1] https://www.facebook.com/

The following subsections expound the details of the major tasks in Sentiment Analysis:

A. *Subjectivity classification*

Typically, any given document will contain sentences that express opinion and some that do not. That is, a document is a collection of objective sentences, sentences that state a fact, and subjective sentences, sentences that represents the author's opinion, point of view or emotion. Subjectivity classification is the task of classifying sentences as opinionated or not opinionated [18, 19]. Tang et al. [2], stated subjectivity classification as follows: Let $S = \{s_1, \ldots, s_n\}$ be a set of sentences in document D. The problem of subjectivity classification is to distinguish sentences used to present opinions and other forms of subjectivity (subjective sentences set S_s) from sentences used to objectively present factual information (objective sentences set S_o), where $S_s \cup S_o = S$.

B. *Sentiment Classification*

Once the task of finding whether a piece of text is opinionated is over we have to find the polarity of the text i.e., whether it expresses a positive or negative opinion. Sentiment classification can be a binary classification (positive or negative) [8], multi-class classification (extremely negative, negative, neutral, positive or extremely positive), regression or ranking [9].

Depending upon the application of the sentiment analysis, sub -tasks of opinion holder extraction and object feature extraction are optional. (They have been represented by dashed boxes in Fig. 3).

C. *Opinion Holder Extraction*

Sentiment Analysis also involves elective tasks like opinion holder extraction, i.e. the discovery of opinion holders or sources [20, 21]. Detection of opinion holder is to recognize direct or indirect sources of opinion. They are vital in news articles and other formal documents because multiple opinions can be expressed in the same article corresponding to different opinion holders. In documents like these, the multiple opinion holders may explicitly be mentioned by name. In social networks, review sites and blogs the opinion holder is usually the author who may be identified by the login credentials.

D. *Object /Feature Extraction*

An additional task is the discovery of the target entity. In contrast with review sites, blogs and social media sites tend not have a set intention or predefined topic and are thus, inclined to discuss assorted topics. In such platforms it becomes necessary to know the target entity.

Also as mentioned before target entities can have features or components that are being reviewed. A reviewer can have differing opinions about the different features or components of the target entity. As a result,

feature based sentiment analysis, i.e. extraction of object feature and the related opinion, is an optional task of sentiment analysis [22,23, 24].

V. Levels of Sentiment Analysis

The tasks described in the previous section can be done at several levels of granularity, namely, word level, phrase or sentence level, document level and feature level. The following Fig. 4 depicts the levels of granularity of sentiment analysis.

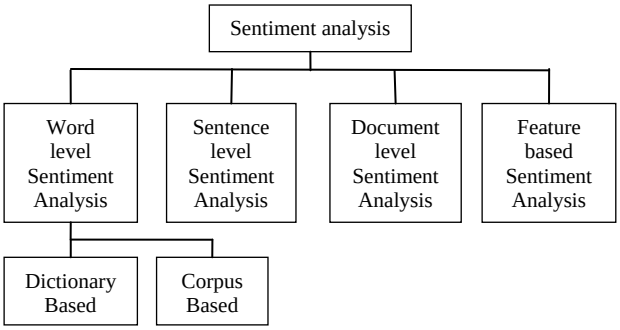

Fig.4 Granularity Levels of Sentiment analysis

The sentiment analysis tasks can be accomplished at the following levels of granularity:

A. *Document Level Sentiment Analysis*

Document-level sentiment analysis considers the whole document as the basic unit whose sentiment orientation is to be determined. To simplify the task, it is presumed that each text's overall opinion is completely held by a single opinion holder and is about a single object. Various machine learning approaches exist for this task. Pang et al. [8] used traditional machine learning methods to classify reviews as positive and negative. They experimented with three classifiers (Naive Bayes, maximum entropy, and support vector machines) and features like unigrams, bigrams, term frequency, term presence and position, and parts-of-speech. They concluded that SVM classifier works best and that unigram presence information was most effective. Document level sentiment analysis has also been formulated as a regression problem by Pang and Lee [9]. Supervised learning was used to predict rating scores. A simple and straightforward method is to find a linear combination of the polarities in the document, as given by Dave et al. [5] and Turney[25].

The difficulty lies in the fact that there could be mixed opinions in a document, and with the creative nature of natural language, people may express the same opinion in vast ways, sometimes without using any opinion words. Also as stated earlier, a text is equally likely to contain objective sentences along with subjective sentences. Therefore, tools are required to extract useful information from subjective sentences instead of objective ones. This leads to sentence level sentiment analysis.

B. *Sentence Level Sentiment Analysis*

At sentence level, research has been done on detection of subjective sentences in a document from a mixture of objective and subjective sentences and then, the sentiment orientation of these subjective sentences is determined. Yu and Hazivassiloglou [26] try to classify subjective sentences and also determine their opinion orientations. For subjective or opinion sentence identification, it uses supervised learning. For sentiment classification of each identified subjective sentence, it used a similar method to Turney[25], but with many more seed words, and log-likelihood ratio as the score function. A simple method used by Liu et al. [27], was to aggregate the orientations of the words in the sentence to get over all polarity of the opinion sentence.

One would expect that subjective sentence detection could be done by using a good sentiment lexicon, but the tricky part is that objective sentences can also contain opinion words

C. *Word Level Sentiment Analysis*

The work to find semantic orientation at phrase level is an important task of sentiment analysis. Most works use the prior polarity [28] of words and phrases for sentiment classification at sentence and document levels. Thus, the manual or semi-automatic construction of semantic orientation word lexicon is popular. Word sentiment classification use mostly adjectives as features but adverbs, and some verbs and nouns are also used by researchers [29, 30]. The two methods of automatically annotating sentiment at the word level are: (1) dictionary-based approaches and (2) corpus-based approaches.

1) *Dictionary based Methods*

In this method, a small seed list of words with known prior polarity is created. This seed list is then extended by extracting synonyms or antonyms iteratively from online dictionary sources like WordNet [1]. Kim and Hovy[31] manually created two seed lists consisting of positive and negative verbs and adjectives. They then expanded these lists by extracting, from WordNet, the synonyms and antonyms of the words of the seed list and assigning them to appropriate list (synonyms were placed in the same list and antonyms in the opposite). The sentiment strength of the words was determined by how the new unseen words interacted with the seed list. Both positive and negative sentiment strengths was computed for each word and their relative magnitudes was compared. Based on WordNet lexical relation, Kamps et al. [32] measured the semantic orientation of words.. They collected words and all their synonyms in WordNet, i.e. words of the same synset. Then a graph was created with edges connecting pairs of synonymous

[1] http://wordnet.princeton.edu/

words. The semantic orientation of a word was calculated by its relative distance from the two seed terms good and bad. The distance was the length of a shortest path between two words w_i and w_j. The values ranged from [-1, 1] with the absolute value indicating the strength of the orientation

The drawback of using a dictionary method is that the polarity classification is not domain specific. For example, "unpredictable" is a positive description for a movie plot but a negative description for a car's steering abilities [25].

2) ***Corpus based Methods***

Corpus based methods rely on syntactic or statistical techniques like co-occurrence of word with another word whose polarity is known. Hatzivassiloglou and McKeown[33] predicted the orientation of adjectives by assuming that pairs of conjoined adjectives have same orientation (if conjoined by and) and opposite orientation (if conjoined by but). Thus they used conjunctions such as "corrupt and brutal" or "simplistic but well-received" to form clusters of similarly and oppositely-oriented words using a log linear regression model. They intuitively assigned the cluster that contained terms of higher average frequency as the positive list. As this method is an unsupervised classification method, the corpus required was immense. Turney [25] assigned semantic orientation by using association. That is it is said to have a positive orientation if they have good associations (e.g. Romantic ambience). The association relationship between an unknown word and a set of manually-selected seeds (like excellent and poor) was used to classify it as positive or negative The degree of association between the unknown word and the seed words was determined by counting the number of results returned by web searches in the AltaVista Search Engine joining the words with the NEAR operator and calculating the point-wise mutual information between them.

With document, sentence and phrase level analysis, we do not know what the opinion holder is expressing opinion on. Furthermore, we do not know the features that are being talked about.

D. ***Feature Based Sentiment Analysis***

In a review, its author talks about the positives and negatives of a product. The reviewer may like some features and dislike some, even though the general opinion of the product may be positive or negative. This kind of information is not provided by document level or sentence level sentiment classification. Thus, feature based opinion sentiment analysis [22, 23, 24] is required. This involves extracting product feature and the corresponding opinion about it. Instinctively, one might think that product features are expressed by nouns and noun phrases, but not all nouns and noun phrases are product features. Yi et al.[29] restricted the candidate words further by extracting only base noun phrases, definite base noun phrase(noun phrases preceded by a definite article "the") and beginning definite base noun phrases(definite base noun phrase at the beginning of a sentence followed by a verb phrase). For each sentiment phrase detected, its target and final polarity is determined based on a sentiment pattern database.

Hu and Lui[30] extract the feature that people are most interested in and thus extract the most frequent noun or noun phrase using association mining. They use simple heuristic method of assigning the nearest opinion word to a feature to determine the sentiment orientation. Popescu and Etzioni[24] greatly improved the task of extracting features. They distinguish between being a part of an object and a property of the object by using WordNet's "is-a" hierarchy and morphological clues. Their algorithm tries to eliminate those noun phrases that probably are not product features. They associated meronymy discriminators with each product class and evaluated noun phrases by computing the PMI (Point-wise Mutual Information) between the phrase and meronymy discriminators.

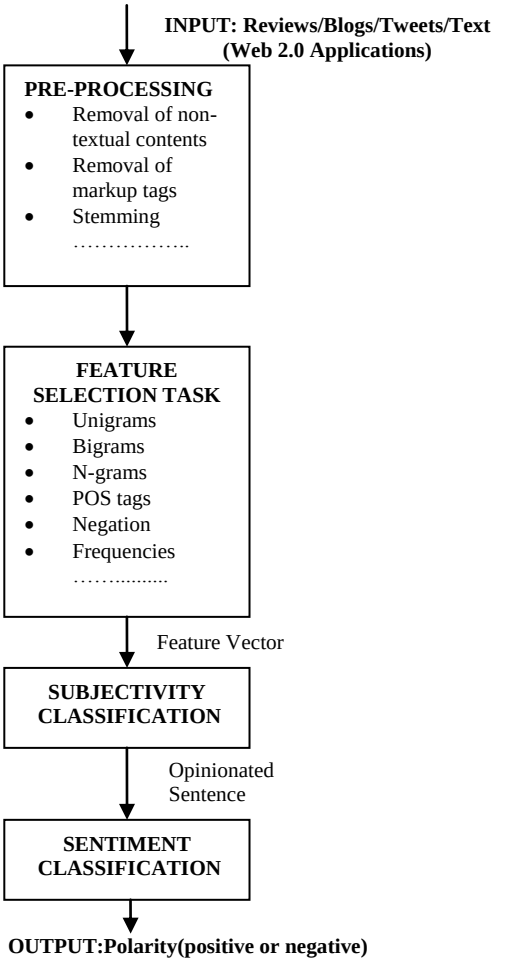

Fig.5 The Sentiment Analysis Model

Table 1 Summary of Sentiment Analysis Tasks

Sentiment Analysis Tasks
At Document Level • Task: Sentiment Classification of whole document • Classes: Positive, negative and neutral • Assumption : Each Document focuses on a single object (not true in discussion posts, blogs ,etc.) and contain opinion from a single opinion holder
At Sentence Level • Task 1: Identifying Subjective/ Objective Sentences o Classes: Objective and Subjective • Task 2: Sentiment Classification of Sentences o Classes: positive and negative o Assumption: A sentence contains only one opinion which may not always be true *Prior polarities of words determined at word level sentiment analysis is used here*
At Feature Level • Task 1: Identify and extract object features that have been commented on by an opinion holder (eg. A reviewer) • Task 2: Determining whether the opinions on features are negative, positive or neutral • Task 3: Find feature synonyms

VI. State-of-Art: The Past and Present of Sentiment Analysis

Most researchers have defined the Sentiment Analysis problem as essentially a text classification problem and machine learning techniques have proved their dexterity in resolving the sentiment analysis tasks [34]. Machine learning techniques require representing the key features of text or documents for processing. These key features are represented as feature vectors which are used for the classification task.. Some examples features that have been reported in literature are:

- **Words and their frequencies**

Unigrams, bigrams and n-grams along with their frequency counts are considered as features. There has been contention on using word presence rather than frequencies to better describe this feature. Pang et al. [8] showed better results by using presence instead of frequencies.

- **Parts of Speech Tags**

Parts of speech like adjectives, adverbs and some groups of verbs and nouns are good indicators of subjectivity and sentiment.

- **Syntax**

Syntactic patterns like collocations are used as features to learn subjectivity patterns by researchers. The syntactic dependency patterns can be generated by parsing or dependency trees.

- **Opinion Words and Phrases**

Apart from specific words, some phrases and idioms which convey sentiments can be used as features, e.g. "cost someone an arm and leg" [3].

- **Position of Terms**

The position of a term within a text can effect on how much the term affects overall sentiment of the text.

- **Negation**

Negation is an important but tricky feature to incorporate. The presence of a negation usually changes the polarity of the opinion but all appearances do it. For e.g., "no doubt it is the best in the market"

As we reviewed the literature for this survey, it was identified that different approaches have been applied to predict the sentiments of words, expressions or documents as to automate the sentiment analysis task. These were either a Natural Language Processing (NLP) research endeavor or addressed by Machine Learning algorithms. Our earlier work [34] probes the role of machine learning as a prominent assisting technology that has ascertained substantial gains in automated sentiment analysis research and practice by developing standards and improving effectiveness. It expounds the unique aspects of the machine learning techniques in sentiment analysis mainly because of the different features involved in case of supervised and semi-supervised techniques. Unsupervised techniques use sentiment driven pattern to obtain labels for words and phrases. While machine learning methods have established to generate good results, there are associated disadvantages. Machine learning classification relies on the training set used, the available literature reports detail classifiers with high accuracy, but they are often tested on only one kind of sentiment source, mostly movie review, thus limiting the performance indication in more general cases. Further, gathering the training set is also arduous; the noisy character of input texts and cross-domain classification add to the complexities and thus push the need for continued development in the area of sentiment analysis.

The research has further substantiated that the existing approaches to sentiment analysis can be grouped into four main categories, namely: *keyword spotting*, where the text is classified in accordance to the presence of reasonably unambiguous affect words; *lexical affinity*, defined as a probabilistic affinity for a particular emotion or opinion polarity to arbitrary words is calculated; *statistical methods*, where the significance of keywords and word co-occurrence frequencies using a large training corpus are computed ; and the most recent *sentic computing* [35], based upon a biologically-inspired and psychologically-motivated affective categorization model which makes use of ontologies and common sense reasoning tools for a conceptual-level analysis of natural language text.

The following Table 2 depicting some previous prominent attempts to study sentiment analysis.

Table 2 Summary of the State-of-Art of Sentiment Analysis

Author	Granularity Level	Model	Features	Data Source
Hatzivassiloglou and McKeown (1997) [33]	Document	Log Linear Regression	Conjunctions and Adjectives	World Street Journal
Das and Chen (2001) [37]	Document	Lexicon and grammar rules	Words	Financial News
Pang et al. (2002) [8]	Document	NB[1], SVM[2], ME[3]	Unigram, bigram, contextual effect of negation, frequency, position	IMBD (Movie Review)
Turney (2002) [25]	Document	PMI-IR[4]	Bigrams	Automobile, bank, movie, travel reviews
Morinaga et al. (2002) [38]	Document	Decision tree induction	Characteristic words, co-occurrence words, and phrases	Cellular phones, PDA and internet service providers
Yi et al. (2003) [22]	Topic	NLP-pattern based	Feature lexical semantics	Digital camera and music reviews
Turney and Littman (2003) [39]	Document	SO-LSA[5], SO-PMI[6], General inquirer	Words and phrases	TASA-ALL corpus(from sources like novel and news articles)
Dave et al. (2003) [5]	Document	Scoring, Smoothing, NB, SVM, ME	Unigrams, bigrams and trigrams	Product reviews
Pang and Lee (2004) [40]	Document	NB, SVM	Unigram; Sentence level subjectivity summarization based on minimum cuts.	Movie Reviews
Kim and Hovy (2004) [31]	Phrase	Probabilistic based		DUC corpus
Gamon (2004) [41]	Document	SVM		Customer feedback
Nigam and Hurst (2004) [42]	Sentence	syntactic rules based chunking	Lexicon of polar phrase and their parts of speech, syntactic pattern	Usenet message board and other online resources
Pang and Lee (2005) [9]	Document	SVM, regression, Metric Labelling		Movie Reviews
Choi et al.(2005) [20]	Extract opinion holder, emotion and sentiment	CRF[7] and AutoSlog	Automatically learned extraction patterns	MQPA corpus
Wilson et al. (2005) [28]	Phrase	BoosTexter	Subjectivity Lexicon	MQPA corpus
Hu and Liu (2005) [23]	Product Feature	Opinion word extraction and aggregation enhanced with WordNet	Opinion words opinion sentences	Amazon Cnn.net
Airoldi et al. (2005) [43]	Document	Two stage Markov Blanket Classifier	Dependence among words, minimal vocabulary	IMBd, Infonic
Aue and Gamon (2005) [30]	Sentence	NB	Stemmed terms, their frequency and weights	Car reviews
Popescu and Etzioni (2005) [24]	Phrase	Relaxation Labelling Clustering	Syntactic dependency template, conjunctions and disjunctions Wordnet	Amazon Cnn.net
Cesarano, (2006) [44]	Sentence	Template based using a hybrid evaluation method	POS, n-grams	Newsarticles, web blogs
K ̈onig and Brill (2006) [45]	Document	Pattern based, SVM, Hybrid		Movie reviews, customer feedback
Kennedy and Inkpen (2006) [46]	Document	SVM, term-counting method, a combination of the two	Term frequencies	General Inquirer dictionary, CTRW dictionary & IMBd
Thomas et al. (2006) [47]	Sentence	SVM	Reference Classification	2005 U.S. floor debate in the House of Representatives

[1] Naïve Bayes
[2] Support Vector Machines
[3] Maximum Entropy
[4] Pointwise Mutual Information and Information Retrieval
[5] Semantic Orientation Latent Semantic Analysis
[6] Semantic Orientation Point wise Mutual Information
[7] Conditional Random Field

Kaji and Kitsuregawa (2007) [36]	Phrase	Phrase trees and word co-occurrence, PMI	lexical relationships, word	HTML documents
Blitzer et al. (2007) [48]	Document	Structural Correspondence Learning	Word frequency and co-occurrence, part of speech	Book, DVD and kitchen appliance product review
Godbole et al. (2007) [49]	Word	Lexical (WordNet)	graph distance measurements between words based on relationships of synonymity and anonymity, commonality of words	Newspaper, blogpost
Annett and Kondrak (2009) [50]	Document	lexical (WordNet) & SVM	number of positive/negative adjectives/adverbs, presence, absence or frequency of words, minimum distance from pivot words	Movie review, blog posts
Zhou and Chaovalit (2008) [51]	Document	ontology-supported polarity mining	n-grams, words, word senses	Movie reviews
Hou and Li (2008) [52]	Sentence	CRF	POS tags, comparative sentence elements	Product reviews, forum discussions; labelled manually and automatically
Ferguson et al. (2009) [53]	Phrase	MNB[1]	binary word feature vectors	Financial blog articles
Tan et al. (2009) [54]	Document	NB Classifier with feature adaptation using Frequently Co-occurring Entropy	words	Education reviews, stock reviews and computer reviews
Wilson et al. (2009) [55]	Phrase	boosting, memory-based learning, rule learning, and support vector learning	words, negation, polarity modification features	MPQA Corpus
Melville et al. (2009) [13]	Document	Bayesian classification with lexicons and training documents	Words	Blog Posts, reviewing software, political blogs, movie reviews
Pak and Paroubek (2010) [15]	Sentence	MNB classifier	N-gram and POS-tags as features	Twitter posts
Barbosa and Feng (2010) [16]	Sentence	SVM	retweet, hashtags, link, punctuation and exclamation marks in conjunction with features like prior polarity of words and POS of words	Twitter posts
Heerschop (2011) [56]	document	Creates a list of adjectives and scored	POS, n-grams, negation	Text documents

[1] Multinomial Naïve Bayes

VII. Applications of Sentiment Analysis

The boom in the availability of opinionated and emotionally charged data from various review sites, blog, forums and social networks has created a wave of interest in sentiment analysis by both academia and businesses. This is because there are many practical and potential applications of sentiment analysis. Sentiment analysis assists organizations and service providers to know the mindset of their customers and users and to accordingly tailor their products and services to the needs of customers and users. It is also of vital interest for scientists such as social psychologists as it allows them to tap into the psychological thinking and responses of online communities. Following is a brief discussion on the potential applications of sentiment analysis:

A. *Bussiness Applications*

Sentiment analysis is being adopted by many businesses who would like an edge and an insight into the "market sentiment" [36]. Potential applications would be extracting product review, brand tracking, modifying marketing strategies and mining financial news. The activities that are aided by sentiment analysis are:

- Automatic tracking of combined user opinions and ratings of brands, products and services from review sites [55].
- Analyzing purchaser inclinations, competitors, and market trends
- Gauging reaction to company-related events and incidents, like during a new product launch it can give them instant feedback about the reception of the new product. It can gauge what their brand image is, whether they are liked or not.
- Monitoring crucial issues to avert harmful viral effects, like dealing with customer complaints that occur in social media and routing the complaints to the particular department that can handle it, before the complaints spread.

Key challenges identified by researchers for this application include, identifying aspects of product, associating opinions with aspects of product, identifying fake reviews and processing reviews with no canonical forms.

B. *Politics*

Sentiment analysis enables tracking of opinion on issues and subjectivity of bloggers in political blogs. Sentiment analysis can help political organization to understand which issues are close to the voter's heart [17]. Thomas et al. [47], try to determine from the transcripts of US Congressional floor debates which speeches support and which are in opposition to proposed legislation. To improve the worth of the information available to voters, the position of public figures, i.e. causes they support or oppose, can also be determined. Mullen and Malouf [58] describe a statistical sentiment analysis method on political discussion group postings to judge whether there is opposing political viewpoint to the original post. Twitter posts have been used to predict election results [59]. Researchers have collectively pointed out some research challenges namely identifying of opinion holder, associated opinion with issues, identifying public figures and legislation.

C. *Recommender System*

Recommender systems can benefit by extracting user rating from text. Sentiment analysis can be used as a sub-component technology for recommender systems by not recommending objects that receive negative feedback [60]. Pang et al. [8] classified movie reviews as "recommended" and "not recommended".

D. *Expert Finding*

There is potential of using sentiment analysis in expert finding systems. Taboada et al. [61], use sentiment analysis techniques to track literary reputation. Piao et al. [62] resolve if an author is referencing a piece of work for substantiation or as research that he or she disregards. Kumar & Ahmad [63] propose mining the expertise from the virtual community using sentiment analysis of each group member's blog & comments received on it. Their combined orientation strength determines the blog score which enables ranking the blogs and identify the expert as the one with the highest blog rank.

E. *Summarization*

Opinion summarization finds application when the number of online review of a product is large. This may make it hard for both the customer and the product manufactured. The consumer may not be able to read all the reviews and make an informed decision and the manufacturer may not be able to keep track of consumer opinion. Liu et al. [27] thus took a set of reviews on a certain product and (i) identified product features commented on (ii) identified review sentences that give opinions for each feature; and (iii) produced a summary using the discovered information. Summarization of single documents [40] or multiple documents (multiple viewpoints) [64] is also an application that sentiment analysis can augment.

F. *Government Intelligence*

Government intelligence is one more application for sentiment analysis. It has been proposed by monitoring sources, the increase in antagonistic or hostile communications can be tracked [65]. For efficient rule making, it can be used to assist in automatically analyzing the opinions of people about pending policies or government-regulation proposals. Other applications include tracking the citizen's opinion about a new scheme, predicting the likelihood of the success of a new legislative reform to be introduced and gauging the mood of the public towards a scandal or controversy.

VIII. Issues and Challenges of Sentiment Analysis

Tackling the fuzzy definition of sentiment and the complexity of its expression in text brings up new questions providing abundant opportunities for quantitative and qualitative work. Major challenges are:

A. *Keyword Selection*

Topic based classification usually uses a set of keywords to classify texts in different classes. In sentiment analysis we have to classify the text in to two classes (positive and negative) which are so different from each other. But coming up with a right set of keyword is not a petty task. This is because sentiment can often be expressed in a delicate manner making it tricky to be identified when a term in a sentence or document is considered in isolation. For example, "If you are reading this because it is your darling fragrance, please wear it at home exclusively, and tape the windows shut." (Review by Luca Turin and Tania Sanchez of the Givenchy perfume Amarige, in *Perfumes: The Guide*, Viking 2008.) No ostensibly negative words occur [4].

B. *Sentiment is Domain Specific*

Sentiment is domain specific and the meaning of words changes depending on the context they are used in. The phrase "*go read the book*" would be considered favorably in a book review, but if expressed in a movie review, it suggests that the book is preferred over the movie, and thus have an opposite result [4].

C. *Multiple Opinions in a Sentence*

Single sentence can contain multiple opinions along with subjective and factual portions. It is helpful to isolate such clauses. It is also important to estimate the strength of opinions in these clauses so that we can find the overall sentiment in the sentence, e.g, "*The picture quality of this camera is amazing and so is the battery life, but the viewfinder is too small for such a great camera*", expresses both positive and negative opinions [4].

D. *Negation Handling*

Handling negation can be tricky in sentiment analysis. For example, "*I like this dress*" and "*I don't like this dress*" differ from each other by only one token but consequently are to be assigned to different and opposite classes. Negation words are called polarity reversers and papers [36, 45] have tried to model negation accurately. But there are many complex polarity reversers like "avoid" in *"[it] avoids all cliché's and predictability found in Hollywood movies*" [4] that have to be addressed.

E. *Sarcasm*

Sarcasm and irony are very quiet difficult to identify. Sarcasm is a very often used in social media.eg *"thank you Janet Jackson for yet another year of Super Bowl classic rock!"* (Twitter). This refers to the supposedly lame music performance in super bowl 2010 and attributes it to the aftermath of the scandalous performance of Janet Jackson in the previous year [66].

F. *Implicit Opinion*

Sentiment that appears in text can be characterized as: explicit where the subjective sentence directly conveys an opinion "*We had a wonderful time*", and implicit where the sentence implies an opinion *"The battery lasted for 3 hours"*. Present sentiment analysis models will not be able to detect this implicit opinion as a negative opinion.

G. *Comparative Sentences*

A comparative sentence expresses a relation based on similarities or differences of more than one object [3]. Research on classifying a comparative sentence as opinionated or not is limited. Also the order of words in comparative sentences manifests differences in the determination of the opinion orientation. E.g. The sentence, "*Car X is better than Car Y*" communicates a completely opposite opinion from "*Car Y is better than Car X*".

H. *Multilingual Sentiment analysis*

Most sentiment analysis research has focused on data in the English language, mainly because of the availability of resources like lexicons and manually labeled corpora. As only 26.8 % of Internet users speak English[1], the construction of resources and tools for subjectivity and sentiment analysis in languages other than English is a growing need. Several methods have been proposed to leverage on the resources and tools available in English by using cross-lingual projections [67].

I. *Opinion Spam*

Opinion spam refers to fake or bogus opinions that try to deliberately mislead readers or automated systems by giving undeserving positive opinions to some target objects in order to promote the objects and/or by giving malicious negative opinions to some other objects in order to damage their reputations [3]. Many review aggregation sites try to recognize opinion spam by procuring the helpfulness or utility score of each review from the reader by asking them to provide helpfulness feedbacks to each review ("Was this review helpful?").

IX. Conclusion

This paper illustrates the research area of Sentiment Analysis and its latest advances. It affirms the terminology, the major tasks, the granularity levels, and applications of sentiment analysis. It also discusses the impact of Web 2.0 applications on this research field. Most work has been done on product reviews – documents that have a definite topic. More general writing with varied domains, such as blog posts, tweets, posts and web pages, have recently been creating & receiving attention. Future work in expanding existing techniques to handle more general writings and crossing domains is an exciting opportunity for both academia and businesses.

References

[1] Tim O'Reilly, Web 2.0 Compact Definition: Trying Again (O'Reilly Media, Sebastopol), http://radar.oreilly.com/archives/2006/12/web_20_compact.html. Accessed 22 Mar 2007

[2] Tang H, Tan S, and Cheng X. A survey on sentiment detection of reviews. Expert Systems with Applications: An International Journal, September 2009, 36(7):10760–10773.

[3] Liu B. Sentiment Analysis and Subjectivity. Handbook of Natural Language Processing, Second edition, 2010

[4] Pang, B and Lee L. Opinion mining and sentiment analysis. Foundations and Trends in Information Retrieva,l 2008,(1-2),1–135

[1] http://www.internetworldstats.com/stats7.htm

[5] Dave K., Lawrence S, and Pennock D.M. Mining the peanut gallery: Opinion extraction and semantic classification of product reviews. In Proceedings of of the 12th international conference on World Wide Web(WWW), 2003, pp.:519–528

[6] Wiebe, J., Wilson, T., Bruce, R., Bell, M., and Martin, M. Learning subjective language. Computational Linguistics, 2004, 30(3):277–308

[7] Theresa Wilson, Janyce Wiebe, and Rebecca Hwa. Just how mad are you? Finding strong and weak opinion clauses. In Proceedings of AAAI, 2004,pages 761–769.

[8] Pang, B., Lee, L., and Vaithyanathan.S. Thumbs up? Sentiment classification using machine learning techniques. In Proceedings of the Conference on Empirical Methods in Natural Language Processing, 2002, (EMNLP):79–86.

[9] Pang B. and Lee L. Seeing stars: Exploiting class relationships for sentiment categorization with respect to rating scales, Proceedings of the Association for Computational Linguistics (ACL),2005:115–124

[10] Anderson, P. What is Web 2.0? Ideas, technologies and implications for education. Technical report, JISC,2007

[11] Mishne G. and Glance N. Predicting movie sales from blogger sentiment. In AAAI Symposium on Computational Approaches to Analyzing Weblogs (AAAI-CAAW),2006: 155–158.

[12] Liu, Y., Huang, J., An, A., and Yu, X. ARSA: A sentiment-aware model for predicting sales performance using blogs. In Proceedings of the ACM Special Interest Group on Information Retrieval (SIGIR),2007

[13] Melville, P., Gryc, W., and Lawrence, R.D. Sentiment analysis of blogs by combining lexical knowledge with text classification. In Proceedings of the 15th ACM SIGKDD international conference on Knowledge discovery and data mining.2009: 1275-1284.

[14] Go, A., Bhayani, R., Huang, L. Twitter sentiment classification using distant supervision. Technical report, Stanford Digital Library Technologies Project.2009.

[15] Pak A. and Paroubek P. Twitter as a corpus for sentiment analysis and opinion mining. In Proceedings of the Seventh Conference on International Language Resources and Evaluation, .2010:1320-1326.

[16] Barbosa, L. and Feng, J. Robust Sentiment Detection on Twitter from Biased and Noisy Data. COLING 2010: Poster Volume, 36-44.

[17] O'Connor B., Balasubramanyan R., Routledge B.R., Smith N. A. From Tweets to Polls: Linking Text Sentiment to Public Opinion Time Series. AAAI. 2010

[18] Hatzivassiloglou, V. and Wiebe, J. Effects of adjective orientation and gradability on sentence subjectivity. In Proceedings of the International Conference on Computational Linguistics (COLING), 2000.

[19] Riloff E. and Wiebe J., Learning extraction patterns for subjective expressions.Proceedings of the Conference on Empirical Methods in Natural Language Processing (EMNLP) , 2003.

[20] Choi, Y., Cardie, C., Riloff, E., and Patwardhan, S., Identifying sources of opinions with conditional random fields and extraction patterns. Proceedings of the Human Language Technology Conference and the Conference on Empirical Methods in Natural Language Processing (HLT/EMNLP), 2005.

[21] Bethard, S., Yu, H., Thornton, A., Hatzivassiloglou, V., and Jurafsky, D., Automatic extraction of opinion propositions and their holders. Proceedings of the AAAI Spring Symposium on Exploring Attitude and Affect in Text, 2004.

[22] Yi, J., Nasukawa, T., Niblack, W., &Bunescu, R.,Sentiment analyzer: extracting sentiments about a given topic using natural language processing techniques. Proceedings of the 3rd IEEE international conference on data mining (ICDM 2003):427–434

[23] Hu, M. and Liu, B. Mining opinion features in customer reviews. In Proceedings of AAAI, 2004: 755–760.

[24] Popescu A-M. and Etzioni O., Extracting product features and opinions from reviews, Proceedings of the Human Language Technology Conference and the Conference on Empirical Methods in Natural Language Processing (HLT/EMNLP),2005

[25] Turney P. Thumbs up or thumbs down? Semantic orientation applied to unsupervised classification of reviews. In Proceedings of the Association for Computational Linguistics (ACL), 2005: 417–424.

[26] Yu H. and Hatzivassiloglou V., Towards answering opinion questions: Separating facts from opinions and identifying the polarity of opinion sentences.In Proceedings of the Conference on Empirical Methods in Natural Language Processing (EMNLP), 2003.

[27] Liu, B., Hu, M., & Cheng, J. Opinion observer: Analyzing and comparing opinions on the web. In Proceedings of the 14th international world wide web conference (WWW-2005). ACM Press: 10–14.

[28] Wilson T., Wiebe J., and Hoffmann P.,Recognizing contextual polarity in phrase-level sentiment analysis. In Proceedings of the Human Language Technology Conference and the Conference on Empirical Methods in Natural

Language Processing (HLT/EMNLP)2005: 347–354

[29] Esuli, A., & Sebastiani, F. Determining the semantic orientation of terms through gloss classification.In Proceedings of CIKM-05, the ACM SIGIR conference on information and knowledge management, Bremen, DE, 2005.

[30] Aue, A. and Gamon, M., Customizing sentiment classifiers to new domains: A case study. Proceedings of Recent Advances in Natural Language Processing (RANLP),2005.

[31] Kim, S. and Hovy, E., Determining the sentiment of opinions.In Proceedings of the International Conference on Computational Linguistics (COLING) ,2004

[32] Kamps, J., Marx, M., Mokken, R.J., de Rijke, M., Using WordNet to measure semantic orientation of adjectives. In Language Resources and Evaluation (LREC),2004.

[33] Hatzivassiloglou, V. and McKeown, K., Predicting the semantic orientation of adjectives. In Proceedings of the Joint ACL/EACL Conference,2004: 174–181

[34] Kumar, A. & Sebastian, T.M., Machine learning assisted Sentiment Analysis. Proceedings of International Conference on Computer Science & Engineering (ICCSE'2012), 123-130, 2012.

[35] Cambria, Erik. Roelandse, Martijn. ed. Sentic Computing: Techniques, Tools and Applications. Berlin: Springer-Verlag., 2012.

[36] Kaji, N. and Kitsuregawa, M., Building lexicon for sentiment analysis from massive collection of html documents. Proceedings of the Conference on Empirical Methods in Natural Language Processing, 2007.

[37] Das, S. and Chen, M., Yahoo! for Amazon: Extracting market sentiment from stock message boards. In Proceedings of the Asia Pacific Finance Association Annual Conference (APFA),2 001.

[38] Morinaga S., Yamanishi K., Tateishi K., and Fukushima T., Mining product reputations on the web.In Proceedings of the ACM SIGKDD Conference on Knowledge Discovery and Data Mining (KDD), 2002: 341–349, Industry track

[39] Turney, P. and Littman, M., Measuring praise and criticism: Inference of semantic orientation from association. ACM Transactions on Information Systems (TOIS),2003, 21(4):315–346.

[40] Pang B. and Lee L., A sentimental education: Sentiment analysis using subjectivity summarization based on minimum cuts. In Proceedings of the Association for Computational Linguistics (ACL), 2004: 271–278.

[41] Gamon, M,. Sentiment classification on customer feedback data: noisy data, large feature vectors, and the role of linguistic analysis. In Proceedings of the International Conference on Computational Linguistics (COLING), 2004.

[42] Nigam, K. and Hurst, M.,.Towards a robust metric of opinion.The AAAI Spring Symposium on Exploring Attitude and Affect in Text,2004

[43] Airoldi, E. M., Bai, X., and Padman, R., Markov blankets and meta-heuristic search: sentiment extraction from unstructured text. Lecture Notes in Computer Science,2006, 3932: 167–187.

[44] Cesarano, C., Dorr, B., Picariello, A., Reforgiato, D., Sagoff, A., Subrahmanian, V.: OASYS: An Opinion Analysis System. AAAI Press In: AAAI Spring Symposium on Computational Approaches to Analyzing Weblogs (CAAW 2006): 21–26.

[45] K ̈onig, A. C. & Brill, E., Reducing the human overhead in text categorization. In proceedings of the 12th ACM SIGKDD conference on knowledge discovery and data mining,2006, pp: 598–603.

[46] Kennedy, A. and Inkpen, D., Sentiment classification of movie reviews using contextual valence shifters. Computational Intelligence, 22(2, Special Issue on Sentiment Analysis), 2006: 110–125.

[47] Thomas M, Pang B., and Lee L., Get out the vote: Determining support or opposition from Congressional floor-debate transcripts. In Proceedings of the Conference on Empirical Methods in Natural Language Processing (EMNLP), 2006: 327–335.

[48] Blitzer, J., McDonald, R., and Pereira, F., Domain adaptation with structural correspondence learning. In Empirical Methods in Natural Language Processing (EMNLP), 2006.

[49] Godbole, N., Srinivasaiah, M., and Skiena, S., Large-scale sentiment analysis for news and blogs. Proceedings of the International Conference in Weblogs and Social Media, 2007.

[50] Annett, M. and Kondrak, G. A comparison of sentiment analysis techniques: Polarizing movie blogs. Advances in Artificial Intelligence,2008, 5032:25–35.

[51] Zhou, L. and Chaovalit, P., Ontology-supported polarity mining.Journal of the American Society for Information Science and Technology,2008, 69:98–110.

[52] Hou, F. and Li, G.-H., Mining chinese comparative sentences by semantic role labeling. Proceedings of the Seventh International Conference on Machine Learning and Cybernetics, 2008.

[53] Ferguson, P., O'Hare, N., Davy, M., Bermingham, A., Tattersall, S., Sheridan, P., Gurrin, C., and Smeaton, A. F., Exploring the use of paragraph-level annotations for sentiment analysis in financial blogs.1st Workshop on Opinion Mining and Sentiment Analysis (WOMSA),2009.

[54] Tan, S., Cheng, Z., Wang, Y., and Xu, H., Adapting naive bayes to domain adaptation for sentiment analysis. Advances in Information Retrieval, 2009, 5478:337–349.

[55] Wilson, T., Wiebe, J., and Hoffmann, P., Recognizing contextual polarity: an exploration of features for phrase-level sentiment analysis. Computational Linguistics, 2009, 35(5):399–433

[56] Heerschop, B., Hogenboom, A., and Frasincar, F. Sentiment lexicon creation from lexical resources, Springer, In 14th International Conference on Business Information Systems (BIS 2011), volume 87 of Lecture Notes in Business Information Processing: 185–196.

[57] Chen Y. Y. and Lee K. V., User-Centered Sentiment Analysis on Customer Product Review. World Applied Sciences Journal 12 (Special Issue on Computer Applications & Knowledge Management),2011: 32-38

[58] Mullen T. and Malouf R.,Taking sides: User classification for informal online political discourse. Internet Research, 2008, 18:177–190.

[59] Tumasjan A., Sprenger T.O., Sandner P.G., Welpe I. M., Predicting Elections with Twitter: What 140 Characters Reveal about Political Sentiment. AAAI ,2010

[60] Terveen L., Hill W., Amento B., McDonald D., and Creter J., PHOAKS: A system for sharing recommendations. In Communications of the Association for Computing Machinery (CACM),2007, 40(3):59–62

[61] Taboada M., Gillies M. A., and McFetridge P., Sentiment classification techniques for tracking literary reputation.In LREC Workshop: Towards Computational Models of Literary Analysis, 2006: 36–43.

[62] Piao S., Ananiadou S., Tsuruoka Y., Sasaki Y., and McNaught J., .Mining opinion polarity relations of citations. In International Workshop on Computational Semantics 84 (IWCS), 2007:366–371.

[63] Kumar, A. & Ahmad, N. ComEx Miner: Expert Mining in Virtual Communities, International Journal of Advanced Computer Science and Applications (IJACSA), Vol.3, No. 6, June 2012, The Science and Information Organization Inc, USA.

[64] Seki Y., Eguchi K., Kando N., and Aono M., Multi-document summarization with subjectivity analysis at DUC 2005. In Proceedings of the Document Understanding Conference (DUC).

[65] Spertus E., Smokey: Automatic recognition of hostile message. In Proceedings of Innovative Applications of Artificial Intelligence (IAAI),1997: 1058–1065.

[66] Davidov, D., Tsur, O., and Rappoport, A., Semi-supervised recognition of sarcastic sentences in twitter and amazon. In Conference on Natural Language Learning (CoNLL), 2010.

[67] Denecke, K.., Using SentiWordNet for Multilingual Sentiment Analysis .Proc. of the IEEE 24th International Conference on Data Engineering Workshop (ICDEW 2008), IEEE Press:507-512.

Authors' Profile

Akshi Kumar is a PhD in Computer Engineering from University of Delhi. She has received her MTech (Master of Technology) and BE (Bachelor of Engineering) degrees in Computer Engineering. She is currently working as a University Assistant Professor in Dept. of Computer Engineering at the Delhi Technological University, Delhi, India. She is editorial review board member for '*The International Journal of Computational Intelligence and Information Security'*, Australia, ISSN: 1837-7823; *'International Journal of Computer Science and Information Security'*, USA, ISSN: 1947-5500; '*Inter-disciplinary Journal of Information, Knowledge & Management'*, published by the Informing Science Institute, USA. (ISSN Print 1555-1229, Online 1555-1237) and '*Webology*', ISSN 1735-188X. She is a life member of Indian Society for Technical Education (ISTE), India, a member of International Association of Computer Science and Information Technology (IACSIT), Singapore, a member of International Association of Engineers (IAENG), Hong Kong, a member of IAENG Society of Computer Science, Hong Kong and a member of Internet Computing Community (ICC), AIRCC. She has many publications to her credit in various journals with high impact factor and international conferences. Her current research interests are in the area of Web Search & Mining, Intelligent Information Retrieval, Web 2.0 & Web Engineering.

Teeja Mary Sebastian is doing M.Tech (Master of Technology) in Computer Technology & Application from Delhi Technological University, Delhi, India and has done her B.Tech (with Distinction) also in Computer Engineering; she is currently working as a scholar in the field of Sentiment Analysis.

SINGLE OTRA BASED PD CONTROLLERS

RAJESHWARI PANDEY

Department of Electronics and Communication Engineering , Delhi Technological University ,

Shahbad Daulatpur, Bawana Road,
Delhi, 110042, India
rajeshwaripandey@gmail.com

SAURABH CHITRANSHI

Department of Electronics and Communication Engineering , Delhi Technological University ,

Shahbad Daulatpur, Bawana Road,
Delhi, 110042, India
chitransi.dtu@gmail.com

NEETA PANDEY

Department of Electronics and Communication Engineering , Delhi Technological University ,

Shahbad Daulatpur, Bawana Road,
Delhi, 110042, India
neetapandey@dce.ac.in

CHANDRA SHEKHAR

Department of Electronics and Communication Engineering , Delhi Technological University ,

Shahbad Daulatpur ,Bawana Road,
Delhi, 110042, India

csr.dtu@gmail.com

Abstract:

This paper presents a single Operational transresistance (OTRA) based voltage-mode proportional-derivative (PD) controller with independent tuning of proportional (Kp) and derivative (Kd) constants. This configuration can be made fully integrated by implementing the resistors using matched transistors operating in linear region. In order to verify the proposed circuit a closed loop control system using the proposed PD controller is designed and simulated using SPICE.

Key Words: OTRA, MOS implementation of a linear resistance, PD Controller, Second order LPF.

1. Introduction

The derivative (D) controllers with adjustable parameters are used to control integrating systems and systems with inertia. In either situation, pure derivative control is not used, for it is too fragile. Instead, proportional and derivative controls are mixed together to maximize the stability. Motor control and robot manipulators are examples of PD controllers.

Literature survey reveals that number of circuits have been reported relating to proportional (P), proportional integral (PI), proportional derivative (PD), and proportional integral & derivative (PID) controllers [1]–[7]. Circuits presented in [1],[2] are based on op-amps and have their own limitation of finite gain bandwidth.

Reference [3] presents OTA based controllers and [4] presents CDBA based controllers whereas CCII based controllers are proposed in [5]-[7]. In this paper an OTRA based controllers has been presented.

It is well known that inherent wide bandwidth which is virtually independent of closed loop gain, greater linearity, and large dynamic range is the key performance features of current mode technique [8]. Operational Transresistance Amplifier (OTRA) is a high gain current input, voltage output amplifier [9]. OTRA, being a current processing analog building block, inherits all the advantages of current mode technique. It is also free from parasitic input capacitances and resistances as its input terminals are virtually grounded and hence, non-ideality problem is less in circuits implemented using OTRA. Several high performance CMOS OTRA topologies have been proposed in literature [9]-[12] leading to growing interest in OTRA based analog signal processing circuits. In recent past OTRA has been extensively used as an analog building block for realizing a number of signal processing circuits such as filters[13]-[16], oscillators[17]-[19], multivibrators [20],[21] and immittance simulation circuits[17],[22]-[24].

This paper aims at presenting a PD controller using single OTRA two resistors and a capacitor having orthogonally tunable proportional and derivative constants. These circuits can be made fully integrated by implementing the resistors using MOS transistors operating in non-saturation region.

2. Circuit Description

2.1. *PD controller*

In PD controller as shown in Fig.1, the actuating signal, a(t) is sum of proportional to the error signal, e(t) and the derivative of e(t). Representing in s-domain can be written as

$$G_c(s) = K_p + K_d\, s \tag{1}$$

where KP and Kd are the proportional and derivative constants, respectively.(1) can alternatively be represented as

$$G_c(s) = K_p(1 + T_d\, s) \tag{2}$$

where Td=Kd / Kp. The amplitude M(ω) and phase Φ(ω) characteristics of (2) are given by

$$M(\omega) = K_p\sqrt{1 + (\omega T_d)^2} \tag{3}$$

$$\Phi(\omega) = \mathrm{arctg}(\omega T_d) \tag{4}$$

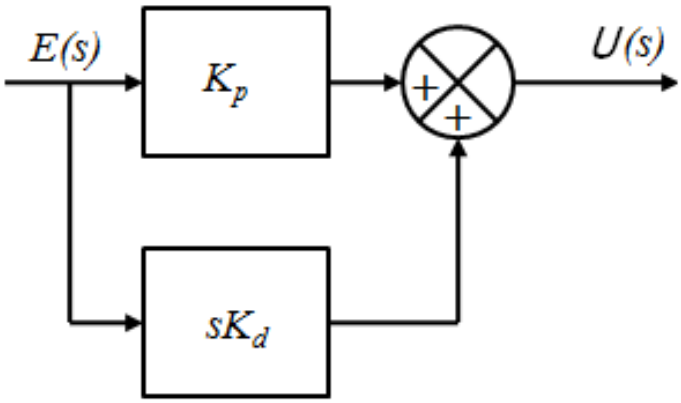

Fig. 1.Block Diagram of PD Controller

2.2. *OTRA based PD controller*

OTRA is a three terminal device [10] shown symbolically in Fig.2 and its port relations can be characterized by matrix (5).

$$\begin{bmatrix} V_p \\ V_n \\ V_o \end{bmatrix} = \begin{bmatrix} 0 & 0 & 0 \\ 0 & 0 & 0 \\ R_m & -R_m & 0 \end{bmatrix} \begin{bmatrix} I_p \\ I_n \\ I_o \end{bmatrix} \tag{5}$$

For ideal operations the transresistance gain Rm approaches infinity and forces the input currents to be equal. Thus OTRA must be used in a negative feedback configuration [9],[10].

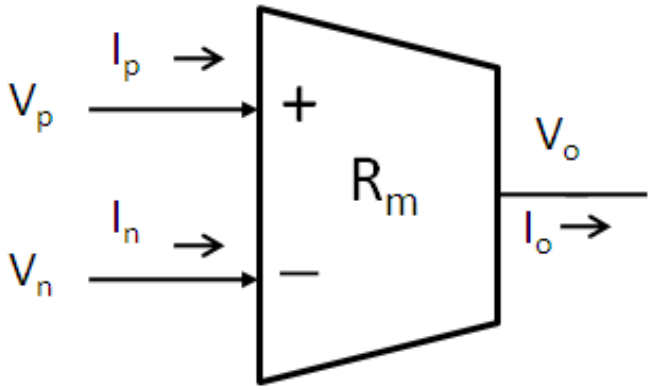

Fig. 2.OTRA Symbol

Proposed PD controller is shown in Fig. 3. The routine analysis of this controller gives the following voltage transfer function

$$\frac{V_o}{V_i} = \frac{R_f}{R} + sCR_f \tag{6}$$

And results in

$$K_p = \frac{R_f}{R} \quad K_d = CR_f \tag{7}$$

From the above equation it is clear that by varying R, Kp value can be adjusted independent of Kd and by simultaneous variation of Rf and R, Kd can be independently controlled.

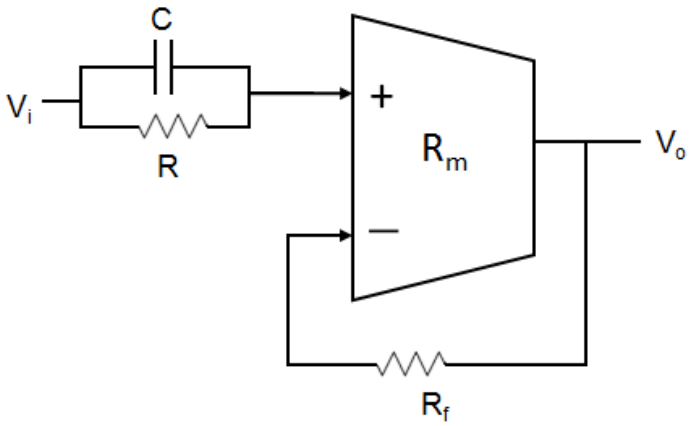

Fig. 3.Proposed PD Controller

These parameters can be electronically tuned by implementing the linear passive resistors using MOS transistors operating in non-saturation region. The resistance value may be adjusted by appropriate choice of gate voltages.

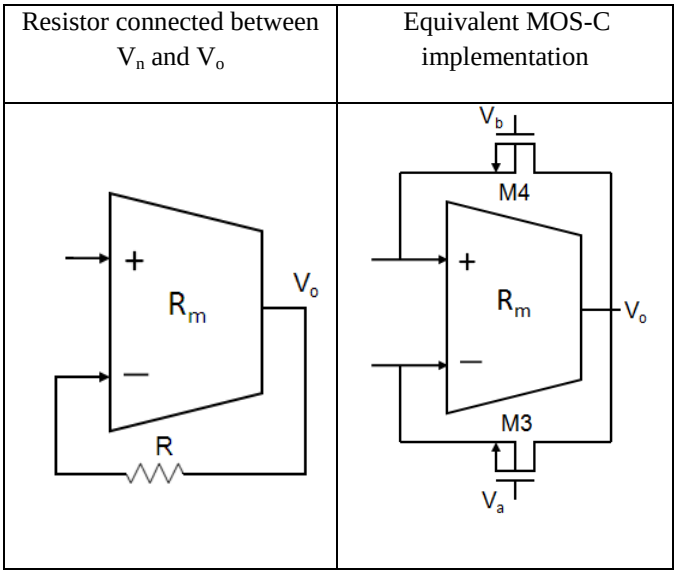

Fig. 4. MOS implementation of a Linear resistance.

The resistors connected to the input terminals of OTRA can easily be implemented using MOS transistors with complete non-linearity cancellation [10]. Fig. 4 shows a typical MOS implementation of resistance connected between negative input and output terminals of OTRA.

The equivalent resistance value is given as

$$R = {}^{1}\Big/_{\mu_n C_{ox}\left({}^{W}\Big/_{L}\right)(V_a - V_b)} \tag{8}$$

where μ_n, C_{ox}, W and L are electron mobility, oxide capacitance per unit gate area, effective channel width, and effective channel length respectively which may be expressed as

$$\mu_n = \frac{\mu_0}{1+\theta(V_{GS}-V_T)} \tag{9}$$

$$C_{ox} = \frac{\varepsilon_{ox}}{T_{ox}} \tag{10}$$

$$W = W_{drawn} - 2W_D \tag{11}$$

$$L = L_{drawn} - 2L_D \tag{12}$$

Va and Vb are the gate voltages and other symbols have their usual meaning. Fig. 5 shows the MOS-C implementation of the circuit of Fig.3.

3.Non-Ideality Analysis

The non-idealities associated with OTRA based circuits may be divided into two groups. The first group results due to finite trans-resistance gain whereas the second one concerns with the nonzero impedances of p and n terminals of OTRA.

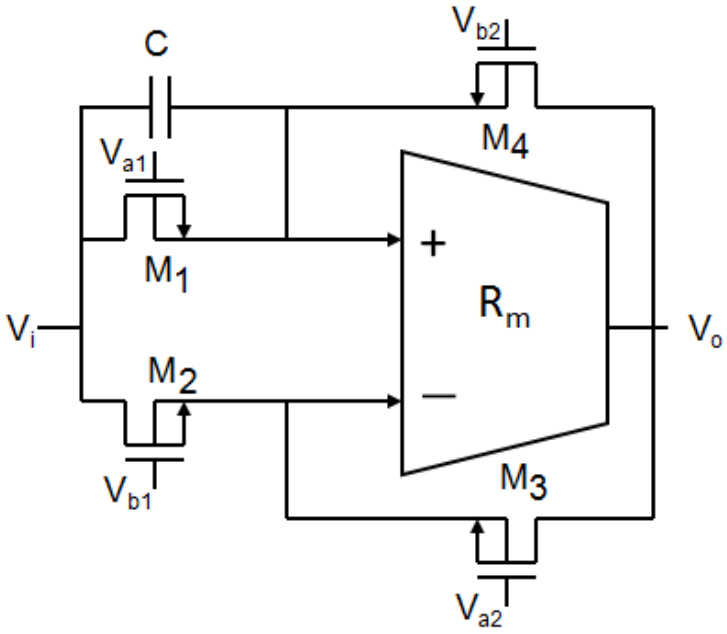

Fig. 5.MOS-C equivalent of Proposed PD Controller

3.1Non- Ideality due to Finite Transresistance Gain

Here the effect of finite trans-resistance gain (R_m) on PD controller is considered and for high frequency applications passive compensation is employed. Ideally the R_m is assumed to approach infinity. However, practically Rm is a frequency dependent finite value. Considering a single pole model for the trans-resistance gain, it can be expressed as

$$R_m = \frac{R_o}{1+{}^{s}/_{\omega_o}} \tag{13}$$

where R_0 is dc transresistance gain.
For high frequency applications the trans-resistance gain, reduces to

$$R_m(s) \approx \frac{1}{sC_p} \quad \text{where} \quad C_p = \frac{1}{R_0\omega_0} \tag{14}$$

Taking this effect into account (6) modifies to

$$\frac{V_o}{V_i} = \frac{R_f}{R(1+sC_pR_f)} + sC\frac{R_f}{1+sC_pR_f} \tag{15}$$

For high-frequency applications, compensation methods must be employed to account for the error introduced in (4). Considering the circuit shown in Fig.6, equation (15) modifies to

$$\frac{V_o}{V_i} = \frac{R_f}{R(1+R_f(sC_p-sY))} + \frac{sCR_f}{1+R_f(sC_p-sY)} \tag{16}$$

By taking Y = C_p, (16) reduces to (6). The effect of R_m can thus be eliminated by connecting a single capacitor between the non inverting terminal and the output as shown in Fig.6, and the passive compensation can be achieved.

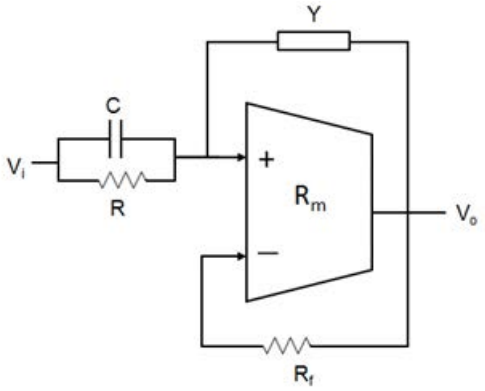

Fig. 6.Compensated PD Controller

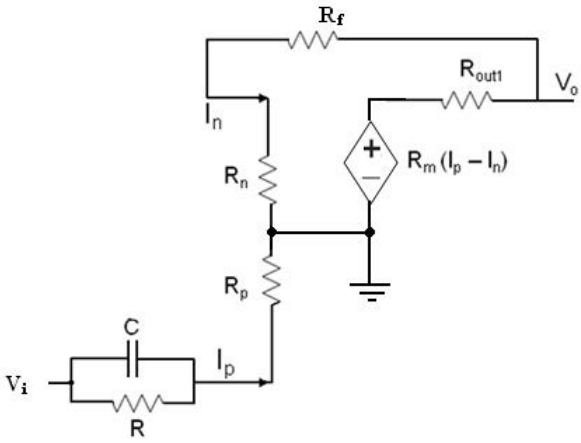

Fig. 7 AC equivalent of proposed PD Controller

3.2 Effect of Nonzero Impedances of p and n Terminals

Ideally input as well as output resistances are assumed to be zero. To consider the effect of and non zero values of input resistances (R_n and R_p) and output resistances (R_{out1}) on proposed PD controller AC equivalent of the controller using AC equivalent of OTRA is drawn and is shown in fig 7.

Routine analysis of Fig. 6(a) results in terminal currents I_p and I_n as

$$I_p = \frac{V_i(1+sCR)}{R+R_p+sCRR_p} \tag{17}$$

$$I_n = \frac{V_o}{R_f+R_n} \tag{18}$$

Thus the output voltage V_o can be written as

$$V_o = R_m(I_p - I_n) - R_{out1}I_n \tag{19}$$

$$V_o = R_mI_p - (R_m + R_{out1})I_n \tag{20}$$

As $R_m >> R_{out1}$ so $R_m+R_{out1} \approx R_m$ and hence

$$V_o \approx R_m(I_p - I_n) \tag{21}$$

Substituting I_p and I_n, (21) results in

$$V_o = R_m\left(\frac{V_i(1+sCR)}{R+R_p+sCRR_p} - \frac{V_o}{R_f+R_n}\right) \tag{22}$$

$$\frac{V_o}{V_i} = \frac{R_m(1+sCR)}{(R+R_p)\left(1+\frac{sCRR_p}{R+R_p}\right)\left(1+\frac{R_m}{R_f+R_n}\right)} \tag{23}$$

As $R >> R_p$, $R_m >> (R_f + R_n)$ and $R_f >> R_n$ and so (23) yields

$$\frac{V_o}{V_i} \approx \frac{R_m(1+sCR)}{R(1+sCR_p)\frac{R_m}{R_f}} \tag{24}$$

$$= \frac{R_f(1+sCR)}{R(1+sCR_p)} \tag{25}$$

Comparing (25) with (6) it is observed a parasitic pole with pole frequency $1/R_pC$ is introduced. The parasitic pole frequency would be much beyond the zero frequency (1/CR) for a selection of $R>>R_p$, and would not influence the performance of the system.

4. Simulation Results

In order to verify the theoretical propositions simulations are performed using PSPICE program. For simulation CMOS implementation of the OTRA proposed in [12] was used. The SPICE simulation was performed using 0.18µm, Level 7, CMOS process parameters provided by MOSIS and supply voltages taken are ±1.5 V. For the proposed controller shown in Fig. 3, the values of passive element are chosen as R = 10KΩ, R_f = 20KΩ and C = 20pF. For time domain analysis, a 3mV peak triangular input voltage is applied. For this input the output of the proposed controller would be given by

$$V_o(t) = \left(\frac{R_f}{R}\right).V_i(t) + CR_f\frac{dV_i(t)}{dt} \quad (26)$$

Both ideal and simulated results are presented in Fig. 8a and are found in agreement with (26). In the magnitude response of the proposed controller given by (3) first term is dominant for low frequencies ($\omega << 1/T_d$) and thus would result in a constant output ($\approx 20 \log K_p$) whereas for high frequencies ($\omega >> 1/T_d$) the second term of the response becomes effective and the output would be represented by a straight line having a slope of 20dB/decade. Similarly for phase response for low frequencies phase would be 0° , at $\omega = 1/T_d$ it would be 45° and would approach 90° for extremely high frequencies. It is observed that the frequency domain response of the proposed controller shown in fig.8b is in close agreement to above discussion.

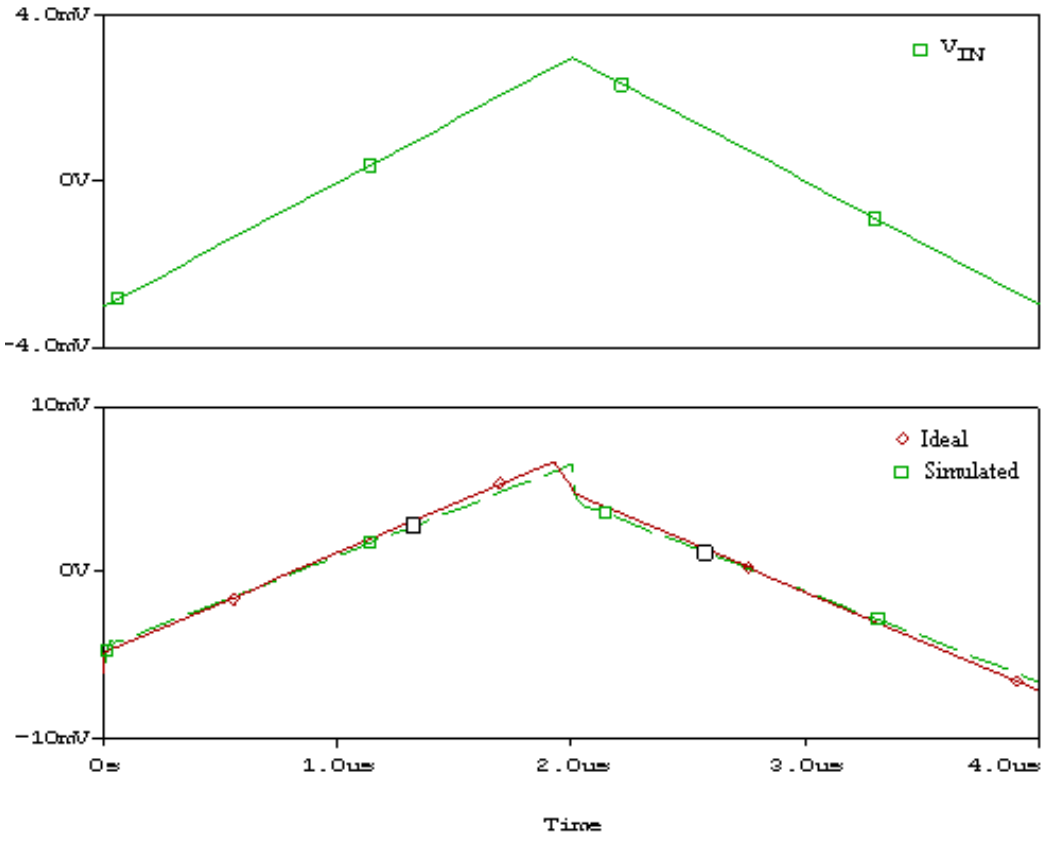

Fig. 8a. Transient response of the PD Controller.

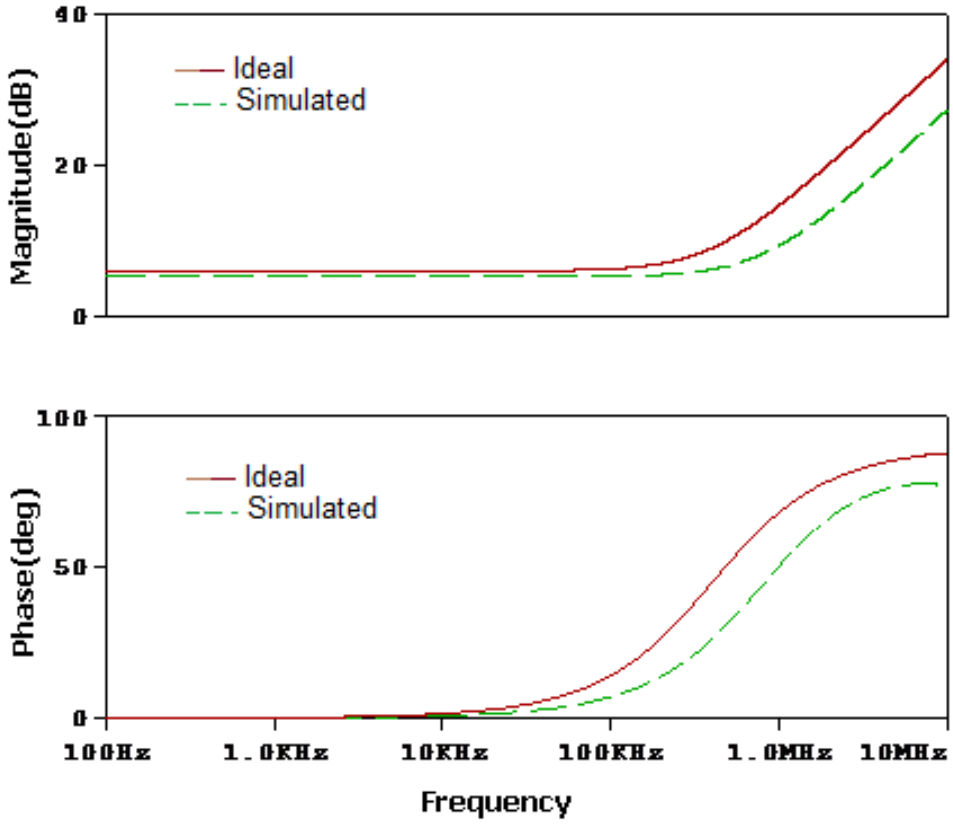

Fig. 8b. Frequency and phase Response of PD controller.

For MOS-C implemented PD controller shown in Fig 5 the aspect ratios of the transistors used for implementing the resistances are listed in Table.1.

Table1.Aspect ratios of transistors used for resistance implementation

Transistor	W(µm)/L(µm)
M1,M2	0.18µ/.54µ
M3,M4	0.18µ/1.08µ

Gate voltages are set as V_{a1}= V_{a2} = 1.2V and Vb1=0.59V, Vb2 =0.64V which result in resistance values as R ≈10KΩ R_f ≈20KΩ and the chosen value of C = 20pF.The ideal and simulated time domain response of MOS-C implemented PD controller, for a 3mV peak triangular input voltage are shown in Fig. 9a. Fig. 9b represents the frequency domain characteristics of the same.

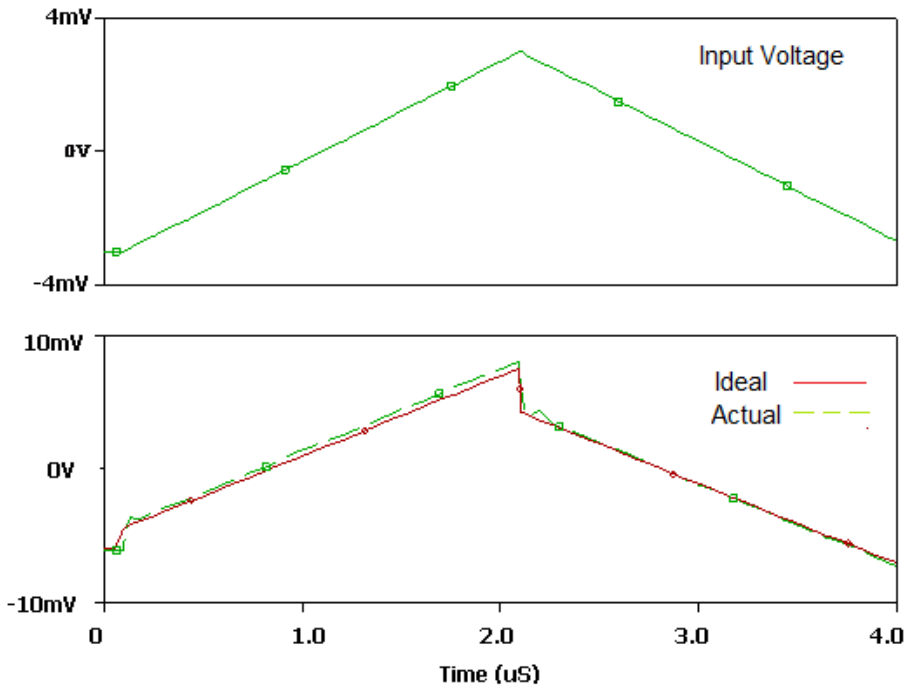

Fig. 9a.Transient response of the MOS-C PD Controller.

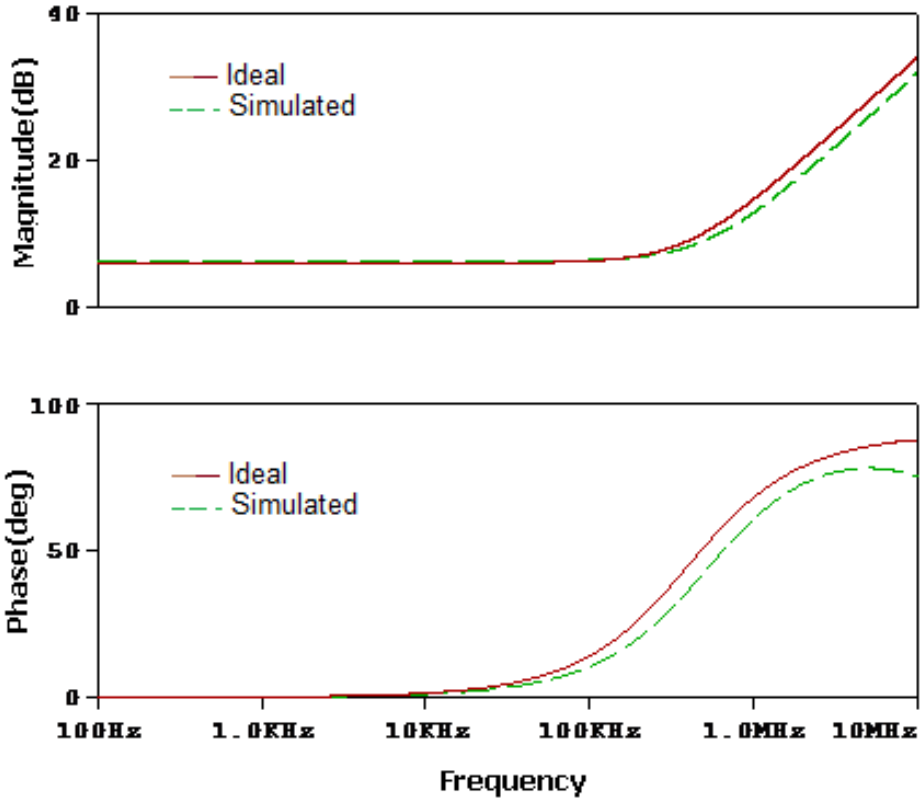

Fig. 9b.Frequency and phase Response of the MOS-C PD Controller.

Fig. 10 shows a closed loop control system realized using the proposed PD controller and a second order low-pass filter (LPF). The LPF is shown in Fig. 11.

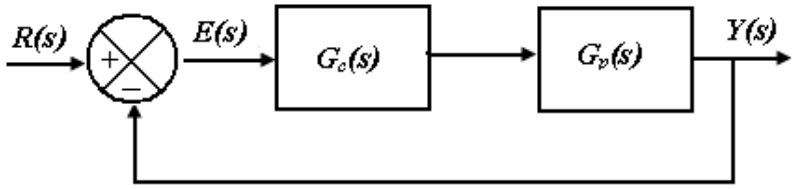

Fig.10.Closed Loop Control System.

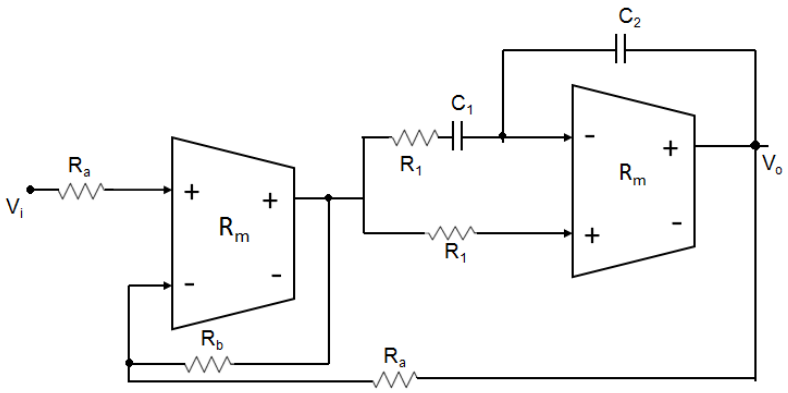

Fig. 11.Second order Low Pass filter.

The transfer function of the LPF is given as

$$\frac{V_0(s)}{V_i(s)} = \frac{G_1{}^2}{s^2C_1C_2+sC_2G_1+KG_1^2} \tag{27}$$

Where $K=R_a/R_b$. The values of passive element for the filters are selected as $R_a=R_b$ =20KΩ, R_1=2KΩ, and $C_1= C_2$=20pF which result in

$$\frac{V_0(s)}{V_i(s)} = \frac{6.25*10^{14}}{s^2+25*10^6s+6.25*10^{14}} \tag{28}$$

Now a PD controller, with the component values R=5K, R_f=15KΩ and C=8pF resulting in K_P=3 and $K_d=0.12\times10^{-6}{}_s$ is added to form control system of Fig. 10.
Fig. 12a shows the step response of the LPF without PD controller for a step input of 50mV whereas Fig.12b depicts the effect of PD controller on step response of the closed loop system.

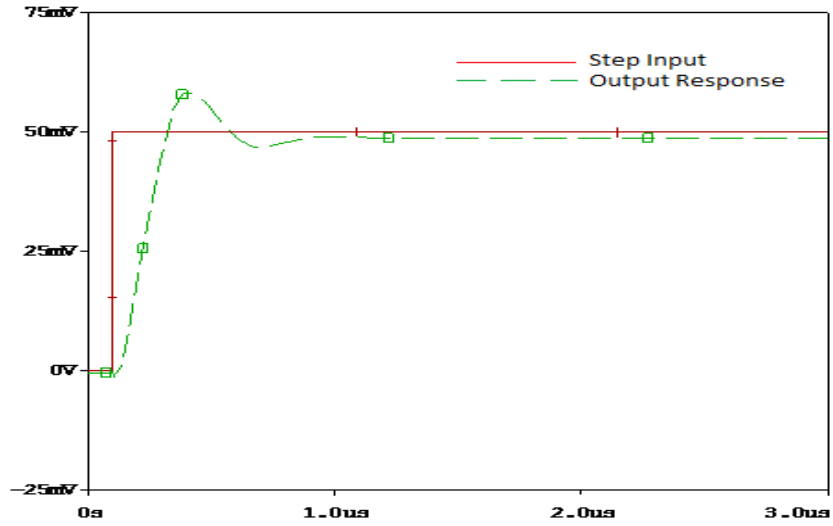

Fig. 12a.Step Response of a second order system without PD controller.

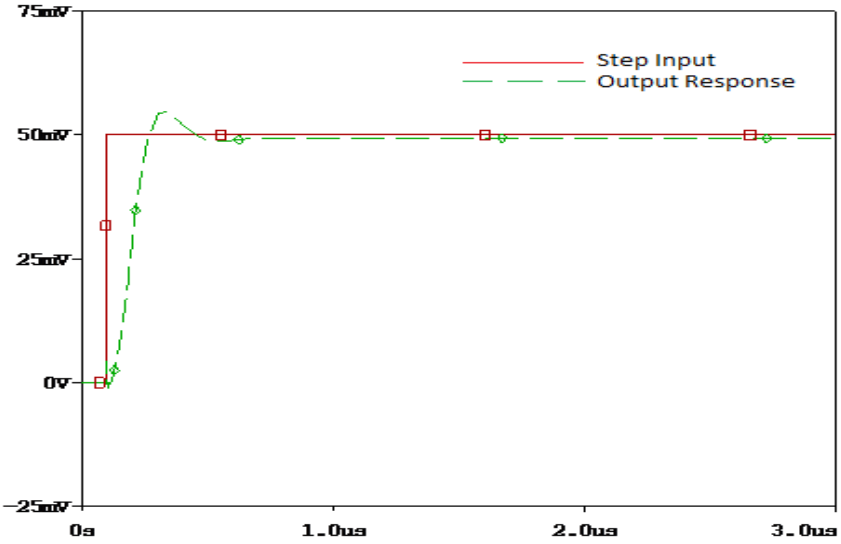

Fig.12b. Step Response of a second order system with PD controller.

Performance comparison of second order system with and without PD controller is shown in Table. 2. It is clearly visible from the table 2 that the response of the system has been improved.

Table. 2. Performance Comparison.

Parameter	Without PD Controller	With PD Controller
Overshoot	19.56%	10.59%
Peak output	58.26mV	54.63mV
Rise time	140.43ns	107.78ns

Conclusion

A single differential Operational transresistance (OTRA) based voltage mode proportional-derivative (PD) controller has been presented which possesses the feature of independent tuning of proportional (Kp) and derivative (Kd) constants. This controller can be made fully integrated by implementing the resistors using MOS transistors operating in linear region. As an application, a second order closed loop system is designed and simulated using SPICE program. The simulated results are in line with the proposed theory.

Reference

[1] S. Franco, *Design with operational amplifiers and analog integrated circuits*. Singapore: Mcgraw-Hill International Edition, 1998.

[2] M.T. Kara, and M.E. Rizkalla, "Single op-amp proportional-integral compensator with anti-windup," In *Proceedings of the IEEE International Symposium on Circuits and System.* Chicago, Illinois, (USA) 1993, pp. 2260 - 2263.

[3] C. Edral, A. Toker, and C. Acar, "OTA-C based proportional- Integral-derivative (PID) controller and calculating optimum parameter tolerances," *Turkish journal of Elec*, vol. 9, no. 2, Nov. 2001, pp.189-198.

[4] A.U. Keskin, "Design of a PID controller circuit employing CDBAs," *International Journal of Electrical Engineering Education*, vol. 43, no.1, Jan. 2006, pp.48-56.

[5] S. Minaei, E. Yuce, S. Tokat and O. Cicekoglu, "Simple realization of current-mode and voltage mode PID, PI and PD controllers," In *Proceeding of IEEE ISIE.* Dubrovnik (Croatia) June 2005, pp.195-198.

[6] E. Yuce, S. Tokat, S. Minaei and O. Cicekoglu, " Low-Component-Count Insensitive Current-Mode and Voltage-Mode PID, PI and PD Controllers," *Frequenz*, vol.60, no. 3-4, April 2006, pp. 65-69.

[7] V. Michal, C. Prémont, G. Pillonet and N. Abouchi, "Single Active Element PID Controllers," In *Proceedings of the Radioelektronika 20th International Conference.* CPE-Lyon, Villeurbanne (France) April 2010, pp. 1 – 4.

[8] C. Toumazou, F. J. Lidgey and D. G. Haigh, "*Analogue IC Design: The Current Mode Approach*," U.K.: Peregrinus, 1990.

[9] J. Chen, H. Tsao and C. Chen, "Operational transresistance amplifier Using CMOS Technology," *Electronics Letters*, vol.28, no.22, Oct. 1992, pp. 2087–2088.

[10] K.N. Salama and A.M. Soliman, "CMOS operational transresistance amplifier for analog signal processing," *Microelectronics Journal*, vol.30 no. 3, March 1999, pp. 235–45.

[11] H. Mostafa and A.M. Soliman, "A Modified CMOS Realization of the Operational Transresistance Amplifier (OTRA)," *Frequenz*, vol.60, No: 3-4, April 2006, pp. 70 -76.

[12] A. K. Kafrawy and A.M. Soliman, "A modified CMOS differential operational transresistance amplifier (OTRA)," *AEU-International Journal of Electronics and Communications*, vol. 63 no. 12, Dec. 2009, pp. 1067-1071.

[13] S. Kilinc, A. U. Keskin and U. Çam, "Cascadable Voltage-Mode Multifunction Biquad Employing Single OTRA," *Frequenz*, vol. 61, No: 3-4, April 2007, pp.84-86.

[14] K.N. Salama and A.M. Soliman, "Universal Filters Using Operational Transresistance Amplifiers," *AEU-International Journal of Electronics and Communications*, vol.53, no. 1, Jan. 1999, pp. 49-52.

[15] J. Chen, H. Tsao and S.I. Liu, "Parasitic- capacitance-insensitive current-mode filters using OTRA," *IEE Proc.-Circuits Devices Syst.*, vol. 142, no. 3, June 1995, pp.186-192.

[16] A. Gokcen and U. Cam, "MOS-C single amplifier biquads using the OTRA," *AEU-International Journal of Electronics and Communications*, vol. 63 no. 8, Aug. 2009, pp. 660-664.

[17] K.N. Salama and A.M. Soliman, "Novel oscillators using operational transresistance amplifier," *Microelectronics Journal*, vol.31, no.1, Jan. 2000, pp. 39-47.

[18] U. Cam, "A Novel Single-Resistance-Controlled Sinusoidal Oscillator Employing Single Operational Transresistance Amplifier," *Analog Integrated Circuits and Signal Processing*, vol. 32, no. 2, Aug. 2002, pp. 183-186.

[19] R. Pandey, N. Pandey, M. Bothra and S.K. Paul, 2011,May . Operational Transresistance Amplifier-Based Multiphase Sinusoidal Oscillators. *Journal of Electrical and Computer Engineering.* Volume 2011,Available: http://www.hindawi.com/journals/jece/2011/586853/

[20] C.L. Hou, H. C. Chien, and Y. K. Lo, "Squarewave generators employing OTRAs," *IEE proc.-Circuits Devices Syst*., Vol.152, no. 6, Dec. 2005, pp. 718–722.

[21] Y. K. Lo, H. C. Chien and H. G. Chiu, "Switch Controllable OTRA Based Bistable Multivibrator," *IET Circuits Devices Syst.*, vol. 2, no. 4, Aug. 2008, pp. 373–382.

[22] U. Cam, F. Kacar, O. Cicekoglu, H. Kuntman and A. Kuntman, "Novel grounded parallel immittance simulator topologies employing single OTRA," *AEU-International Journal of Electronics and Communications*, vol. 57, no.4, 2003, pp. 287-290.

[23] S. Kilinc, K. N. Salama and U. Cam, "Realization of fully Controllable negative Inductance with single operational Transresistance Amplifier," *Circuits Systems Signal Processing*, vol. 25, no.1, Feb. 2006, pp.47-57.

[24] U. Cam, F. Kacar, O. Cicekoglu, H. Kuntman and A. Kuntman, "Novel two OTRA-based grounded Immittance simulator topologies," *Analog Integrated circuit and Signal Processing*, vol. 39 no. 2, May 2004, pp.169-175.

[25] C. Sanchez, F.V. Fernandez and E. Tlelo-Cuautle, "Generalized Admittance matrix models of OTRA and COAs," *Microelectronics Journal*, vol.41, no.8, Aug. 2010, pp.502-505.

J Supercond Nov Magn
DOI 10.1007/s10948-012-1761-4

ORIGINAL PAPER

Structural, Optical and Multiferroic Properties of $BiFeO_3$ Nanoparticles Synthesized by Soft Chemical Route

Manisha Arora · P.C. Sati · Sunil Chauhan · Sandeep Chhoker · A.K. Panwar · Manoj Kumar

Received: 27 July 2012 / Accepted: 21 August 2012

Abstract $BiFeO_3$ nanoparticles were prepared via a soft chemical method using citric acid and tartaric acid routes followed by calcination at low temperature. Structural characterization showed remarkably different conditions for pure phase formation from both routes. The tartaric acid route was effective in obtaining pure phase $BiFeO_3$ nanoparticles while citric acid route required leaching in dilute nitric acid to remove impurity phases. Further optical, magnetic, and dielectric characterizations of pure phase $BiFeO_3$ nanoparticles obtained by tartaric acid route were done. X-ray diffraction and Raman spectroscopy confirmed the distorted rhombohedral structure of $BiFeO_3$ nanoparticles. The average crystallite size of $BiFeO_3$ nanoparticles was found to vary in the range 30–50 nm. Fourier Transformed Infrared spectra of $BiFeO_3$ samples calcined at different temperatures were studied in order to analyze various bond formations in the samples. UV-Visible diffuse absorption showed that BFO nanoparticles strongly absorb visible light in the wavelength region of 400–580 nm with absorption cut-off wavelength of 571 nm. The band gap of $BiFeO_3$ nanoparticles was found to be 2.17 eV as calculated from absorption coefficient spectra. Magnetic measurement showed saturated hysteresis loop indicating ferromagnetic behavior of $BiFeO_3$ nanoparticles at room temperature. Temperature dependent dielectric constant showed anomaly well below the antiferromagnetic Néel temperature indicating decrease in antiferromagnetic Néel temperature of $BiFeO_3$ nanoparticles.

Keywords Bismuth ferrite · Nanoparticles · Optical property · Magnetism

1 Introduction

Materials that possess electric and magnetic ordering simultaneously in the same phase are known as multiferroics. These materials can exhibit magnetoelectric (ME) effect i.e. induction of magnetization by electric field or of polarization by magnetic field at room temperature. Multiferroic materials have become the topic of great interest to the researchers because of its applications in various fields of electrical, magnetic and optical devices [1, 2]. $BiFeO_3$ (BFO) is the most studied multiferroic material due to the existence of both ferroelectric and (anti) ferromagnetic ordering in the same phase above room temperature. $BiFeO_3$ possesses distorted rhombohedral structure with Curie temperature $T_c \sim 1100$ K and magnetic ordering is G type antiferromagnetic with Néel temperature $T_N \sim 640$ K [3]. The magnetic structure of $BiFeO_3$ is spatially modulated with a cycloid spin structure with period 620 Å in which all magnetic spins are oriented antiparallel to each other resulting in no magnetization at room temperature [4]. Further it is very difficult to synthesize single phase $BiFeO_3$ because of the very narrow range of the synthesis temperature for phase stability. However, decrease in particle size below 62 nm gives rise to suppression of spiral structure which improves magnetization in BFO [5]. Modern synthesis techniques such as solid state route, sol gel technique and sonochemical route have been applied to obtain pure phase BFO [6–8].

In addition to multiferroic properties, BFO has potential to be used in variety of devices because of its interesting op-

M. Arora · P.C. Sati · S. Chauhan · S. Chhoker · M. Kumar (✉)
Department of Physics and Materials Science and Engineering, Jaypee Institute of Information Technology, Noida 201307, India
e-mail: manoj.chauhan@jiit.ac.in

A.K. Panwar
Department of Applied Physics, Delhi Technological University, Delhi 110042, India

Published online: 05 September 2012

tical properties in visible region. It can be used as a photocatalytic material due to its narrow band gap which allows carrier excitation, especially in commercially available femto second laser pulses [9]. Recently the photocatalytic properties of BFO powders under visible light illumination have been reported [10]. Gao et al. also suggested that BFO nanowires might also be useful for photocatalytic decomposition of organic contaminants [11]. Apart from all these applications photocatalytic properties of BFO degraded due to the presence of impurity phases and structure instability. In the present communication we compared citric acid and tartaric acid routes of sol gel technique to obtain phase pure BFO nanoparticles. Further detailed structural, optical, magnetic and dielectric properties of BFO nanoparticles are reported in this paper.

2 Experimental Details

BFO nanoparticles were synthesized by metal ions complexing with citric acid and tartaric acid using soft chemical route. For the synthesis of BFO powder from citric acid, $Bi(NO_3)_3{\cdot}5H_2O$, $Fe(NO_3)_3{\cdot}9H_2O$, citric acid and ethylene glycol were used to prepare precursor solution. An aqueous solution of citric acid was prepared in distilled water and then $Bi(NO_3)_3{\cdot}5H_2O$ and $Fe(NO_3)_3{\cdot}9H_2O$ were added with constant stirring at 50–60 °C followed by addition of ethylene glycol to the solution with citric acid/ethylene glycol proportion (70:30). The solution was heated at 100 °C on hot plate until gel formation occurs after evaporation of water. The dried powder was then sintered at 550 °C for 2 hrs to get desired phase of BFO nanoparticles. On the other hand, synthesis of BFO powder by tartaric acid route involved tartaric acid as a template material and dilutes nitric acid as oxidizing agent. Stoichiometric amount of $Bi(NO_3)_3{\cdot}5H_2O$ (Sigma Aldrich, 98 %) and $Fe(NO_3)_3{\cdot}9H_2O$ (Sigma Aldrich, 98 %) were dissolved in deionized water along with small amount of dilute nitric acid. This was followed by addition of tartaric acid (ratio of tartaric acid and metal nitrates was 1:2 mole). This solution was heated up to 60 °C for 12 hrs with constant stirring followed by heat treatment in an oven for 4–5 hrs in order to obtain fluffy light yellow color gel. The dried powder was calcined at 550 °C for 2 hrs in order to get crystalline phase. After the heat treatment, samples were characterized by X-ray diffraction (XRD) using Panalytical X'Pert Pro X-ray diffractometer. Rietveld Refinement was carried out to find various structural parameters. Transmission electron microscopy (Philips CM 10) was used to study the particle size. Fourier Transform infrared (FTIR) spectra were obtained (Perkin Elmer Spectrum BS-III) at a resolution of 4 cm^{-1} using a photo detector. Optical properties were studied by using UV–Visible diffuse reflectance (Ocean optics UV–Visible 4000). Magnetization measurements were taken on Lake shore Vibrating Sample Magnetometer (VSM). The dielectric measurements were carried on silver coated pellets in the temperature range 40–450 °C at various frequencies.

3 Results and Discussion

Figure 1 shows XRD patterns of BFO nanoparticles (sintered at 550 °C) prepared by sol gel method via citric and tartaric acid routes, respectively. It can be seen in Fig. 1(a) that majority of the peaks belong to distorted rhombohedral structure of $BiFeO_3$ along with some impurity peaks of $Bi_{36}Fe_{24}O_{57}$ and $Bi_2Fe_4O_9$ for sample prepared by citric acid route. Leaching was done in dilute nitric acid to remove impurity phases present in BFO powder prepared by citric acid route. Figure 1(b) shows XRD pattern of BFO nanoparticles prepared by citric acid route after leaching in dilute nitric acid. Leaching was effective in reducing impurity phases; however, few impurity peaks still appeared in the XRD pattern. On the contrary, we obtained pure phase BFO nanoparticles via tartaric acid route (Fig. 1(c)) even without leaching in dilute nitric acid. Further characterizations of BFO nanoparticles prepared by tartaric acid route were done and discussed in this paper. All XRD peaks for sample prepared by tartaric acid route has been indexed according to rhombohedrally distorted perovskite structure with space group *R3c*. Rietveld Refinement of XRD pattern of BFO nanoparticles prepared by tartaric acid route has been performed to investigate various structural parameters. The lattice parameters and unit cell volume were calculated as $a = b = 5.5785$ Å, $c = 13.8654$ Å and 373.6829 $(Å)^3$, respectively. The difference in the experimental and simulated data is shown in Fig. 1(d). It was observed from fitting parameters that the structure is very well fitted for rhombohedral system where the weight pattern factor R_{wp} and the expected pattern factor R_{exp} are 14.2 and 20.6, respectively. The average crystallite size as calculated using Debye-Scherer formula was found to be 40 nm assuming that small crystallite size to be the only reason for line broadening of XRD peaks.

To investigate the particle size and morphology of the nanoparticles, transmission electron microscopy (TEM) was performed using carbon coated copper grid. Figure 2(a) shows the TEM image for BFO nanoparticles with particle size varying from 30–50 nm with quasi spherical morphology. Figure 2(b) shows the selected area electron diffraction (SAED) pattern taken from Fig. 2(a). The well resolved electron diffraction spots confirmed the highly polycrystalline nature of BFO nanoparticles. The observed lattice spacing is measured to be 3.9 Å, 2.7 Å, 2.2 Å and 1.9 Å which correspond to (012), (110), (202) and (024) lattice planes of BFO, respectively.

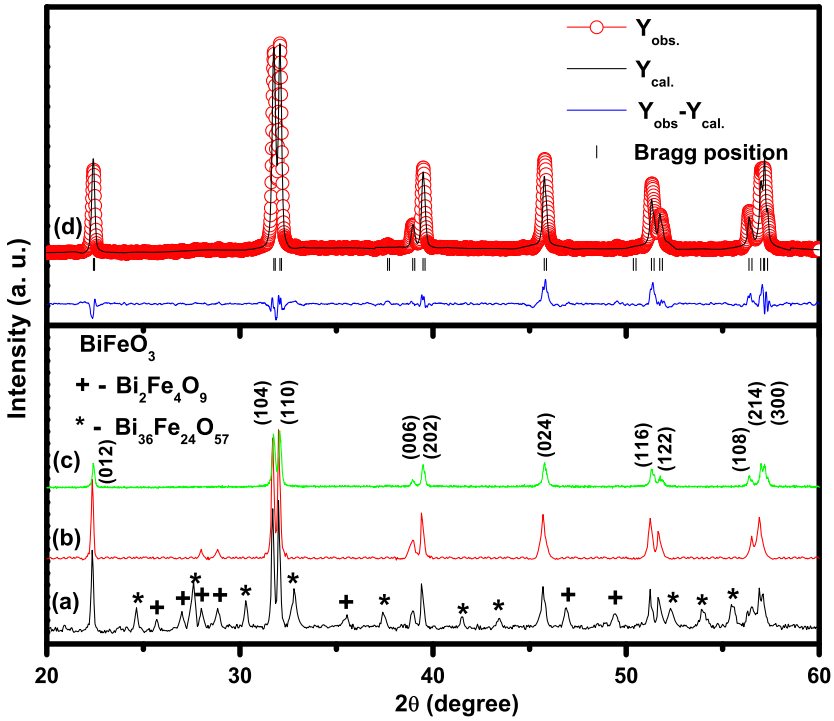

Fig. 1 (**a**) XRD patterns of BFO nanoparticles prepared by Citric acid route and (**b**) followed by leaching. (**c**) XRD pattern of BFO nanoparticles prepared by tartaric acid route and (**d**) Rietveld refinement of XRD pattern of BFO nanoparticles prepared by Tartaric acid route

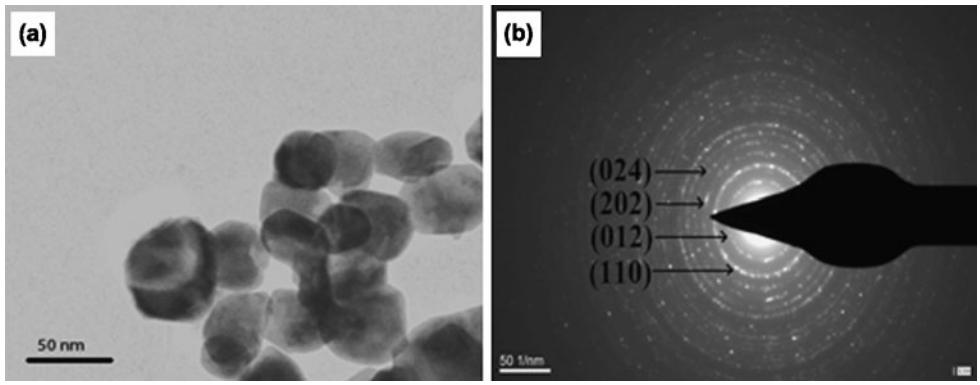

Fig. 2 (**a**) TEM image of BFO nanoparticles, (**b**) SAED pattern of BFO nanoparticles

Further Raman spectroscopy was used to study the structural characteristics of BFO nanoparticles prepared by tartaric acid route. More often, 13 Raman active modes ($4A_1 + 9E$) for BFO having distorted rhombohedral structure with R3c space group are observed. The room temperature Raman spectrum of BFO nanoparticles is shown in Fig. 3(a). Here we fitted 10 Raman modes in the range 100–700 cm^{-1}. Three intense peak at 136 cm^{-1}, 170 cm^{-1} and 217 cm^{-1} and a weak intensity peak at 475 cm^{-1} are assign to $A_1 1$, $A_1 2$, $A_1 3$ and $A_1 4$ modes, respectively. The peaks around 260 cm^{-1}, 278 cm^{-1}, 345 cm^{-1}, 365 cm^{-1}, 469 cm^{-1} and 520 cm^{-1} are assigned to E1, E2, E3, E4, E5, and E6 modes, respectively. Raman spectrum of BFO nanoparticles is in good agreement with previous reports on single crystal BFO [12] and thin film BFO [13] as shown in Table 1.

Figure 3(b) shows FTIR spectra of BFO nanoparticles (sintered at 250 °C, 350 °C, 450 °C and 550 °C) in the wave number range 1000–400 cm^{-1}. It is clear that BFO nanoparticles sintered at 250 °C and 350 °C did not show any absorption indicating the absence of bond formation. However, the sample sintered at 450 °C showed two weak broad absorption peaks around 450 cm^{-1} and 550 cm^{-1}, respectively. On further increasing the sintering temperature, intensity of broad absorption peaks increases indicating the completion of bond formation and high degree of crystallization. The broad absorption peaks at 550 cm^{-1} and 440 cm^{-1} are due to overlapping of Fe–O and Bi–O group vibration. Absorption peaks at 550 cm^{-1} and 440 cm^{-1} are the characteristics of Fe–O stretching and bending vibrations of octahedral FeO_6 group, respectively [14]. BiO_6 octahedral structure unit also possesses absorption peaks at 525 cm^{-1} and 450 cm^{-1} [15]. Peak corresponding to 667 cm^{-1} is attributed to water absorption from environment. As the calcination temperature increases these peaks becomes promi-

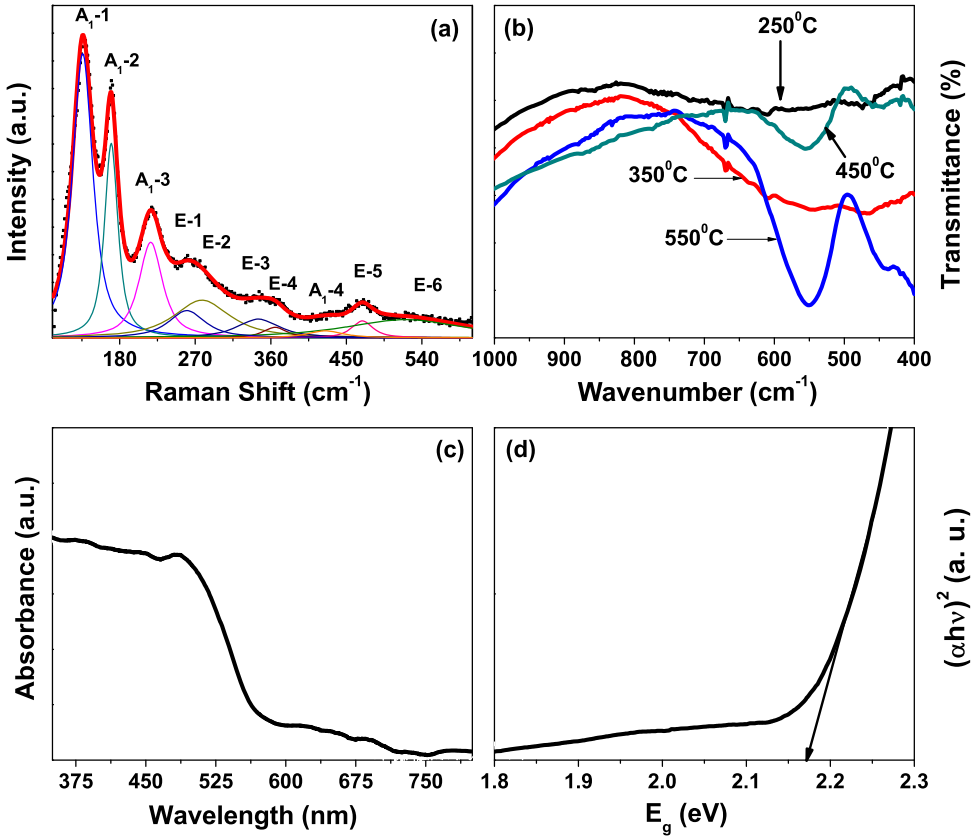

Fig. 3 (**a**) Raman spectra of BFO nanoparticles, (**b**) FTIR spectra of BFO nanoparticles sintered at different temperatures, (**c**) UV–Visible absorption spectra of BFO nanoparticles and (**d**) the plot between $(\alpha h\nu)^2$ and binding energy for BFO nanoparticles

Table 1 Comparison of Raman Mode positions (cm^{-1}) in our study with the reported data on single crystal BFO by Fukumura et al. [12] and data on thin film of BFO by Singh et al. [13]

Raman modes	Our study (cm^{-1})	Fukumura et al. (cm^{-1})	Singh et al. (cm^{-1})
A_1-1	136	147	136
A_1-2	170	176	168
A_1-3	217	227	211
A_1-4	425	490	425
E-1	260	265	275
E-2	278	279	335
E-3	345	351	365
E-4	365	375	456
E-5	469	437	549
E-6	520	525	597

nent which confirms the Bi–O and Fe–O bonds formation at 550 °C.

BFO is a small band gap metal oxide semiconductor which is very useful as a visible light irradiated photocatalyst. In order to examine the optical properties of BFO, optical response such as the absorption from BFO nanoparticles were observed. Figure 3(c) shows UV–Visible absorption spectra in the range of 350–800 nm for BFO nanoparticles in the diffuse reflectance mode. It is observed that the absorption spectrum of BFO nanoparticles features three unambiguous absorption regions. The broad absorption band from 450–600 nm confirmed that BFO nanoparticles can absorb higher percentage of visible light. This absorption band arises due to two types of electronic transition. The first excitation is due to electronic transitions from $^6A_1$ state to $^4T_1(^4G_1)$ state and the second excitation is due to $^6A_1$ to $^4E, ^4A_1(^4G)$ ligand field transitions and the field transfer band tail [16]. These transitions get overlapped and form a broad region of absorption band. The absorption below 450 nm is associated with the charge transfer transition (d–d). The energy band gap at $\sim$ 571 nm is associated with the metal to metal transitions while the band $\sim$ 728 nm is associated with the crystal field transitions [17].

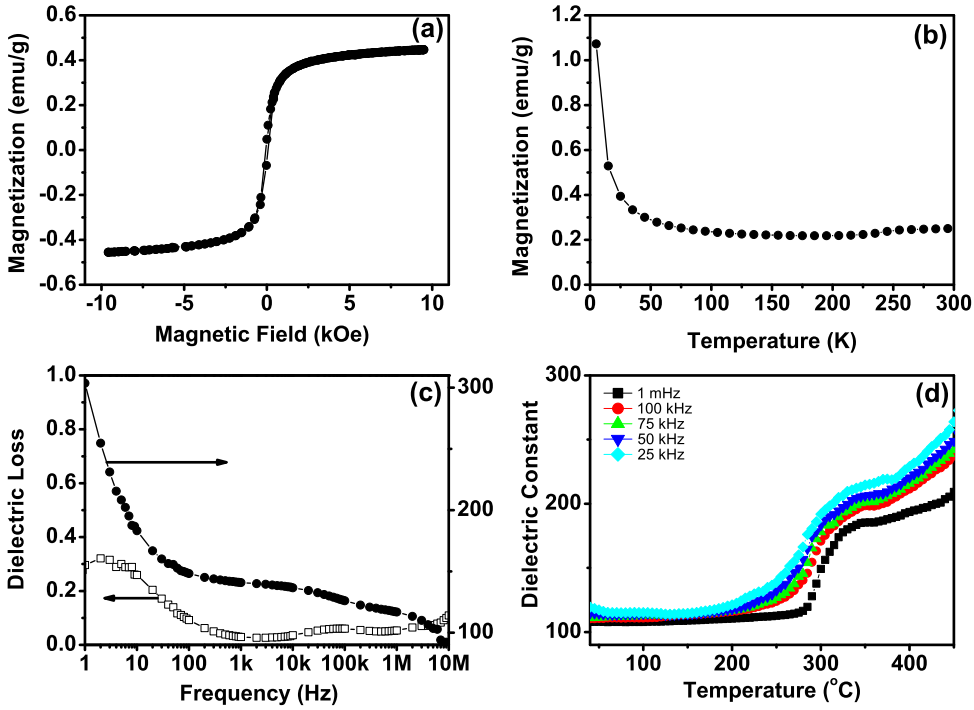

Fig. 4 (**a**) Magnetic hysteresis loop of BFO nanoparticles at room temperature, (**b**) temperature Dependent magnetization curve of BFO nanoparticles, (**c**) room temperature frequency dependence of dielectric constant and dielectric loss and (**d**) temperature dependent dielectric constant of BFO nanoparticles

Band gap E_g for the direct band gap materials can be calculated by using the formula

$$\alpha h\nu = K(h\nu - E_g)^{1/2}$$

where K is a constant, E_g is the band gap and $h\nu$ is the photon energy. According to classical Tauc's approach [18], the value of the band gap is estimated by extrapolating the linear portion of the graph intersecting X-axis at 0. Figure 3(d) shows $(\alpha E_{\text{photon}})^2$ versus E_{photon} curve based on the spectrum data of pure BFO nanoparticles. The energy band gap of BFO nanoparticles is estimated to be 2.17 eV which is in good agreement with the earlier reported band gap values for BFO nanoparticles [19] but this value of band gap is smaller as compared to BFO thin films [9]. This smaller value of the band gap indicates high ability of BFO nanoparticles to utilize visible light for the photocatalytic activities.

Figure 4(a) shows the magnetic hysteresis loop of BFO nanoparticles measured at room temperature, indicating ferromagnetic behavior. It is well known that bulk bismuth ferrite possesses cycloid spin of order 62 nm and no net magnetization at room temperature. The possible explanation which can describe the origin of net magnetization in nanoparticles of BFO ceramics could be its size dependent properties; As the particle size reduces, surface to volume ratio becomes very large which results in the structure distortion and the modification of the spiral G type antiferromagnetic ordering to the collinear G type antiferromagnetic structure in which the canted components becomes measureable. Further the cycloid spin structure is partly destroyed in BFO nanoparticles due to the average particle size (30–50 nm) being less than that of cycloid spin order (62 nm). Figure 4(b) shows the temperature dependent magnetization of BFO nanoparticles. The magnetization increases slowly with decreasing temperature up to 50 K. The sharp increase in magnetization below 50 K indicates the ferromagnetic behavior of BFO nanoparticles at low temperature.

Figure 4(c) shows frequency dependence of dielectric constant and dielectric loss of BFO nanoparticles at room temperature. Dielectric constant and dielectric loss decreases slowly with increasing frequency in low frequency region and becomes frequency independent in high frequency region. This can be explained on the basis of dipole relaxation. High value of the dielectric constant at the low frequencies and low value of the dielectric constant at high frequencies indicates large dispersion due to the Maxwell-Wagner type of interfacial polarization in agreement with Koop's phenomenological theory (the inability of the dipoles to follow the alternating field at high frequencies) [20, 21]. The variation of dielectric constant at various frequencies as a function of temperature is shown in Fig. 4(d). A dielectric anomaly in dielectric constant has been observed around $\sim 290\,^{\circ}\text{C}$ which could be related to antiferromagnetic Néel temperature (T_N). This type of behavior is also predicted by Landau-Devonshire theory of phase transition in magnetoelectrically ordered system as an influence of magnetic order on electric order. The appearance of dielectric anomaly around $\sim 290\,^{\circ}\text{C}$ which is well below the antiferromagnetic temperature ($370\,^{\circ}\text{C}$) also indi-

cates the decrease in Néel temperature of BFO nanoparticles.

4 Conclusions

In summary, pure phase BFO nanoparticles were successfully synthesized by sol gel method via tartaric acid as a template material. XRD patterns confirmed distorted rhombohedral structure of BFO nanoparticles. XRD calculations and TEM micrographs revealed that the average crystallite/particle size varied in the range 30–50 nm. Raman spectroscopy also confirmed rhombohedral structure of BFO nanoparticles. FTIR studies showed the presence of Bi–O and Fe–O bonds in BFO samples sintered at 450 °C and 550 °C. BFO nanoparticles showed enhanced absorption of visible light with a broad absorption band (400–650 nm) indicating an energy band gap of 2.17 eV. Room temperature weak ferromagnetism and decrease in Néel temperature were observed for BFO nanoparticles. Pure phase BFO nanoparticles having improved ferromagnetic and enhanced optical properties in visible region may find potential applications in optoelectronic devices.

Acknowledgements This work was financially supported by Department of Science and Technology (DST) India through grant No. SR/FTP/PS-91/2009. Manisha Arora is thankful to JIIT Noida for providing Teaching Assistance.

References

1. Fiebig, M., Lottermoser, Th., Frohlich, D., Goltsev, A.V., Pisarev, R.V.: Nature **419**, 818 (2002)
2. Hill, N.A.: J. Phys. Chem. B **104**, 6694 (2000)
3. Fischer, P., Polomska, M., Sosnowska, I., Szymanskig, M.: J. Phys. C **13**, 1931 (1980)
4. Wang, Y.P., Zhou, L., Zhang, M.F., Chen, X.Y., Liu, J.M., Liu, Z.G.: Appl. Phys. Lett. **84**, 1731 (2004)
5. Selbach, S.M., Tybell, T., Einarsrud, MA, Grande, T.: Chem. Mater. **19**, 6478 (2007)
6. Dai, H., Li, T., Xue, R., Chen, Z., Xue, Y.: J. Supercond. Nov. Magn. **25**, 109 (2012)
7. Tang, Y.H., Han, T.C., Liu, H.L., Lin, J.G.: J. Supercond. Nov. Magn. (2011). doi:10.1007/s10948-011-1257-7
8. Mazumder, R., Ghosh, S., Mondal, P., Bhattacharya, D., Dasgupta, S., Das, N., Sen, A., Tyagi, A.K., Sivakumar, M., Takami, T., Ikuta, H.: J. Appl. Phys. **100**, 033908 (2006)
9. Takahashi, K., Kida, N., Tonouchi, M.: Phys. Rev. Lett. **96**, 117402 (2006)
10. Gao, F., Chen, X., Yin, K., Dong, S., Ren, Z., Yuan, F., Yu, T., Zou, Z., Liu, J.M.: Adv. Mater. **19**, 2889 (2007)
11. Gao, F., Yuan, Y., Wang, K.F., Chen, X.Y., Chen, F., Liu, J.M.: Appl. Phys. Lett. **89**, 102506 (2006)
12. Fukumura, H., Matsui, S., Harima, H., Takahashi, T., Itoh, T., Kisoda, K., Tamada, M., Noguchi, Y., Miyayama, M.: J. Phys. Condens. Matter **19**, 365224 (2007)
13. Singh, M.K., Jang, H.M., Ryu, S., Jo, M.H.: Appl. Phys. Lett. **88**, 42907 (2006)
14. Yang, H., Xian, T., Wei, Z.Q., Dai, J.F., Jiang, J.L., Feng, W.J.: J. Sol-Gel Sci. Technol. **58**, 238 (2011)
15. Bhushan, B., Basumallick, A., Bandopadhyay, S.K., Vasanthacharya, N.Y., Das, D.: J. Phys. D, Appl. Phys. **42**, 065004 (2009)
16. Jaiswal, A., Das, R., Vivekanand, K., Abraham, P.M., Adyanthaya, S., Poddar, P.: J. Phys. Chem. C **114**, 2108 (2010)
17. Zhang, S.T., Lu, M.H., Wu, D., Chen, Y.F., Ming, N.B.: Appl. Phys. Lett. **87**, 262907 (2005)
18. Chang, D.A., Lin, P., Tseng, T.Y.: J. Appl. Phys. **77**, 4445 (1995)
19. Joshi, U.A., Jang, J.S., Borse, P.H., Lee, J.S.: Appl. Phys. Lett. **92**, 242106 (2008)
20. Maxwell, P.C.: Electricity and Magnetism, vol. 1. Oxford University Press, Oxford. Section 328
21. Koops, C.G.: Phys. Rev. **83**, 121 (1951)

Mathematical Theory and Modeling
ISSN 2224-5804 (Paper) ISSN 2225-0522 (Online)
Vol.2, No.8, 2012

Study of Average Losses Caused by Ill-Processing in a Production Line with Immediate Feedback and Multi Server Facility at Each of the Processing Units

Abhimanu Singh [1] * Prof. C. K. Datta[2] Dr. S. R. Singh[3]
1. Faculty of Technology, University of Delhi, Delhi, India
2. PDM College of Engineering, Bahadurgarh, Haryana, India
3. DN College, Meerut, India
*E-.mail address of corresponding author: asingh19669@yahoo.co.in

Abstract
In this paper, we have modeled a production line consisting of an arbitrary number of processing units arranged in a series. Each of the processing units has multi-server facility. Arrivals at the first processing unit are according to Poisson distribution and service times at each of the processing units are exponentially distributed. At each of the processing units, the authors have taken into account immediate feedback and the rejection possibility. Taking into account the stationary behavior of queues in series, the solution for infinite queuing space have been found in the product form. Considering the processing cost at each of the processing units, the average loss to the system due to rejection, caused by ill processing at various processing units, is obtained.
Keywords: Queuing Network, Processing Units, Production Line, Multi-Server, Immediate Feedback, Stationary behavior.

1. Introduction

A production line is a sequence of a finite number of processing units arranged in a specific order. At each of the processing units, service may be provided by one person or one machine that is called single- server facility, or it can be provided by more than one persons or more than one machines that is called multi-server facility at the respective processing unit. In this paper we have considered multi-server facility at each of the processing units. At each of the processing units a specific type processing is performed i.e. at different processing units material is processed differently. At a processing unit the processing times of different jobs or materials are independent and are exponentially distributed around a certain value, called mean processing time. To estimate the required measures, we represent a production line by a serial network of queues with multi- server facility at each of the node.

Several researches have been considered the queues in series having infinite queuing space before each servicing unit. Specifically, Jackson had considered finite and infinite queuing space with phase type service taking two queues in series. In [7] has found that the steady state distribution of queue length taking two queues in the system, where each of the two non-serial servers is separately in service. O.P. Sharma [1973] studied the stationary behavior of a finite space queuing model consisting of queues in series with multi-server service facility at each node.

In an production line the processing of raw material starts at the first processing unit. It is processed for a certain time interval at the first processing unit and then it is transferred to the second processing unit for other type of processing, if its processing is done correctly at the first processing unit. This sequence is followed til the processing at the last processing unit is over.

End of processing at each of the processing units give rise to the following three possibilities:

(a) Processing at a unit is done correctly and the job or material is transferred to the next processing unit for other type of processing.
(b) Processing at a unit is not done correctly but can be reprocessed once more at the same processing unit.
(c) Processing at a unit is neither done correctly nor it can be reprocessed at the same processing unit i.e. this job or material is lost, in this situation the job or material is rejected and put into the scrap.

2. Modeling

Let us consider an assembl line consisting of *an* arbitrary number(r) processing units arranged in a series in a specific order. Each of the processing units has multi- server facility.

Let λ = Mean arrival rate to the first processing unit from an infinite source, following Poisson's rule.

μ_i = Mean service rate of an individual server at the i^{th} processing unit having exponentially distributed service times.

s_i = Number of servers at the i^{th} processing unit.

n_i = Number of unprocessed jobs before the i^{th} processing unit waiting for service, including one in service, if any, at any time t.

$p_{i,i+1}$ = Probability that the processing of a job or material at the i^{th} processing unit is done correctly and it is transferred to the $(i+1)^{st}$ processing unit.

$p_{i,i}$ = Probability that the processing of a job or material at the i^{th} processing unit is not done correctly but it can be reprocessed once more, so, it is transferred to the same processing unit for processing once more.

$p_{i,o}$ = Probability that the processing of a job or material at the i^{th} processing unit is neither done correctly nor it remains suitable for reprocessing.

C_i= Processing cost per unit at i^{th} processing unit.

L = Average loss to the system due to rejection of items at various processing units.

$P(n_1, n_2, ...n_r, t)$ = Probability that there are n_1 jobs for processing before the first processing unit, n_2 jobs before the second processing unit, and so on, n_r jobs before the r^{th} processing unit at time t, with $n_i \geq 0 (1 \leq i \leq r)$ and $P(n_1, n_2, ...n_r, t)$=0, if some n_i <0 (because number of jobs cannot be negative).

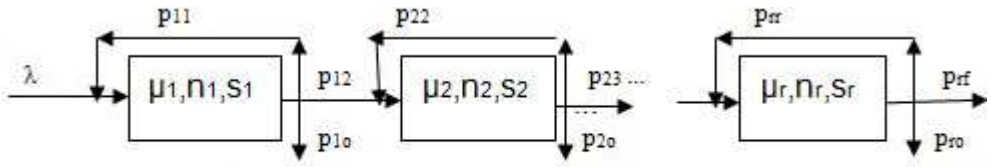

Fig. 1. A Production line

The above production line can be represented by a serial network of queues in which each processing unit is equivalent to a queue with the same number of similar servers and the same numbers of jobs waiting for service. In the above serial network of queues, each queue has immediate feedback. To analyze this serial network of queues firstly we remove the immediate feedback. After the removal of immediate feedback the above serial network of queues is replaced by one as follows:

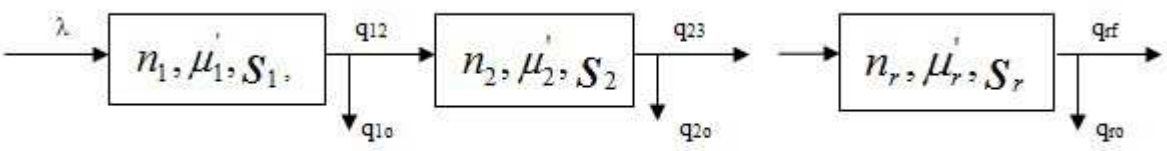

Fig.2 Equivalent Serial Network of Queues

Here $\mu_i^{'} = \mu_i(1-p_{i,i})$, where $\mu_i^{'}$ is the effective service at the i^{th} processing unit after the removal of the immediate feedback as given by J.Warland (1988). We define the respective probabilities as follows

$$q_{io} = \frac{p_{io}}{(1-p_{ii})} \quad , \quad q_{ii+1} = \frac{p_{ii+1}}{(1-p_{ii})} \tag{1}$$

3. Equations Governing the Queuing System

Under the steady state conditions, we have,

$$\left[\lambda + n_1\mu_1^{'} + n_2\mu_2^{'} + ... + n_r\mu_r^{'}\right].\mathrm{P}(n_1, n_2, ...n_r)$$

$$= \lambda \mathrm{P}(n_1 - 1, n_2 n_3, ...n_r) + \sum_{i=1}^{r} n_i\mu_i^{'}.q_{i,i+1}.P(n_1, n_2, ...n_i + 1, n_{i+1} - 1, ...n_r) +$$

$$\sum_{i=1}^{r} n_i\mu_i^{'}.q_{i,o}.P(n_1, n_2, ...n_i + 1.n_{i+1}, ...n_r) \tag{2}$$

Dividing the above steady state equation by the factor $\left[\lambda + \mu_1^{'} + \mu_2^{'} + ... + \mu_r^{'}\right]$the above equation is reduced to P.Q=P, where P is the row vector of the steady state probability matrix and Q is the stochastic transition matrix.

4. Solution for Infinite Queuing System

Under the steady state conditions all the queues behave independently and thus the solution of steady state equation in product form is given by

$$\mathrm{P}(n_1, n_2, ...n_r) = \prod_{i=1}^{r}(1-\rho_i)\rho_i^{n_i}, \tag{3}$$ where

$n_i \geq 0 (1 \leq i \leq r)$ and $\rho_i < 1 \ (1 \leq i \leq r)$

If any $\rho_i \ (1 \leq i \leq r)$>1 then the stability is disturbed and the behavior of the system will not remain stationary consequently solution will not remain valid
Here, we have

$$\rho_i = \frac{\lambda_i}{n_i\mu_i'},$$

Where $\lambda_i = \lambda \prod_{k=1}^{i} \frac{p_{k-1,k}}{(1-p_{k-1,k-1})}, \quad p_{0,0} = 0$

Thus

$$\rho_i = \frac{\lambda}{n_i\mu_i} \prod_{k=1}^{i} \frac{p_{k-1,k}}{(1-p_{k,k})}, \text{ With } p_{0,1} = 1 \tag{4}$$

It can be seen that $\sum_{i=1}^{r} \lambda_i.q_{i,o} + \lambda_r.q_{r,f} = \lambda$ (5)

5. Evaluation of Average Loss

Let c_1 be the processing cost at the first processing unit, c_2 the processing cost at the second processing unit and so on … c_r, the processing cost at the r^{th} processing unit.

If an item is rejected just after its processing at the first processing unit is over, then it causes a loss c_1 to the system. If an item is rejected just after its processing at the second processing unit is over, then it causes a loss (c_1+c_2) to the system. Thus, in general if an item is rejected just after its processing at the r^{th} processing unit is over, then it causes a loss $(c_1+c_2+c_3+\ldots+c_r)$ to the system.

L, the average loss per unit time to the system due to rejection of items just after the processing at various processing units, due to ill-processing (processing of an item is neither done correctly nor it can be reprocessed) is

$$L = c_1 \lambda q_{1,o} + (c_1+c_2)\lambda q_{1,2} q_{2,o} + \ldots + (c_1+c_2+\ldots c_r) \lambda q_{1,2} q_{2,3} \ldots q_{r-1,r} q_{r,o}$$

$$= \sum_{i=1}^{r} (c_1+c_2+\ldots c_i) \lambda q_{1,2} . q_{2,3} \ldots q_{i-1,i} q_{i,o},$$

With $q_{0,1} = 1$

$$= \sum_{i=1}^{r} (c_1+c_2+\ldots c_i) \lambda \frac{p_{1,2}}{1-p_{1,1}} \frac{p_{2,3}}{1-p_{2,2}} \ldots \frac{p_{i-1,i}}{1-p_{i-1,i-1}} \frac{p_{i,o}}{1-p_{i,i}},$$

$$= \lambda \sum_{i=1}^{r} (c_1+c_2+\ldots c_i) \prod_{k=1}^{i} \left(\frac{p_{k-1,k}}{1-p_{k-1,k-1}} \right) \cdot \frac{p_{i,o}}{(1-p_{i,i})} \qquad \textbf{(6)}$$

With $p_{0,0} = 0, and \quad p_{0,1} = 1$

6. Conclusion

The work can be used to find the approximate loss in a manufacturing system and can be extended to make decision policies.

7. Acknowledgements

Author is thankful to Siddhartha Sirohi, Assistant Professor, Delhi University, Delhi, and Achal Kaushik, Assistant Professor, BPIT, Rohini, Delhi, for their continuous encouragement and support. I am thankful to management of BPIT also, for providing research oriented environment in the institute.

8. Biography

Abhimanu Singh born on 4th may 1969, got his M.Sc. Degree in mathematics from Ch. Charan Singh University, Meerut, U. P., India, in 1996.

He started teaching Mathematics to B. Sc. Students in 1996. He has been teaching Engineering Mathematics for the last fifteen years at Delhi Technological University (formerly Delhi College of Engineering), Delhi, and GGSIP University, Delhi, affiliated institutions. He has authored three books on Engineering Mathematics.

1. Applied Mathematics-I, Delhi, Delhi, Ane books Pvt. Ltd., 2010.
2. Engineering Mathematics-I, Delhi, Delhi, Ane books Pvt. Ltd., 2011.
3. Applied Mathematics-II Delhi, Delhi, Ane books Pvt. Ltd., 2011.

His current area of research is modeling with applications of Queuing Theory.

References

1) T.L.Saaty, *Elements of Queueing Theory*, New York, McGraw-Hill, 1961, ch. 12, pp. 260.
2) U. Narayan Bhat, *An Introduction to Queueing Theory*, Birkhäuser Boston, 2008, ch. 7, pp 144-147.
3) D.Gross and C.M.Harris, *Fundamentals of Queueing Theory*, John-Wiley New York, 1985, ch. 4, pp. 220-226
4) Guy L. Curry. Richard M. Feldman, *Manufacturing System*, Springer-Verlag Berlin Heidelberg, 2011, ch. 3, pp. 77-80.
5) Kishor.S.Trivedi., *Probability & Statistics with Reliability, Queuing and Computer Science Applications*. Wiley India (P.) Ltd., 4435/7, Ansari Road, Daryaganj, New Delhi, (2002), ch. 9, pp. 564
6) J. R. Jackson (1957), "Networks of waiting lines", Oper. Res.,5, pp. 518-521. http://or.journal.informs.org/content/5/4/518.full.pdf
7) K.L.Arya (1972), Study of a Network of Serial and Non-serial Servers with Phase Type Service and Finite Queueing Space, *Journal of Applied Probability* [online] 9(1), pp198-201. http://www.jstor.org/stable/3212649
8) O. P. Sharma (1973), A Model for Queues in Series. *Journal of Applied Probability* [Online] 10(3), pp. 691-696.
Available: http://www.jstor.org/stable/3212791
9) J. Walrand, *An Introduction to Queueing Networks*, Prentice Hall, Englewood Clifs, New Jersey, (1988), ch 4, pp. 160.
10) **10) R. R. P. Jackson,(1954) "Queueing Systems with Phase Type Service,"** Operations Research Quarterly, 5(2), pp. 109-120.
11) Abhimanu Singh, (2012) "evaluation of measures of performance of a production line with immediate feedback and single server at each of the processing units", *International Journal of Physics and Mathematical Sciences ISSN: 2277-2111* (Online), 2(1), pp. 173-177,
available:http://*www.cibtech.org/jpms.htm*

This academic article was published by The International Institute for Science, Technology and Education (IISTE). The IISTE is a pioneer in the Open Access Publishing service based in the U.S. and Europe. The aim of the institute is Accelerating Global Knowledge Sharing.

More information about the publisher can be found in the IISTE's homepage: http://www.iiste.org

The IISTE is currently hosting more than 30 peer-reviewed academic journals and collaborating with academic institutions around the world. **Prospective authors of IISTE journals can find the submission instruction on the following page:** http://www.iiste.org/Journals/

The IISTE editorial team promises to the review and publish all the qualified submissions in a fast manner. All the journals articles are available online to the readers all over the world without financial, legal, or technical barriers other than those inseparable from gaining access to the internet itself. Printed version of the journals is also available upon request of readers and authors.

IISTE Knowledge Sharing Partners

EBSCO, Index Copernicus, Ulrich's Periodicals Directory, JournalTOCS, PKP Open Archives Harvester, Bielefeld Academic Search Engine, Elektronische Zeitschriftenbibliothek EZB, Open J-Gate, OCLC WorldCat, Universe Digtial Library , NewJour, Google Scholar

International Journal of Materials and Chemistry 2012, 2(2): 79-85
DOI: 10.5923/j.ijmc.20120202.07

Thermal Behaviour of Chemically Synthesized Polyanilines/Polystyrene Sulphonic Acid Composites

Gupta Neetika[1,*], Kumar D.[2], Tomar S. K.[3]

[1]Department of Chemistry, Meerut International Institute of Technology, Meerut, 250002, India
[2]Department of Chemistry, Delhi Technological University, Delhi, India
[3]Institute of Engineering & Technology, JK Lakshmipat University; Jaipur, India
neetikamanglik@yahoo.co.in, sandeeptomar@jklu.edu.in

Abstract Polyanilines are synthesized by free radical chemical oxidative polymerization of aniline & o-toluidine using ammonium persulphate as an oxidant in protonic acid medium. These polymers have been introduced into polystyrene sulphonic acid (PSSA) in 2:1, 1:1, 1:2 compositions for the preparation of composite materials. The composite samples so obtained are thermally characterized by thermogravimetric analysis (TGA), differential scanning calorimetry (DSC), X-ray diffraction, and FTIR spectra. The incorporation of polymer in PSSA has been endorsed by FTIR analysis. TGA data reveals that the (Polyaniline/Polystyrene sulphonic acid) PANI/PSSA (2:1) and (Poly o-toluidine/Polystyrene sulphonic acid) POT/PSSA (2:1) composites show better thermal stability than their 1:1 and 1:2 counterparts. Steric hindrance of $-CH_3$ group present in ortho position and sulphonic acid group of PSSA affects the thermal behaviour of composites. Two-step transitions are clearly reported from the DSC thermograms of polyanilines/PSSA composites and non-reversing chemical cross-linking reaction was further confirmed by X-ray diffraction and DSC thermograms.

Keywords Polyanilines, Chemical Oxidative Polymerization, Composites, PSSA

1. Introduction

Conducting polymers have become a popular basic material for advanced applications including plastic batteries, EMI shielding, electrochromic displays and sensors[1-7]. Among conducting polymers, polyaniline (PANI) has been extensively studied for its environmental stability in the conducting form, ease of synthesis, low cost and high conductivity. Nevertheless, a few applications have been reported where conducting polymers like PANI exhibit poor physical and mechanical properties. Numerous methods have been developed to overcome such shortcomings. It has been reported that the composite system by blending PANI with a commodity polymer improves its mechanical properties[8-11]. It has also been proposed that the incorporation of side groups into the main chain[12], grafting of the conducting PANI chain to a non-conductive polymer[13] and electrochemical polymerization of aniline in a polymer matrix[14] improve their processibility and thus broaden their applicability. A large amount of PANI-inorganic composites like PANI/V_2O_5[15], PANI/TiO_2[16-18], PANI/CdS[19], PANI/graphite oxide[20] and PANI/clay[21,22], etc have been synthesized and studied to enhance the overall properties in the past few years. Similarly composites of PANI with polyacrylonitrile, Polyure thane/polymethylmeth acrylate (PU/PMMA), Acrylonitrile butadiene styrene (ABS), PVC, Polyvinyledene fluoride/ Nanocrystalline Nickel Composites, Ag-CrO_2 Nanocomposite, Polyvinyledene fluoride (PVDF) Based Composites, LiFe1/2Ni1/2VO_4 composite were also studied in recent years[23-28].

Here, we have developed a simple but interesting method to prepare composites of polyaniline with polystyrene sulphonic acid and poly(o-toluidine) with polystyrene sulphonic acid[29,30] to get better and some new synergistic properties which could not be attained from individual materials. The procedure involves oxidative polymerization of aniline and o-toluidine and synthesis of polystyrene sulphonic acid by the sulphonation of polystyrene separately and subsequently reinforcement of polyaniline and poly(o-toluidine) in polystyrene sulphonic acid. This paper addresses the preparation of composite samples and their thermal behaviour to explore the synergistic properties.

2. Experimental Procedure

2.1. Materials

Aniline and o-toluidine monomer were double distilled and stored at low temperature prior to use. Polystyrene of grade M110 was procured from Haldia Petrochemicals, India. All other chemicals used were procured from CDH, India.

* Corresponding author:
neetikamanglik@yahoo.co.in (Gupta Neetika)
Published online at http://journal.sapub.org/ijmc

Silver sulphate, ammonium persulphate, HCl and H_2SO_4 were used as received. Double distilled water was deionized by Millipore used throughout the studies.

2.2. Synthesis of Polyaniline and Poly(o-toluidine)

The polymerization of freshly distilled aniline has been carried out by free radical chemical oxidative polymerization method by using ammonium persulphate (APS) as an oxidant in non-oxidizing protonic acid like HCl. In a chemical reaction 0.1 M of aniline was mixed to precooled 1 M HCl solution at 0-5℃. An aqueous solution of APS (0.1 M) was added drop wise to reaction mixture with constant stirring for 4-5 h resulted with the stabilization of temperature of reaction mixture till the completion of reaction. The dark green precipitate so obtained was filtered and then washed repeatedly with distilled water till the pH of the filterate became neutral. This precipitate was then dried under dynamic vacuum till constant weight. The polymer was also treated with 1M aqueous ammonia with constant stirring for 3-4 h for converting it into the base/undoped form. The blue black precipitate (undoped form) so obtained was filtered and then washed repeatedly with water to neutral pH. A similar procedure is also employed for the preparation of poly (o-toluidine) undoped form and finally dried under dynamic vacuum.

2.3. Sulphonation of Polystyrene

Before going to prepare composites of PANI and its derivatives with PSSA, we prepared PSSA from polystyrene through its sulphonation. A mixture of polystyrene granules (3g), silver sulphate (0.034 g) and concentrated H_2SO_4 (44 mL) was heated at 90℃ for 2 h until it becomes dark brown and highly viscous. This liquid pours into excess of ice-cold distilled water which on constant stirring resulted into a white gummy mass. This precipitate was dissolved in distilled water to make 100 mL solution of PSSA.

2.4. Synthesis of Composites of Polyanilines with PSSA

For the preparation of composite materials, undoped PANI and POT were mixed with polystyrene sulphonic acid in different compositions, i.e., 1:2, 1:1 and 2:1 by weight. A dark green colour paste was obtained in each case, which was dried in oven at 120℃. These samples of composite materials have been abbreviated as (Polyaniline/Polystyrene sulphonic acid) PANI/PSSA (2:1), PANI/PSSA (1:1), PANI/PSSA (1:2), (Polyo-toluidine/Polystyrene sulphonic acid) POT/PSSA (2:1), POT/PSSA (1:1) and POT/PSSA (1:2) composites.

2.5. Characterization

The composite material samples along with polyanilines were thermally characterized by TGA, DSC, XRD and FTIR spectra. TGA and DSC were performed on Perkin Elmer by pursuing N_2 gas as a carrier at a flow rate of 100 mL/min within a temperature range 50-800℃ for TGA and 50-600℃ for DSC, respectively at a heating rate of 10℃/min. Wide angle X-ray differactometer (model Philips X'pert 1830) using Ni filter and CuKα radiation as a source at 36kV and 15 mA. FTIR spectrum of all composites were taken on FTIR spectrophotometer (Model RX-I Perkin Elmer, UK) in the region of 400-4000 cm^{-1} at 4 cm^{-1} resolutions with atleast 32 scans for each sample.

3. Results and Discussion

3.1. Thermogravimeric Analysis

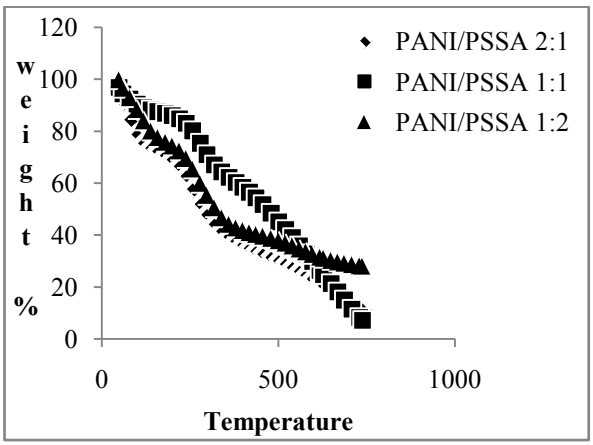

Figure 1. TGA thermogram of PANI/PSSA composite materials

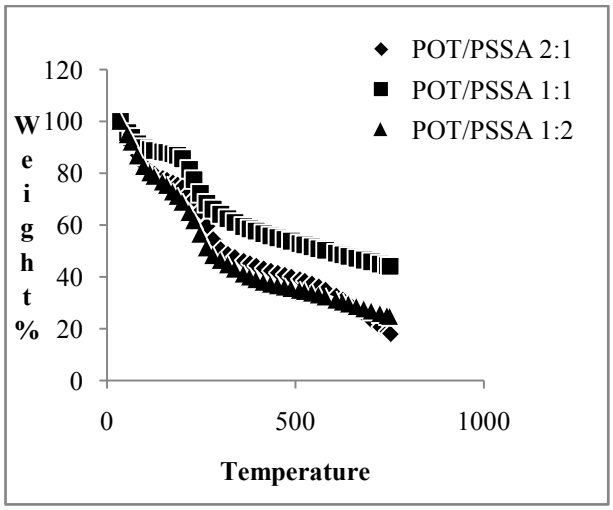

Figure 2. TGA thermogram of POT/PSSA composite materials

The thermogram of polyaniline emeraldine base form shows a weight loss of 7-8% upto 100℃, a weight loss of 22% from 100-450℃ and a weight loss of 40% from 450-800℃. Our data are found in good agreement with the data reported in literature[31-33], which confirms the reliability of our results. When polyaniline was mixed with polystyrene sulphonic acid in different compositions, i.e. in (2:1), (1:1) and (1:2) compositions, a different thermal behaviour with respect to the parent polymer, i.e., polyaniline is shown in Figure1. Thermogram suggests that weight loss mainly occurs in two steps. First step corresponds to the loss of water molecules, slow removal of oligomers and loss of impurities upto 120℃ with a total weight loss of ca. 6% in

PANI/PSSA (2:1) composition, upto 150℃ with a weight loss of 9% in PANI/PSSA (1:1) composition and upto 100℃ with a weight loss of 12% in PANI/PSSA (1:2) composition. Second step corresponds to the degradation of polymeric backbone and polystyrene sulphonate ions in the range of 200-400℃ (weight loss of ca. 33%) in PANI/PSSA (2:1), in the range of 160-360℃ (weight loss ca. 25%) in PANI/PSSA (1:1), in the range of 140-360℃ (weight loss of ca. 38%) in PANI/PSSA (1:2) composition. Thus, the thermal stabilities of all the composites are considerably less than that of polyaniline. This may be attributed to the decreased chain length and presence of bulky groups in the composites.

POT in its base form shows a negligible weight loss upto 410℃ and a continuous weight loss (ca. 15%) is observed upto 650℃, which is possibly due to the degradation of POT matrix in its thermogram. This implies that the base form of PANI brings about thermally more stable than undoped POT. It is possibly due to the lower steric hindrance of the $–CH_3$ group of toluidine present in ortho-position.

In case of composites of poly(o-toluidine) with PSSA a different behaviour of thermogram is shown in figure2. In case of POT/PSSA (2:1) first weight loss due to loss of moisture occurs upto 100℃, where as in POT/PSSA (1:1) weight loss occurs upto 110℃ and in POT/PSSA (1:2) composition, thermogram shows first weight loss upto 100℃. Second major weight loss due to degradation of polymeric backbone and polystyrene sulphonate ion occurs from 150-300℃ (27%) in POT/PSSA (2:1) composition, from 140-300℃ (ca. 24%) in POT/PSSA (1:1) composition and from 120-400℃ (ca. 22%) in POT/PSSA (1:2) composition.

Thus, the thermal stability of the composites depends upon the actual amount of PSSA incorporated, which in turn is governed, by the competition between reactivity and steric hindrance of $–CH_3$ group of toluidine in ortho-position.

3.2. Differential Scanning Calorimetry

DSC thermogram of the polyaniline (EB) form shows an endothermic peak at 50-140℃ and an exothermic peak at 185-350℃. The first peak is most likely attributed to the removal of water and the second peak may be related to the cross-linking reaction [34]. In comparison to polyaniline base form, the composite materials in different compositions show entirely different thermogram as shown in figure3.The thermogram of PANI/PSSA (2:1) composition shows an endothermic peak at 99℃, which may be attributed to the loss of water molecules present in polymer matrix. Another endothermic peak at 272℃ may be assigned to the cross-linking/oxidation of composite backbone, where as the small change above 400℃ onwards may be assigned due to the degradation of the composite backbone. In case of PANI/PSSA (1:1) also, an endothermic peak at 265℃ may be assigned to the cross-linking/oxidation of composite. A transition is observed at about 356℃, which may be attributed due to the decomposition of polymeric system, while in case of PANI/PSSA (1:2) composition, DSC thermogram shows an endothermic peak at about 140℃ due to the evaporation of water molecules trapped inside the composite or bound to the polymer backbone. Other exothermic peak at 298℃ may be assigned due to the cross-linking/oxidation in composite backbone, whereas the change above 360℃ may be assigned due to the degradation of composite. The glass transition was not observable in these composites, because the glass transition is buried in the peak due to the removal of water and it does not exhibit hysteresis. When the polymer powder is heated, cooled and reheated, no exotherm is observed upon heating. However, if the transition is a T_g, it should be observed repeatedly upon heating and cooling. Cross-linking in these polymers is an irreversible chemical reaction and therefore would be observed only upon heating the polymer for the first time.

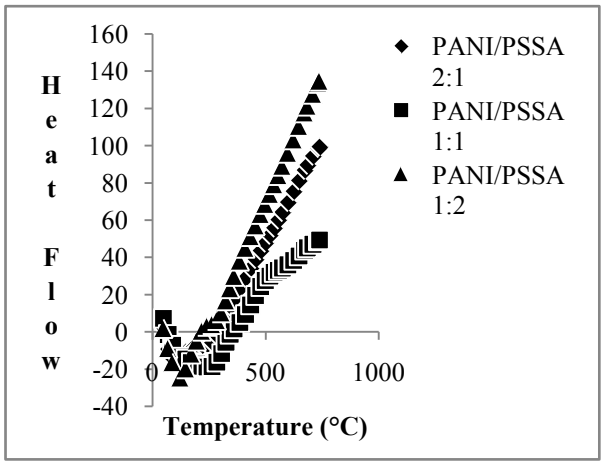

Figure 3. DSC thermogram of PANI/PSSA composite materials

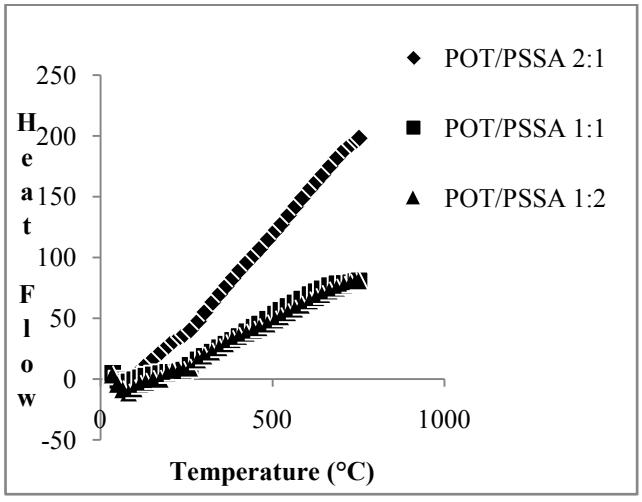

Figure 4. DSC thermograms of POT/PSSA composite materials

DSC thermogram of poly(o-toluidine) (EB) form shows an endothermic peak at 100-120℃ followed by exothermic peaks at 235 and 310℃. The exothermic peak at 235℃ may be assigned due to the oxidation or cross-linking in polymer chain whereas a change in thermogram above 310℃ may be assigned due to the degradation of composite backbone [Kumar et al 2004]. However, in the thermogram of POT/PSSA (2:1) composition as shown in fig.4, an endothermic peak at 80℃ may be assigned due to the release of

water and impurities present in composite. Another endothermic peak at 268℃ may be assigned due to the cross-linking or oxidation of composite backbone and onset of exothermic transition above 300℃ onwards attributed due to the degradation of polymeric backbone. In case of POT/PSSA (1:1) composite, the endothermic peak at 82℃ appears due to the release of moisture and an endothermic peak at about 235℃ may be assigned to the cross-linking/oxidation of composite backbone while an exothermic transition above 350℃ shows the degradation of polymeric matrix. In case of POT/PSSA (1:2) composite, endothermic peak at 84℃ may be assigned due to removal of water. Another endothermic peak at 255℃ in POT/PSSA (1:2) may be assigned due to the cross-linking or oxidation of composite. The transition above 360℃ onwards may be assigned due to the degradation of polymeric backbone.

Thus, on the basis of thermal profile of these materials, we can say that among polyanilines/PSSA composite materials, cross-linking or oxidative reaction starts at higher temperature in PANI/PSSA rather than POT/PSSA composites, which indicates that the stability of PANI composites is higher than POT composites. These DSC results of composite materials are also found in good agreement with TGA results.

3.3. X-ray Diffraction

In PANI/PSSA (2:1) composite, the XRD pattern shows sharp peaks centered on 2θ value of 15, 17 and small peak at 25°, while in case of PANI/PSSA (1:1) composition small peaks at 10, 39 and 45° and in case of PANI/PSSA (1:2) composition small hump at 10, 16, 19, 25 and 39^0 are observed. The intensity of above peaks decreases abruptly with the increase in PSSA content in the composite material. Thus the peaks appear as weak shoulders in PANI/PSSA (1:1) and PANI/PSSA (1:2) compositions.

In POT/PSSA (2:1) composite, the XRD pattern shows sharp peaks centered on 2θ value of 14, 17 20, 39 and 45°, while in case of POT/PSSA (1:1) a small hump at 14, and a broad amorphous peak at 25 are observed. In POT/PSSA (1:2) composite, small hump at 20, 39 and 43 are observed. Thus POT/PSSA (2:1) composite is found more crystalline than POT/PSSA (1:1) and POT/PSSA (1:2) composite, because as PSSA content increases in the composite material, the intermolecular chain spacing and amorphous nature of composites increases due to steric hindrance of methyl group. The amorphous nature in PANI/PSSA (1:2) and POT/PSSA (1:2) composition also attributes the reason that PSSA acts as a plasticizer and it distorts the lattice. Thus instead of entering inside the emplty lattice, it first forms attachment through suitable bonding at the reactive site and simultaneously engulfs the whole polymer in a very regular manner-because of its miceller type morphology. This type of morphology destroys the regular arrangement of polymeric backbone and thus leads towards the amorphous character. The Bragg angles and d-spacing obtained from the wide angle X-ray diffractograms of powdered samples of composite materials are presented in Table-1.

Table 1. X-ray diffractogram data of composite materials

Sample	Value of 2θ (in degree)	Value for d spacing (Å)
PANI/PSSA (2:1)	15, 17, 25	6.23, 5.23, 3.57
PANI/PSSA (1:1)	10, 39, 45	8.98, 2.33, 2.02
PANI/PSSA (1:2)	10, 16, 19, 25, 39	8.90, 5.45, 4.66, 3.55, 2.33
POT/PSSA (2:1)	14, 17, 20, 39, 45	6.30, 5.24, 4.46, 2.33, 2.02
POT/PSSA (1:1)	14, 25	6.37, 3.61
POT/PSSA (1:2)	20, 39, 43	4.47, 2.33, 2.11

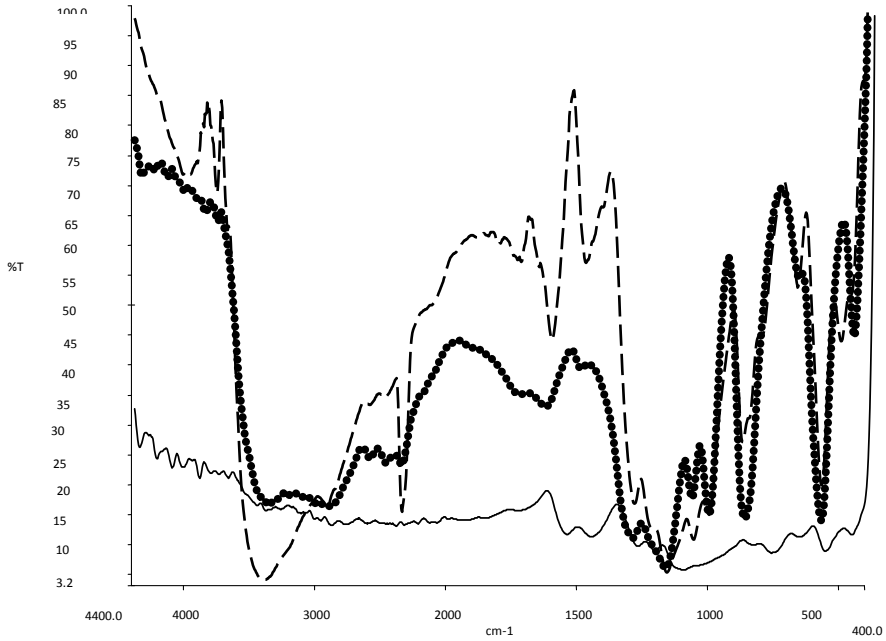

[PANI/PSSA (2:1), PANI/PSSA (1:1), PANI/PSSA (1:2)]

Figure 5. FTIR spectra of PANI/PSSA composite materials

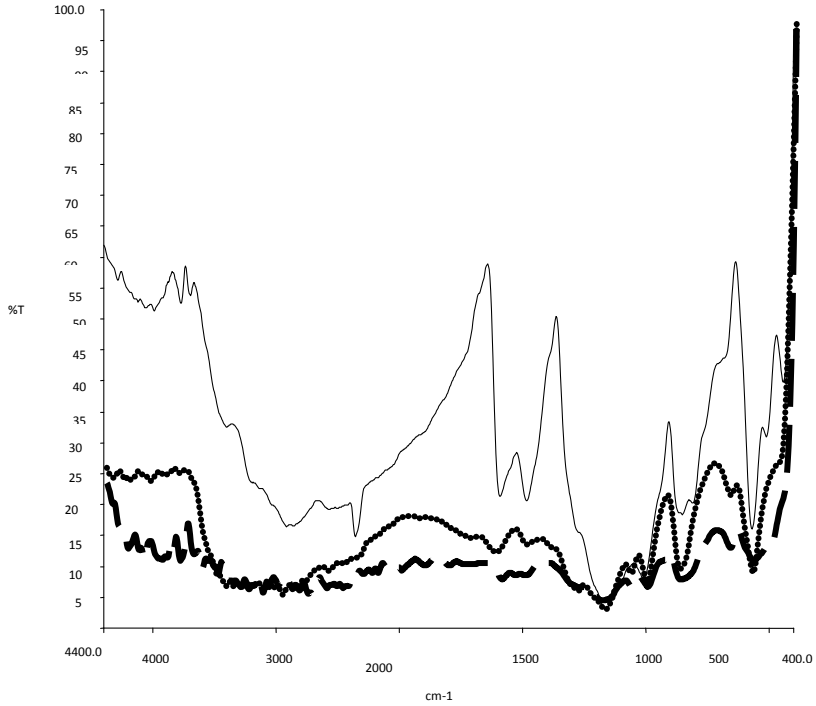

Figure 6. FTIR spectra of POT/PSSA composite materials[POT/PSSA (2:1), POT/PSSA (1:1),POT/PSSA (1:2)]

3.4. FTIR Analysis

The FTIR spectra of emeraldine base form of aniline are observed in the range of 1650 cm^{-1} to 1220 cm^{-1}, which arises due to the aromatic ring breathing, -NH- deformation and due to the -C-N- stretching. The bands at 1577 cm^{-1} and at 1484 cm^{-1} are the characteristic bands of N- quinoid and benzenoid rings and their presence shows a prominence in the conducting state of the polymer. The absorption band at 1227 cm^{-1} arises due to C-N benzenoid ring stretching in the polymer. The peak at 818 cm^{-1} attributes due to the para coupled ring while peak at 886 cm^{-1} represents the deformed vibrational mode of benzene ring, which is caused due to attachment of specific group present on the ring. Figure5. Shows the FTIR spectra of composite materials prepared by reinforcement of polymer, i.e. polyaniline to PSSA in different compositions such as PANI/PSSA (2:1), PANI/PSSA (1:1) and PANI/PSSA (1:2) compositions. The FTIR studies reveal the formation of composite materials and help to obtain their compositions qualitatively. In case of composites, the out of plane H deformation, i.e. para coupling was observed at ~ 800 cm^{-1}. The band at 1470-1490 cm^{-1} corresponds to C=C ring vibrations of benzenoid ring. The peak at 1130-1140 corresponds to sulphonic acid group in all these compositions, i.e. due to the symmetric $-SO_3$ stretching. The intensity of this band goes on increasing with the increase in PSSA content. The characteristic bands of both PSSA and PANI confirms the presence of both phases in composite materials, but all these bands shows a systematic shifting that indicates existence of significant interaction between PANI and PSSA in the composite material.

The FTIR spectra of poly(o-toluidine) giving peaks at 1591 and 1491 cm^{-1} are due to the C=C vibration of quinoid and benzenoid rings. The characteristic peak at 1304 cm^{-1} has been attributed due to C-N in Q-B-Q sequence. The peak at 807 cm^{-1} attributes to the para coupled phenyl ring and a strong peak at 878 cm^{-1} appears due to the methyl group attached to phenyl ring. The band at 1155 cm^{-1} could be attributed to the $-CH_3$ rocking mode. The FTIR spectra of composite materials are shown in figure6. The C=C vibrations of quinoid ring is observed at 1590-1620 cm^{-1} in all composites. The peak due to C=C vibration of benzenoid ring is observed at 1485-1510 cm^{-1} in composite materials. The peak due to methyl group attached to the phenyl ring is observed at 850-870 cm^{-1} . The characteristic peaks observed at 1170-1190 cm^{-1} are due to symmetric stretching vibrations of $-SO_3$ (polystyrene sulphonic acid). The peak at 3100-3400 cm^{-1} shows the presence of N-H stretching vibration in all compositions. The intensity of these peaks goes on increasing with the increase in PSSA content.

4. Conclusions

Polyaniline and poly(o-toluidine) have been reinforced into PSSA in 2:1, 1:1 and 1:2 compositions for the preparation of composite material. TGA-DSC result show that thermal stability of PANI/PSSA (2:1) and POT/PSSA (2:1) is higher than their 1:1 and 1:2 compositions, respectively. In all thermograms, the first peak is observed due to loss of water/moisture and oligomers while the second peak may be due to the crosslinking/oxidation followed by degradation of composite material. From XRD pattern, we infer that crystallinity of PANI/PSSA (2:1) and POT/PSSA (2:1) is higher than their 1:1 and 1:2 conuterparts. PANI/PSSA (2:1) and POT/PSSA (2:1) compositions find an easy way to attack on

the suitable sites of polymer, which facilitates the easy movements of polyaniline and poly(o-toluidine) molecular chain, ultimately causes a change and contributes towards the higher crystallinity. The FTIR data demonstrated the interaction between PSSA and polyanilines with the presence of sulphonic acid peaks in all composites. The characteristic bands of PSSA, PANI and POT also confirm the presence of both phases in the materials.

ACKNOWLEDGEMENTS

A financial support for major research project from the University Grants Commission, New Delhi is acknowledged gratefully. Authors are also thankful to Prof. P.B.Sharma, vice chancellor, Delhi Technological University, Delhi for his kind support and keen interest in the work.

REFERENCE

[1] V. P. Parkhutik, J. M. Martinez-Duart, R. D. Calleja, E. M. Matveeva, J. Electrochem. Soc, 1993, "Deposition of Polyaniline Films onto Porous Silicon Layers, 140, L94-L95.

[2] K.H.Chen, S. M. Yang, 2003" Polyaniline-montmorillonite composite synthesized by electrochemical method" Synth. Met. 135, 151-152.

[3] J. A. Conklin, S. C. Huang, S. M. Huang, T. Wan, R. B. Kaner, 1995, "Thermal properties of polyaniline and poly(aniline-co-o-ethylaniline)" Macromol., 28, 6522-6527.

[4] L. H. Dao, M. Leclerc, J. Guay, J. W. Chevalier,1989, "Synthesis and characterization of substituted poly anilines"Synth. Met. 29, 377-382.

[5] L. Ding, X. Wang, R. V. Gregory, 1999, "Thermal properties of chemically synthesized polyanilines (EB)powder", Synth. Met., 104, 73-78.

[6] S. H. Goh, H. S. O. Chan, C. H. Ong, 1998, "Miscible blends of conductive polyaniline with tertiary amide polymers" J. Appl. Polym. Sci. 68, 1839-1844.

[7] N. Gupta, 2010,"Investigations on electronically conducting polymers" Ph.D.Thesis, C.C.S.Univ., Meerut,

[8] N. Gupta, D. Kumar, 2009 "Investigation on poly (aniline-co-o-toluidine) / polystyrene sulphonic acid composite", Ind. J. Eng Mat. Sci, 16, 403-409.

[9] N. Gupta, S. Sharma, I. Mir, D. Kumar, 2006, "Advances in sensors based on conducting polymers", J. Sci. Ind. Res. 65, 549-557.

[10] K. Gurunathan, D. C. Trivedi, 2000, "Studies on polyaniline and colloidal TiO composites" Mater. Lett.45, 262-268.

[11] K. Gurunathan, D. P. Amalnerkar, D. C. Trivedi, 2003, "Synthesis and characterization of conducting polymer composite (PAn/TiO_2) for cathode material in rechargeable battery"Mater. Lett.57, 1642-1648.

[12] T. Jeevananda, Siddaramaiah, 2003, "Synthesis and characterization of polyaniline filled PU/PMMA IPNs" Eur. Polym. J., 39 (3) 569-578.

[13] V. Jousseaume, M. Morsli, A. Bonnet, O. Tesson, S. Lefrant, 1998, "Electrical properties of polyaniline–polystyrene blends above the percolation threshold" J. Appl. Polym. Sci. 67, 1205-1208.

[14] A. Kaynak, J. Unsoworth, R. Clout, A. Mohan, G. Bears, 1994, "A study of microwave transmission, reflection, absorption, and shielding effectiveness of conducting polypyrrole films" J. Appl. Polym. Sci. 54, 269-278.

[15] P. S. Khiew, N. M. Huang, S. Radiman, M. S. Ahmad, 2004, "Synthesis and characterization of conducting polyaniline-coated cadmium sulphide nanocomposites in reverse microemulsion" Mater. Lett., 58, 516-521.

[16] T. Kobayashi, H. Yoneyama, H. Tamura, 1984, "Polyaniline film-coated electrodes as electrochromic display devices" J. Electroanal. Chem. 161, 419-423.

[17] D. Kumar, R. Chandra, 2001, "Thermal behavior of synthetic metals, Polyanilines", Ind. J. Eng. Mater. Sci., 8 209-214.

[18] D. Kumar, R. C. Sharma, 1998 "Advances in conducting polymers" Eur. Polym. J. 34 1053-1060.

[19] X. Li, G. Wang, D. Lu, 2004, "Surface properties of polyaniline/nano-TiO_2 composites" Appl. Surf. Sci, 229, 395-401.

[20] L. F. Malmonge, L. H. Mattoso, 1995, "Electroactive blends of poly(vinylidene fluoride) and polyaniline derivatives" Polymer, 36, 245-249.

[21] M. Mermillod, J. Tanguy, F. Petiot, 1986, "A study of chemically synthesized polypyrrole as electrode material for battery applications" J. Electrochem. Soc.133, 1073-1079.

[22] H. S. Nalwa, 2006, "Handbook of organic conductive molecules and polymer",Vol. 2, Wiley, New York.

[23] T. F. Otero, J. Rodriguez, E. Angulov, C. Santamarias, 1993, "Artificial muscles from bilayer structures", Synth. Met., 57, 3713-3717.

[24] W. Pan, S. Yang, G. Li, J. M. Jiang, 2005, "Electrical and structural analysis of conductive polyaniline/polyacrylonitrile composites", Eur. Polym. J., 41 2127-2133.

[25] M. Panda, V. Srinivas, A. K. Thakur 2008, "On the question of percolation threshold in polyvinylidene fluoride/nanocrystalline nickel composites", Appl. Phys. Lett., 92 (1) 132905-132907, 2010 "Thermal effects on the percolation behavior of polyvinylidene fluoride/nickel composites", Appl. Phys. Lett., 117, 3023-3028

[26] Y. H. Park, H. C. Shin, Y. Lee, Y. Son, D. H. Baik, 1999 "Electrochemical preparation of polypyrrole copolymer films from PSPMS precursor", Macromol, 32 4615-4618.

[27] Y. H. Park, C.R. Park, 2001, "Preparation of conducting polyacrylonitrile / polyaniline composite films by electrochemical synthesis and their electroactivity", Synth. Met. 118(1), 187-192.

[28] M. Ram, R. N. P. Choudhary, A.K. Thakur, 2007 " Preparation and characterization of LiFe1/2Ni 1/2Vo4" Mater. Chem. & Phys., 101 455-463.

[29] N. Shukla, A. Shukla, A. K. Thakur, R. N. P. Choudhary,

2008, "Low temperature ferroelectric behavior of PVDE based composites", Ind. J. Eng. Mater. Sci., 15 126-128.

[30] G. P. Singh, S. Ram, A. K. Thakur, R. N. P. Choudhary, 2008 "Electrical properties of ferromagnetic AgCro2 particles", Ind. J. Eng. Mater. Sci., 15 171-175.

[31] S. Wang, Z. Tan, Y. Li, L. Sun, T. Zhang, 2006, " Synthesis, characterization and thermal analysis of polyaniline/Zro2 composites" Thermochim. Acta, 441, 191-194.

[32] C. G. Wu, Y. C. Liu, S. S. Hsu, 1999 "Assembly of conducting polymer/ metal oxide multilayer in one step" Synth. Met. 102, 1268-1269.

[33] P. Xiao, M. Xiao, P. Liu, K. Gong, 2000, " Direct synthesis of a polyaniline intercalated graphite oxide nanocomposite" Carbon, 38 626-628.

[34] S. M. Yang, K. H. Chen, 2003, "Synthesis of polyaniline montmorillonite nanocomposites" Synth. Met., 135, 51-52.